

## Supplementary Material

### Novel tetrahydropyrimidinyl-substituted benzimidazoles and benzothiazoles:

#### Synthesis, antibacterial activity, DNA interactions and ADME profiling

Valentina Rep,<sup>a</sup> Rebeka Štulić,<sup>a</sup> Sanja Koštrun,<sup>b</sup> Bojan Kuridža,<sup>c</sup> Ivo Crnolatac,<sup>c</sup> Marijana Radić Stojković,<sup>\*c</sup> Hana Čipčić Paljetak,<sup>d</sup> Mihaela Perić,<sup>d</sup> Mario Matijašić<sup>d</sup> and Silvana Raić-Malić<sup>\*a</sup>

<sup>a</sup>Department of Organic Chemistry, Faculty of Chemical Engineering and Technology, University of Zagreb, Marulićev trg 19, 10 000 Zagreb, Croatia.

<sup>b</sup>Selvita d.o.o., Prilaz baruna Filipovića 29, 10 000 Zagreb, Croatia.

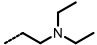
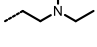
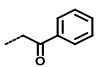
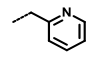
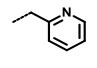
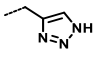
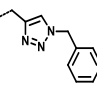
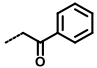
<sup>c</sup>Ruđer Bošković Institute, Division of Organic Chemistry and Biochemistry, Bijenička cesta 54, 10 000 Zagreb, Croatia.

<sup>d</sup>Department for Intercellular Communication, Center for Translational and Clinical Research, University of Zagreb School of Medicine, Šalata 2, 10 000 Zagreb, Croatia

Content	Pages
1. Cytotoxic activity assessment of selected compounds <b>12a</b> , <b>12c</b> , <b>15a-c</b> , <b>16a</b> , <b>16c</b> , <b>17a</b> , <b>18a</b> and <b>21b</b>	S1
2. Spectroscopic characterization of <b>15a-c</b> , <b>16a</b> , <b>16c</b> , <b>17a</b> , <b>21a</b> and <b>21b</b>	S2–S5
3. Interactions of <b>15a-c</b> , <b>16a</b> , <b>16c</b> , <b>17a</b> , <b>21a</b> and <b>21b</b> with ds-polynucleotides in neutral medium (pH=7.0)	
3.1. Fluorimetric titrations	S5–S15
3.2. Thermal melting experiments	S16–S17
3.3. Circular dichroism (CD) titration	S18–S21
4. <sup>1</sup> H and <sup>13</sup> C NMR spectra of novel compounds	S22–S52

## 1. Cytotoxic activity

Table S1. Cytotoxic activity of selected compounds against HepG2 cell lines

Compd	X	R <sub>1</sub>	R <sub>2</sub>	IC <sub>50</sub> (μM)
				HepG2
<b>12a</b>	NH	H		>100
<b>12c</b>	NH	OCH <sub>3</sub>		>100
<b>15a</b>	NH	H		>100
<b>15b</b>	NH	F		>100
<b>15c</b>	NH	OCH <sub>3</sub>		>100
<b>16a</b>	NH	H		>100
<b>16c</b>	NH	OCH <sub>3</sub>		>100
<b>17a</b>	NH	H		>100
<b>18a</b>	NH	H		>100
<b>21b</b>	S	F		>100

<sup>a</sup>50% inhibitory concentration or compound concentration required to inhibit tumour cell proliferation by 50%.

## 2. Spectroscopic characterization of 15a-c, 16a, 16c, 17a, 21a and 21b

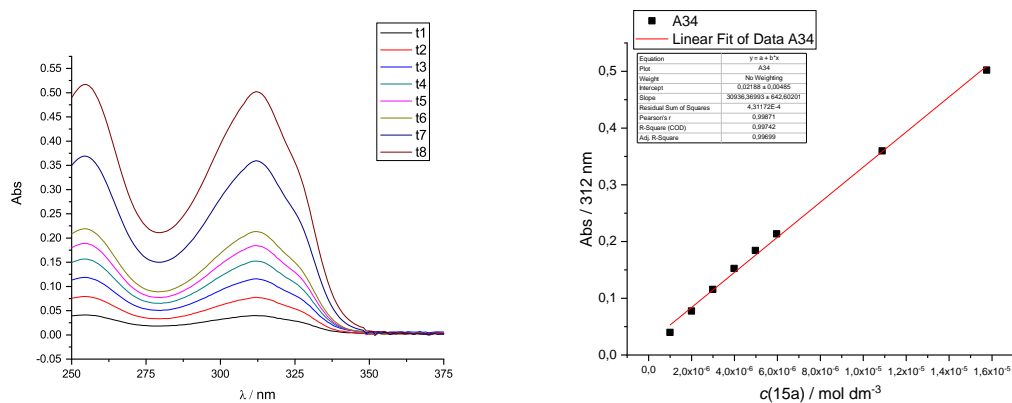


Figure S1. UV/Vis spectra changes of **15a** at different concentrations (concentration range from  $1 \times 10^{-6}$  –  $1.6 \times 10^{-5}$  mol dm<sup>-3</sup>) at pH=7, sodium cacodylate buffer,  $I=0.05$  M.

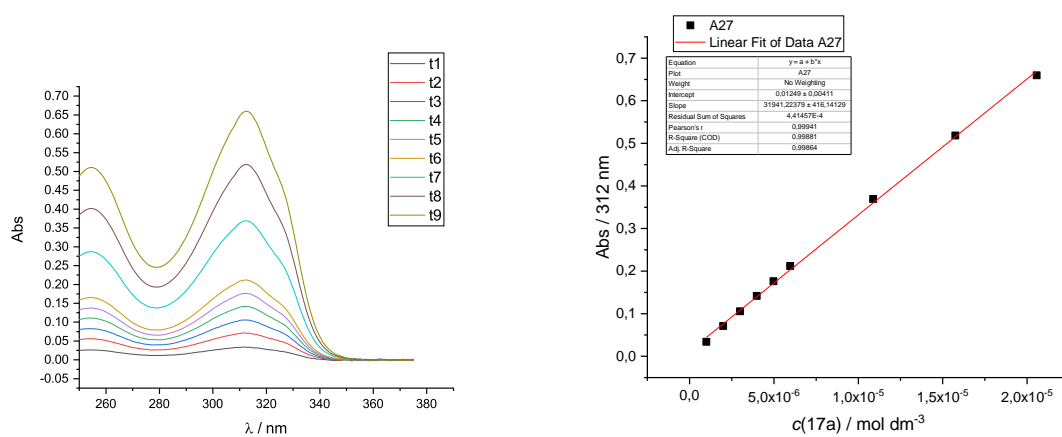


Figure S2. UV/Vis spectra changes of **17a** at different concentrations (concentration range from  $1 \times 10^{-6}$  –  $2 \times 10^{-5}$  mol dm<sup>-3</sup>) at pH=7, sodium cacodylate buffer,  $I=0.05$  M.

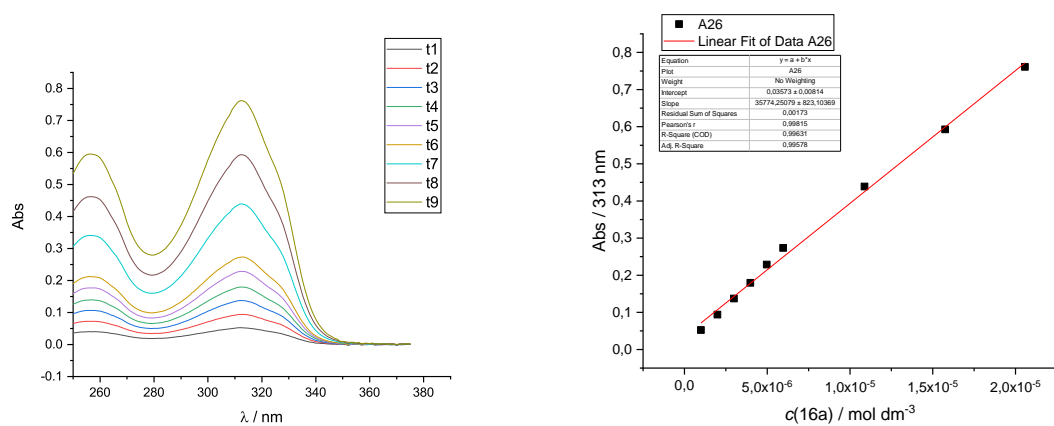


Figure S3. UV/Vis spectra changes of **16a** at different concentrations (concentration range from  $1 \times 10^{-6} - 2 \times 10^{-5} \text{ mol dm}^{-3}$ ) at pH=7, sodium cacodylate buffer,  $I=0.05 \text{ M}$ .

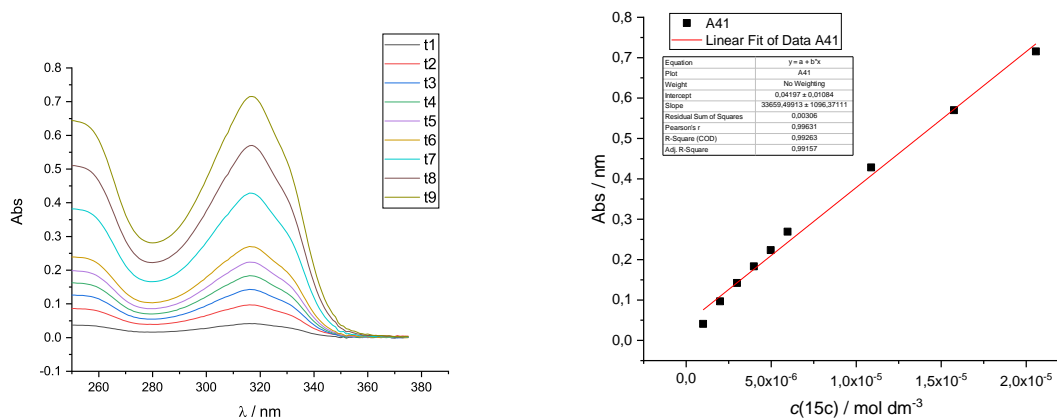


Figure S4. UV/Vis spectra changes of **15c** at different concentrations (concentration range from  $1 \times 10^{-6} - 2 \times 10^{-5} \text{ mol dm}^{-3}$ ) at pH=7, sodium cacodylate buffer,  $I=0.05 \text{ M}$ .

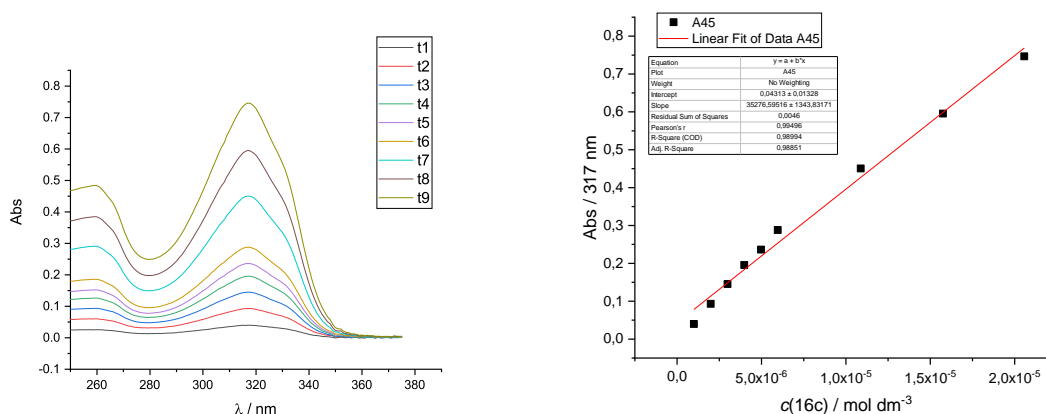


Figure S5. UV/Vis spectra changes of **16c** at different concentrations (concentration range from  $1 \times 10^{-6} - 2 \times 10^{-5} \text{ mol dm}^{-3}$ ) at pH=7, sodium cacodylate buffer,  $I=0.05 \text{ M}$ .

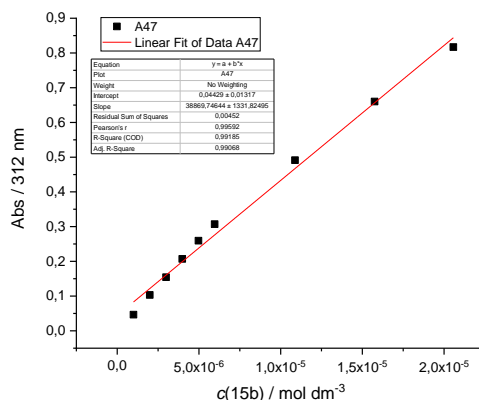
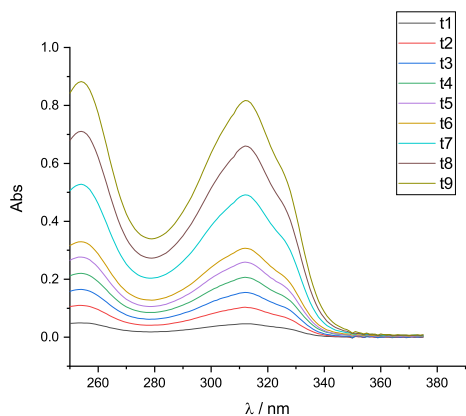


Figure S6. UV/Vis spectra changes of **15b** at different concentrations (concentration range from  $1 \times 10^{-6} - 2 \times 10^{-5} \text{ mol dm}^{-3}$ ) at pH=7, sodium cacodylate buffer,  $I=0.05 \text{ M}$ .

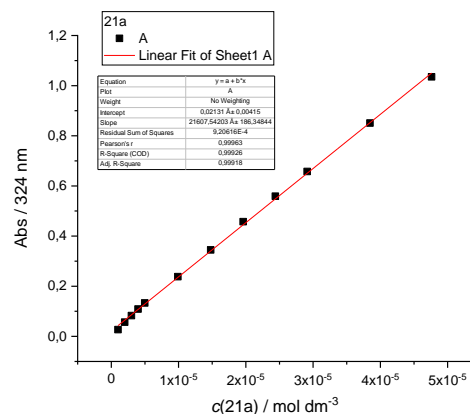
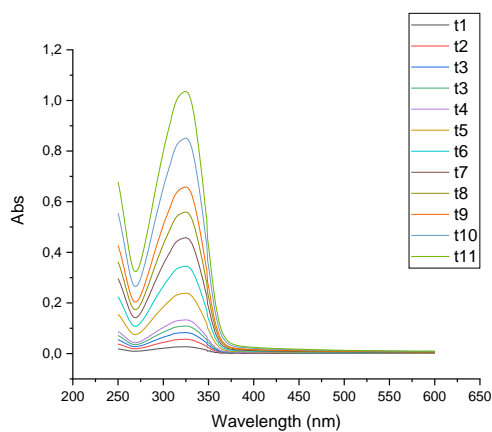


Figure S7. UV/Vis spectra changes of **21a** at different concentrations (concentration range from  $1 \times 10^{-6} - 2 \times 10^{-5} \text{ mol dm}^{-3}$ ) at pH=7, sodium cacodylate buffer,  $I=0.05 \text{ M}$ .

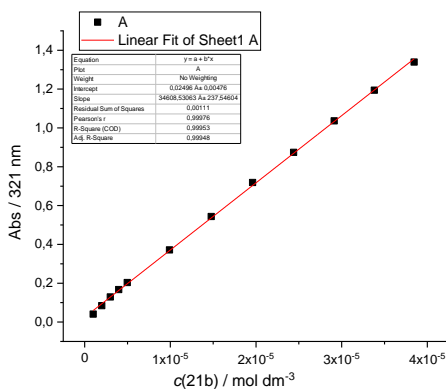
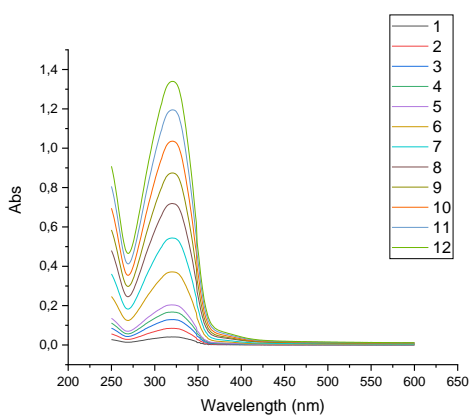


Figure S8. UV/Vis spectra changes of **21b** at different concentrations (concentration range from  $1 \times 10^{-6} - 2 \times 10^{-5} \text{ mol dm}^{-3}$ ) at pH=7, sodium cacodylate buffer,  $l=0.05 \text{ M}$ .

**Table S2.** Electronic absorption data **15a-c**, **16a**, **16c**, **17a**, **21a** and **21b**

	pH = 7,0 <sup>a</sup>	
	$\lambda_{\text{max}} / \text{nm}$	$\epsilon \times 10^3 / \text{mmol}^{-1} \text{cm}^2$
<b>15a</b>	312	30.94
<b>15b</b>	312	38.87
<b>15c</b>	317	33.66
<b>16a</b>	313	35.77
<b>16c</b>	317	35.27
<b>17a</b>	312	31.94
<b>21a</b>	324	21.61
<b>21b</b>	321	34.61

<sup>a</sup> Sodium cacodylate buffer,  $l = 0.05 \text{ mol dm}^{-3}$ , pH = 7.0.

### 3. Interactions of 15a-c, 16a, 16c, 17a, 21a and 21b with ds-polynucleotides in neutral medium (pH=7.0)

#### 3.1. Fluorimetric titrations

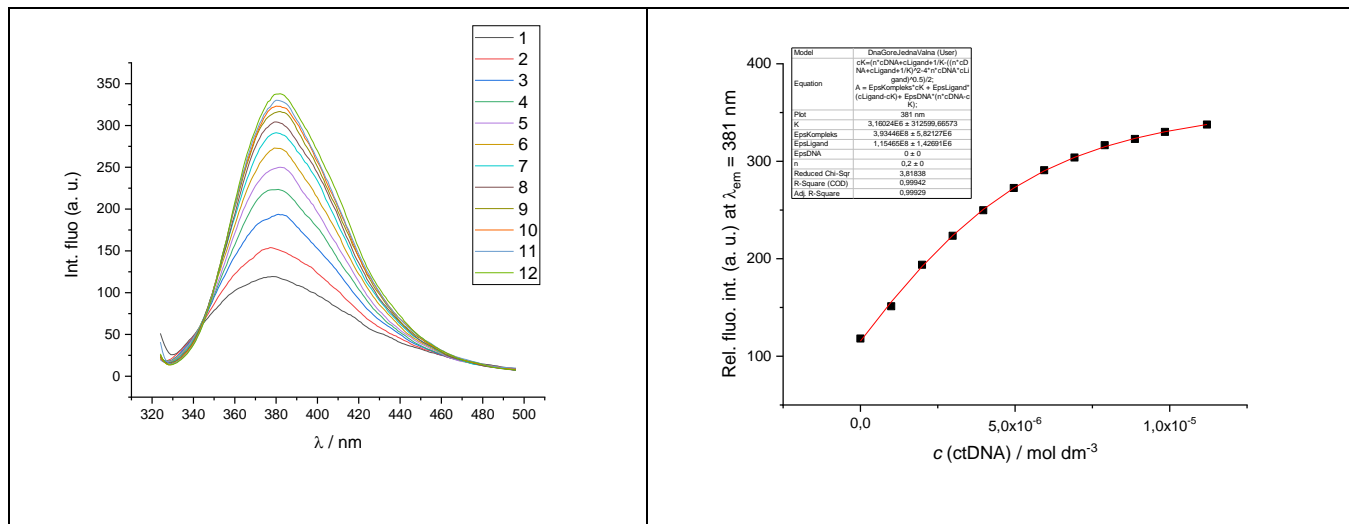


Figure S9. a) Changes in fluorescence spectrum of **15a** ( $c = 1 \times 10^{-6} \text{ mol dm}^{-3}$ ,  $\lambda_{\text{exc}}=312 \text{ nm}$ ) upon titration with ctDNA ( $c = 1.0 \times 10^{-6} - 1.1 \times 10^{-5} \text{ mol dm}^{-3}$ ); b) Dependence of **15a** absorbance at  $\lambda = 381 \text{ nm}$  on  $c(\text{ctDNA})$ , at pH=7, sodium cacodylate buffer,  $l = 0.05 \text{ mol dm}^{-3}$ .

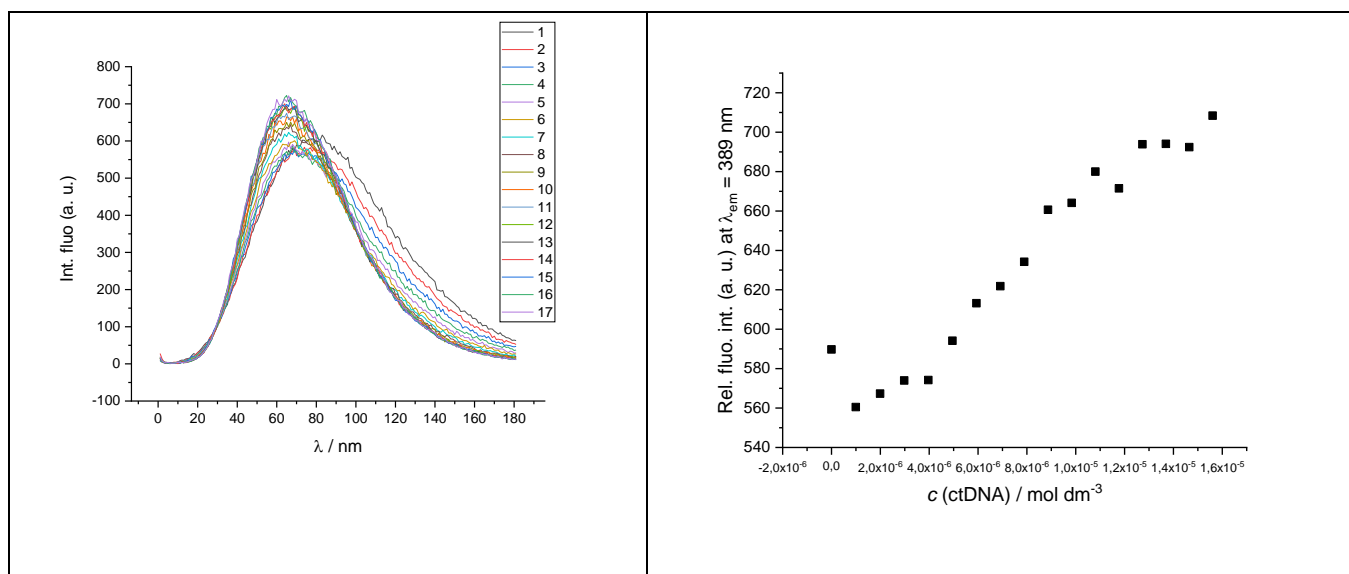


Figure S10. a) Changes in fluorescence spectrum of **17a** ( $c = 1 \times 10^{-6} \text{ mol dm}^{-3}$ ,  $\lambda_{\text{exc}}=312 \text{ nm}$ ) upon titration with ctDNA ( $c = 1.0 \times 10^{-6} - 1.6 \times 10^{-5} \text{ mol dm}^{-3}$ ); b) Dependence of **17a** absorbance at  $\lambda = 389 \text{ nm}$  on  $c(\text{ctDNA})$ , at pH=7, sodium cacodylate buffer,  $l = 0.05 \text{ mol dm}^{-3}$ .

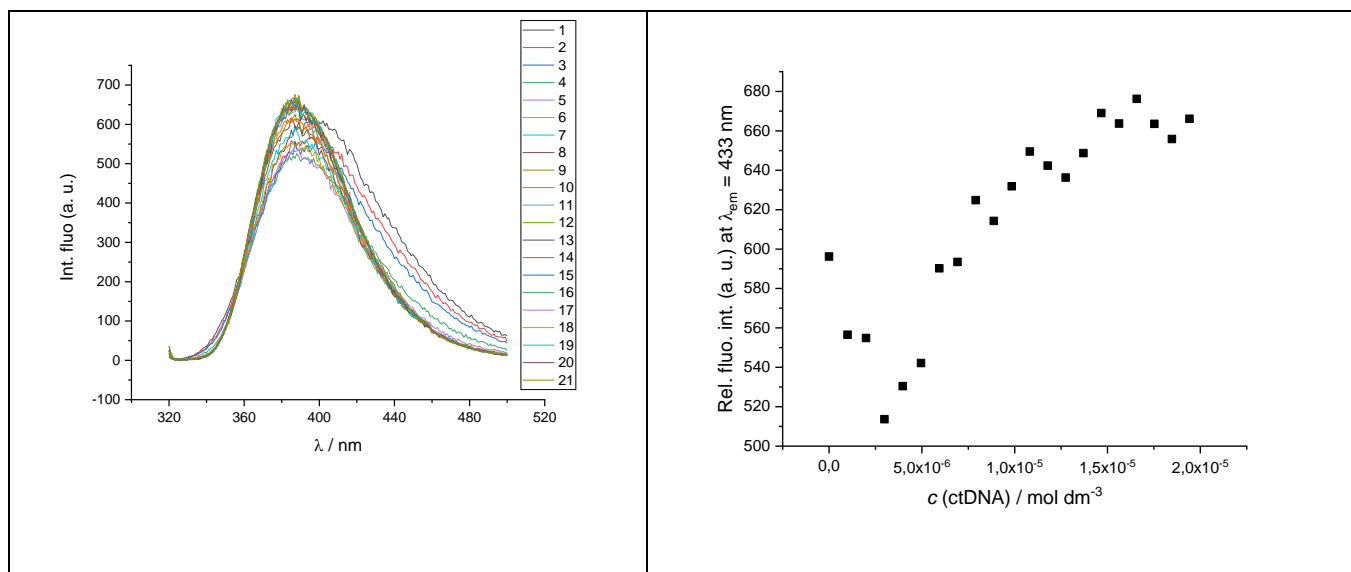


Figure S11. a) Changes in fluorescence spectrum of **16a** ( $c = 1 \times 10^{-6} \text{ mol dm}^{-3}$ ,  $\lambda_{\text{exc}} = 313 \text{ nm}$ ) upon titration with ctDNA ( $c = 1.0 \times 10^{-6} - 1.9 \times 10^{-5} \text{ mol dm}^{-3}$ ); b) Dependence of **16a** absorbance at  $\lambda = 433 \text{ nm}$  on  $c(\text{ctDNA})$ , at  $\text{pH} = 7$ , sodium cacodylate buffer,  $I = 0.05 \text{ mol dm}^{-3}$ .

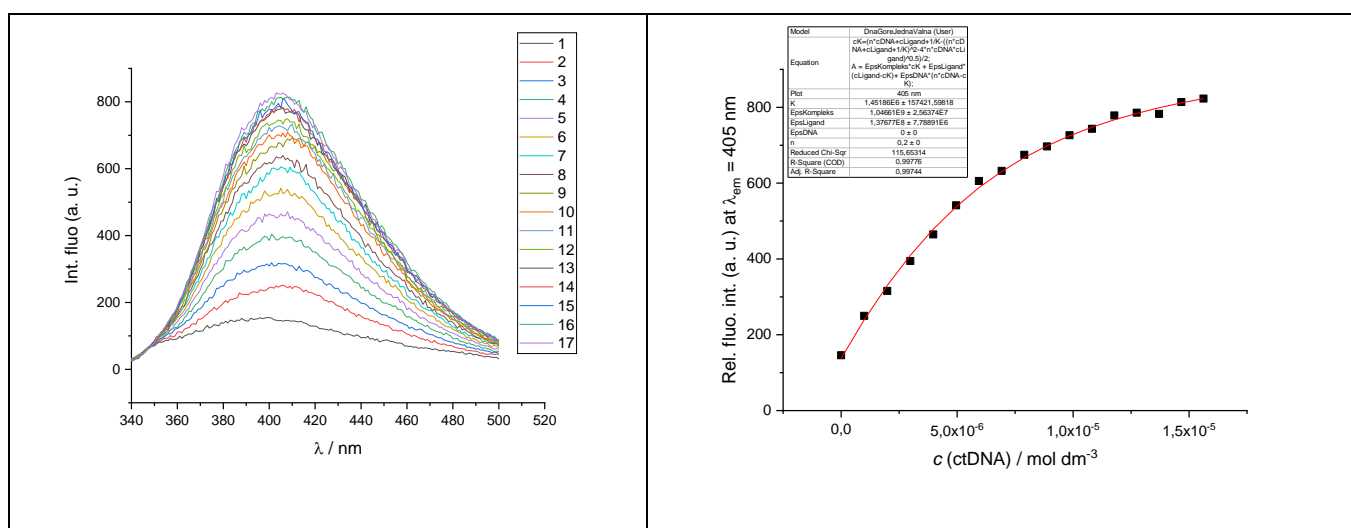


Figure S12. a) Changes in fluorescence spectrum of **15c** ( $c = 1 \times 10^{-6} \text{ mol dm}^{-3}$ ,  $\lambda_{\text{exc}} = 317 \text{ nm}$ ) upon titration with ctDNA ( $c = 1.0 \times 10^{-6} - 1.6 \times 10^{-5} \text{ mol dm}^{-3}$ ); b) Dependence of **15c** absorbance at  $\lambda = 405 \text{ nm}$  on  $c(\text{ctDNA})$ , at  $\text{pH} = 7$ , sodium cacodylate buffer,  $I = 0.05 \text{ mol dm}^{-3}$ .



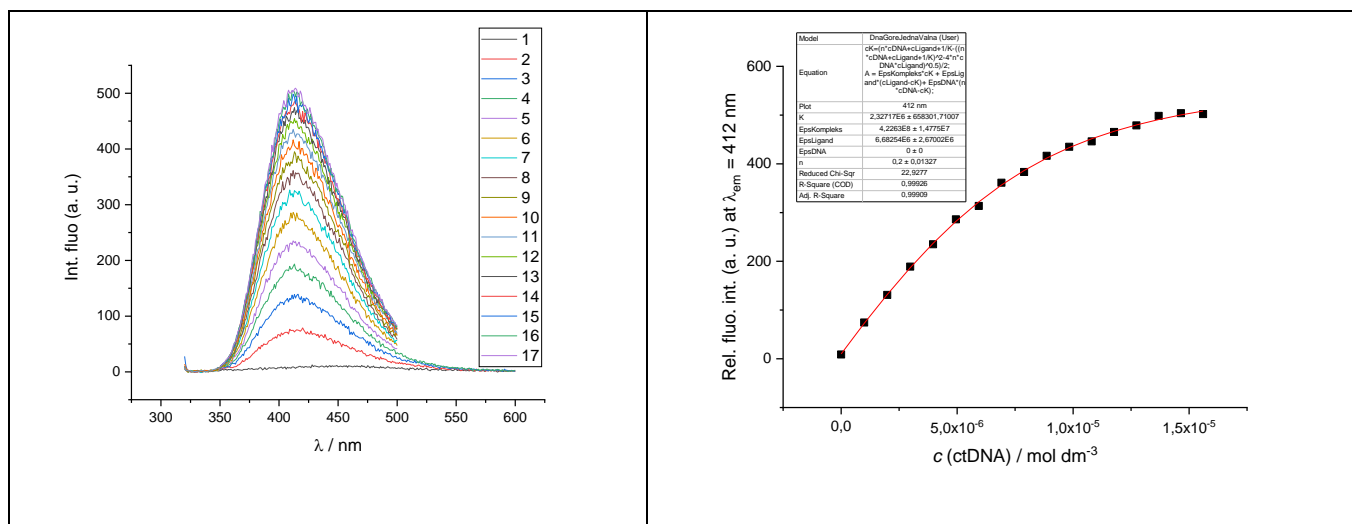


Figure S13. a) Changes in fluorescence spectrum of **16c** ( $c = 1 \times 10^{-6} \text{ mol dm}^{-3}$ ,  $\lambda_{exc} = 317 \text{ nm}$ ) upon titration with ctDNA ( $c = 1.0 \times 10^{-6} - 1.6 \times 10^{-5} \text{ mol dm}^{-3}$ ); b) Dependence of **16c** absorbance at  $\lambda = 412 \text{ nm}$  on  $c(\text{ctDNA})$ , at pH=7, sodium cacodylate buffer,  $I = 0.05 \text{ mol dm}^{-3}$ .

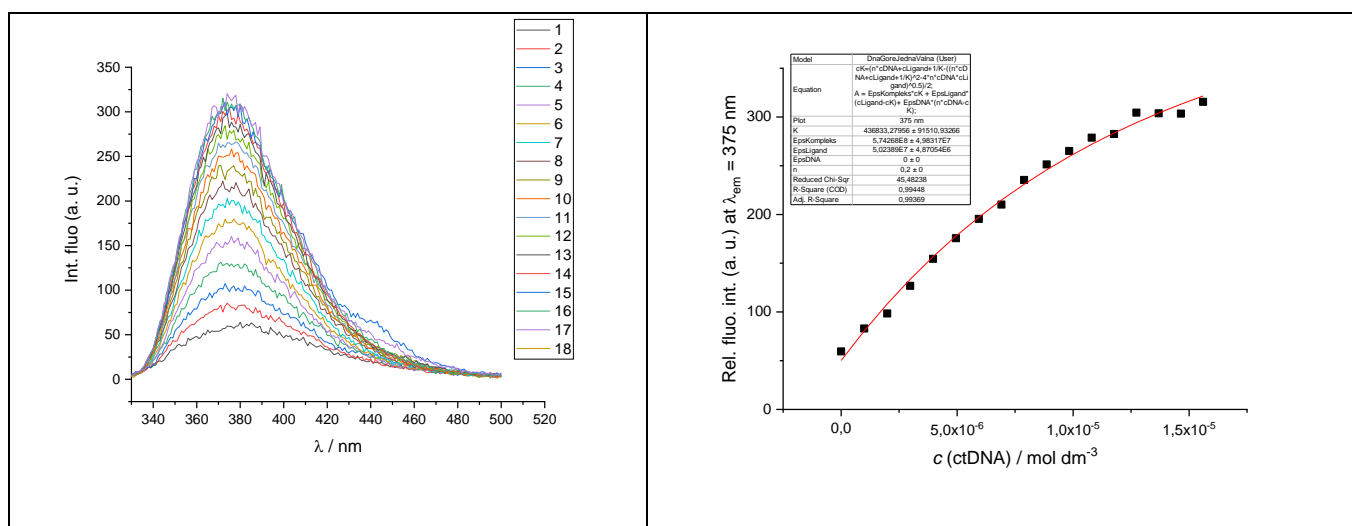


Figure S14. a) Changes in fluorescence spectrum of **15b** ( $c = 1 \times 10^{-6} \text{ mol dm}^{-3}$ ,  $\lambda_{exc} = 312 \text{ nm}$ ) upon titration with ctDNA ( $c = 1.0 \times 10^{-6} - 1.6 \times 10^{-5} \text{ mol dm}^{-3}$ ); b) Dependence of **15b** absorbance at  $\lambda = 375 \text{ nm}$  on  $c(\text{ctDNA})$ , at pH=7, sodium cacodylate buffer,  $I = 0.05 \text{ mol dm}^{-3}$ .

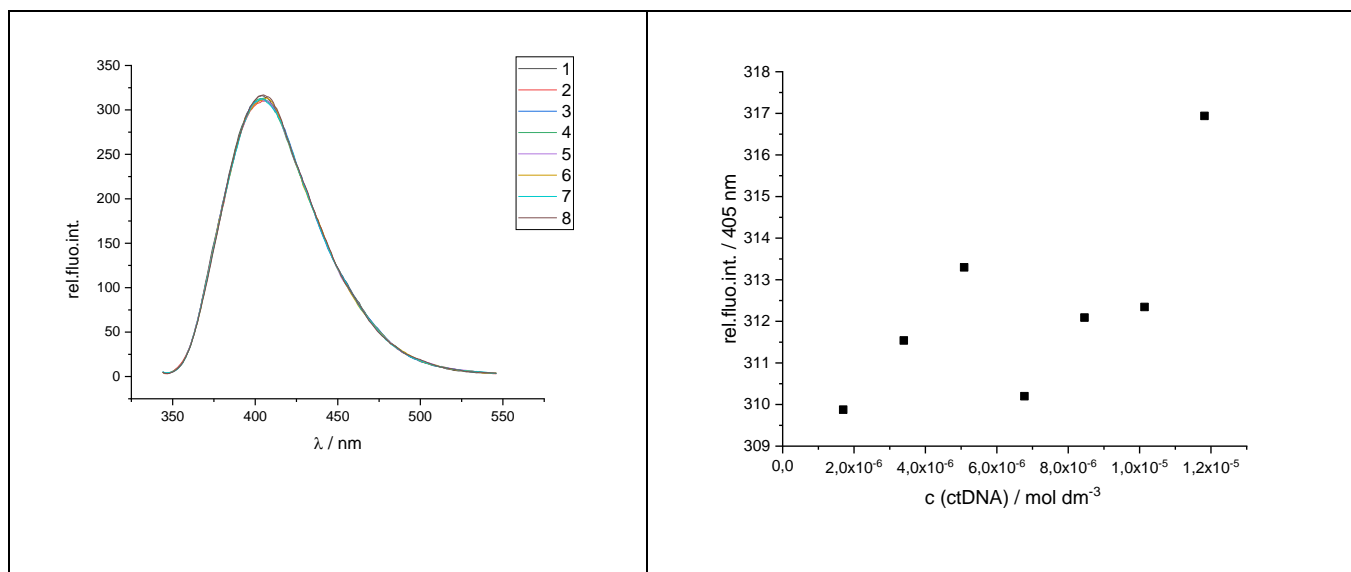


Figure S15. a) Changes in fluorescence spectrum of **21a** ( $c = 2 \times 10^{-6} \text{ mol dm}^{-3}$ ,  $\lambda_{\text{exc}} = 324 \text{ nm}$ ) upon titration with ctDNA ( $c = 1.7 \times 10^{-6} - 1.2 \times 10^{-5} \text{ mol dm}^{-3}$ ); b) Dependence of **21a** absorbance at  $\lambda = 405 \text{ nm}$  on  $c(\text{ctDNA})$ , at  $\text{pH} = 7$ , sodium cacodylate buffer,  $l = 0.05 \text{ mol dm}^{-3}$ .

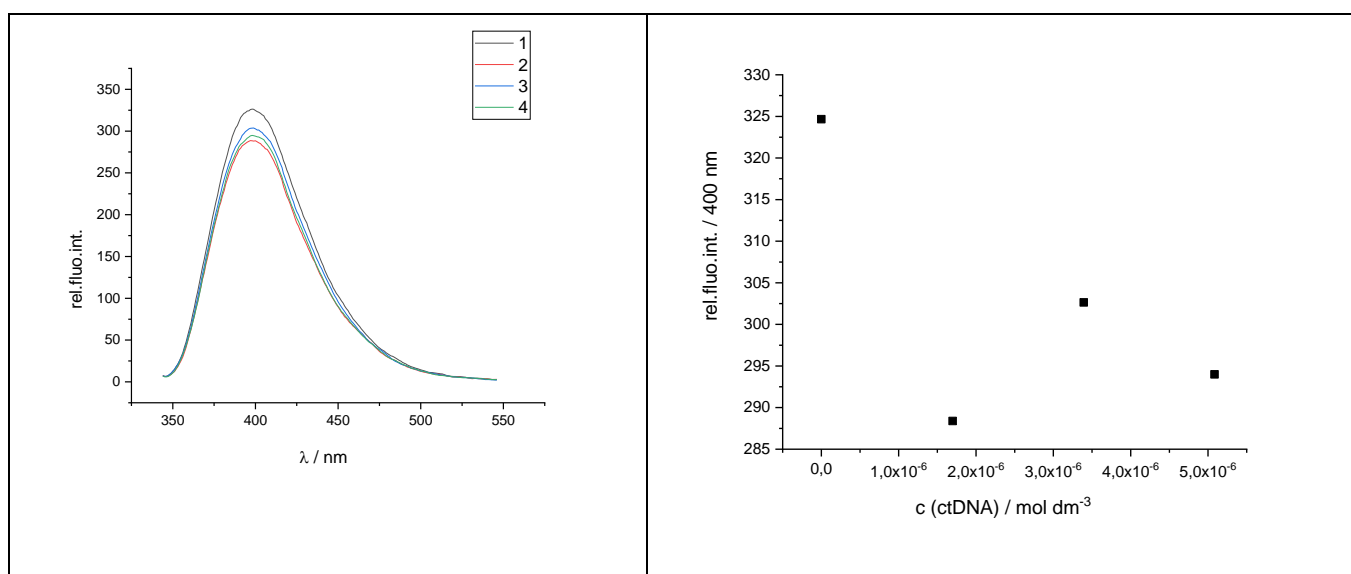


Figure S16. a) Changes in fluorescence spectrum of **21b** ( $c = 2 \times 10^{-6} \text{ mol dm}^{-3}$ ,  $\lambda_{\text{exc}} = 321 \text{ nm}$ ) upon titration with ctDNA ( $c = 1.7 \times 10^{-6} - 1.2 \times 10^{-5} \text{ mol dm}^{-3}$ ); b) Dependence of **21b** absorbance at  $\lambda = 400 \text{ nm}$  on  $c(\text{ctDNA})$ , at  $\text{pH} = 7$ , sodium cacodylate buffer,  $l = 0.05 \text{ mol dm}^{-3}$ .

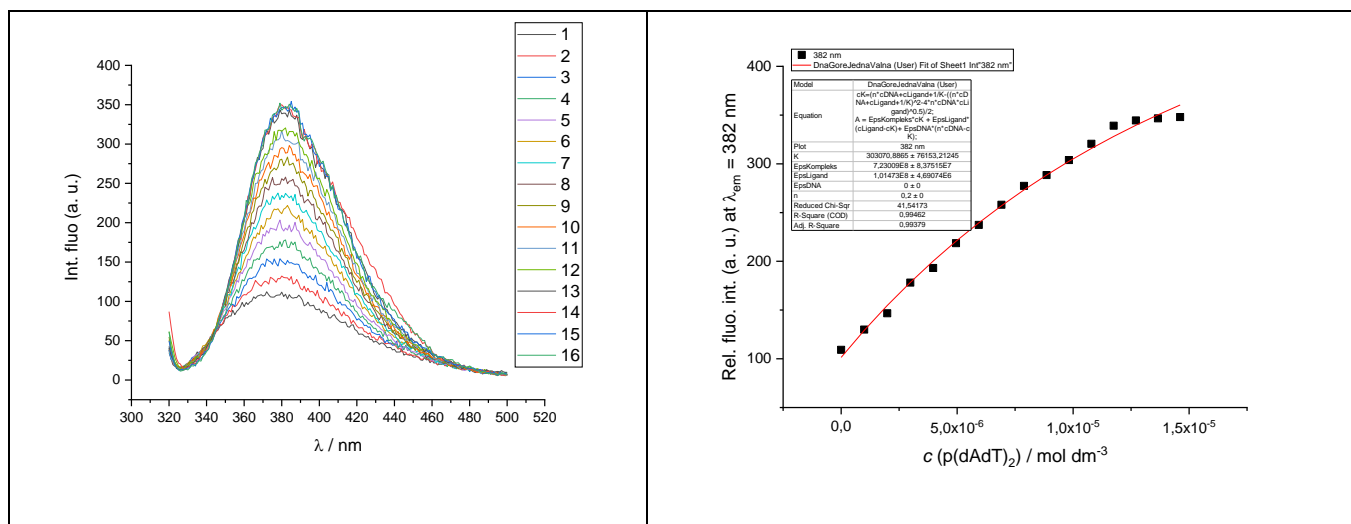


Figure S17. a) Changes in fluorescence spectrum of **15a** ( $c = 1 \times 10^{-6} \text{ mol dm}^{-3}$ ,  $\lambda_{\text{exc}} = 312 \text{ nm}$ ) upon titration with  $\text{p(dAdT)}_2$  ( $c = 1.0 \times 10^{-6} - 1.5 \times 10^{-5} \text{ mol dm}^{-3}$ ); b) Dependence of **15a** absorbance at  $\lambda = 382 \text{ nm}$  on  $c(\text{p(dAdT)}_2)$ , at pH=7, sodium cacodylate buffer,  $l = 0.05 \text{ mol dm}^{-3}$ .

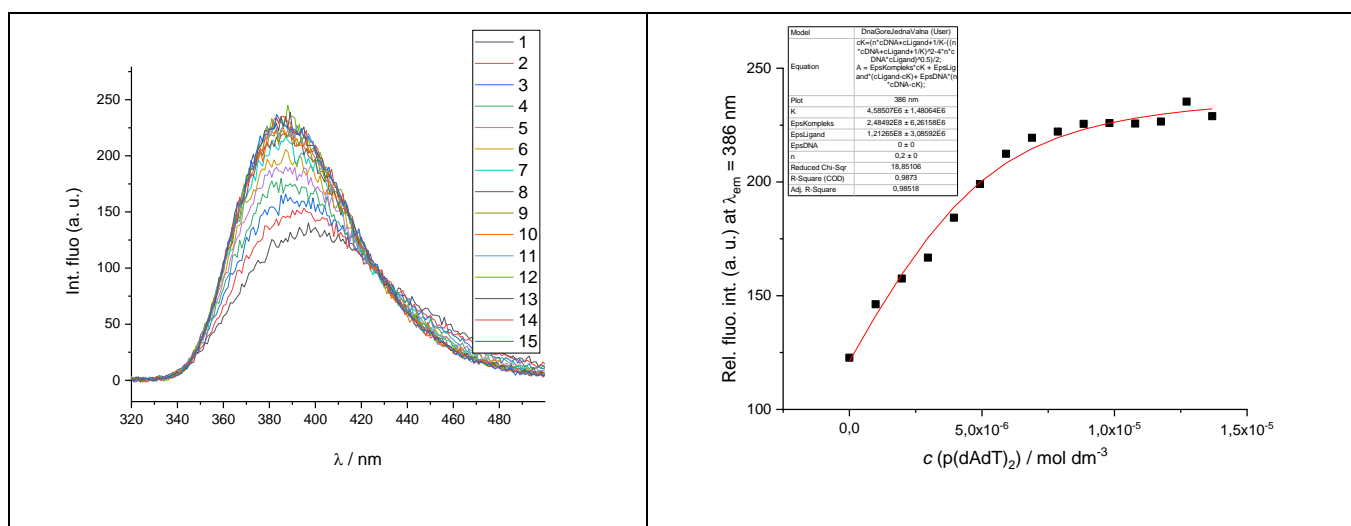


Figure S18. a) Changes in fluorescence spectrum of **17a** ( $c = 1 \times 10^{-6} \text{ mol dm}^{-3}$ ,  $\lambda_{\text{exc}} = 312 \text{ nm}$ ) upon titration with  $\text{p(dAdT)}_2$  ( $c = 1.0 \times 10^{-6} - 1.4 \times 10^{-5} \text{ mol dm}^{-3}$ ); b) Dependence of **17a** absorbance at  $\lambda = 386 \text{ nm}$  on  $c(\text{p(dAdT)}_2)$ , at pH=7, sodium cacodylate buffer,  $l = 0.05 \text{ mol dm}^{-3}$ .

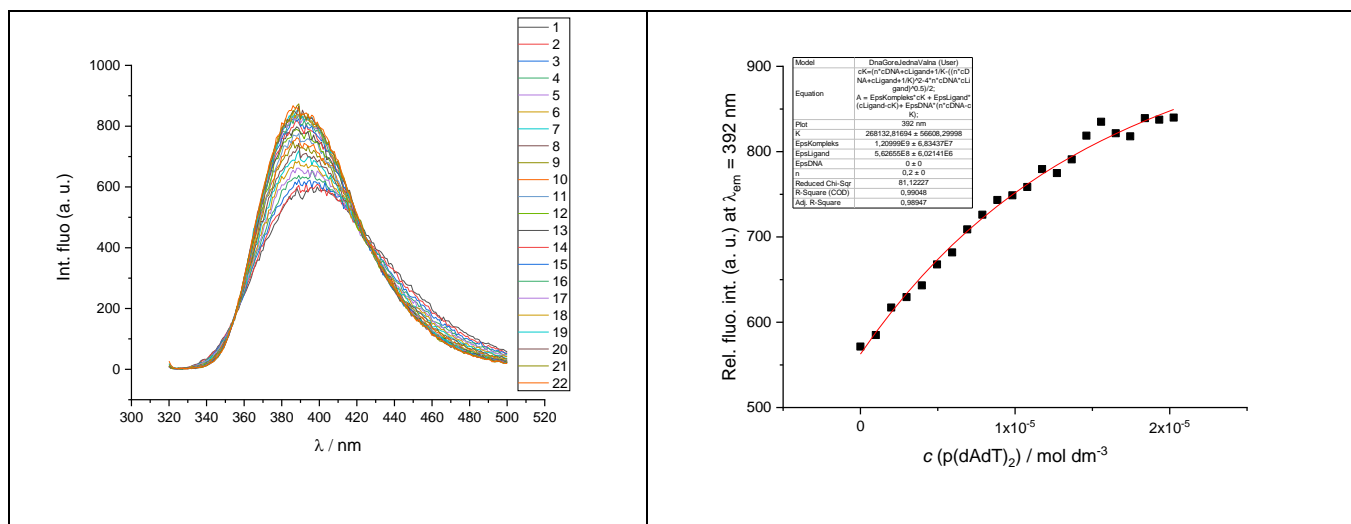


Figure S19. a) Changes in fluorescence spectrum of **16a** ( $c = 1 \times 10^{-6} \text{ mol dm}^{-3}$ ,  $\lambda_{exc} = 313 \text{ nm}$ ) upon titration with  $p(dAdT)_2$  ( $c = 1.0 \times 10^{-6} - 2.0 \times 10^{-5} \text{ mol dm}^{-3}$ ); b) Dependence of **16a** absorbance at  $\lambda = 392 \text{ nm}$  on  $c(p(dAdT)_2)$ , at pH=7, sodium cacodylate buffer,  $l = 0.05 \text{ mol dm}^{-3}$ .

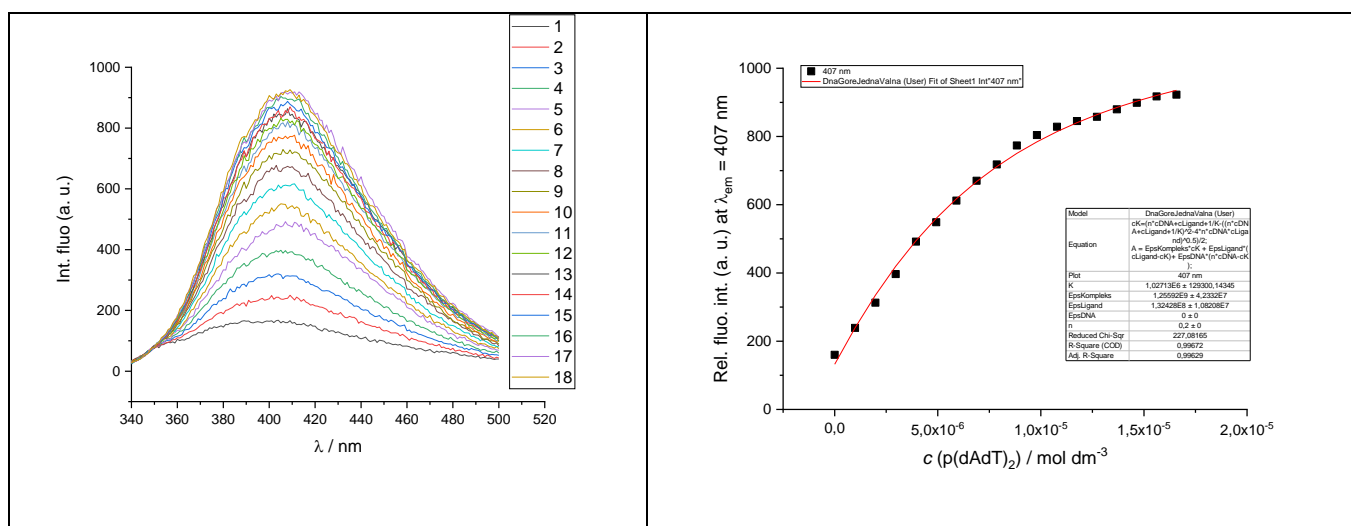


Figure S20. a) Changes in fluorescence spectrum of **15c** ( $c = 1 \times 10^{-6} \text{ mol dm}^{-3}$ ,  $\lambda_{exc} = 317 \text{ nm}$ ) upon titration with  $p(dAdT)_2$  ( $c = 1.0 \times 10^{-6} - 1.7 \times 10^{-5} \text{ mol dm}^{-3}$ ); b) Dependence of **15c** absorbance at  $\lambda = 407 \text{ nm}$  on  $c(p(dAdT)_2)$ , at pH=7, sodium cacodylate buffer,  $l = 0.05 \text{ mol dm}^{-3}$ .

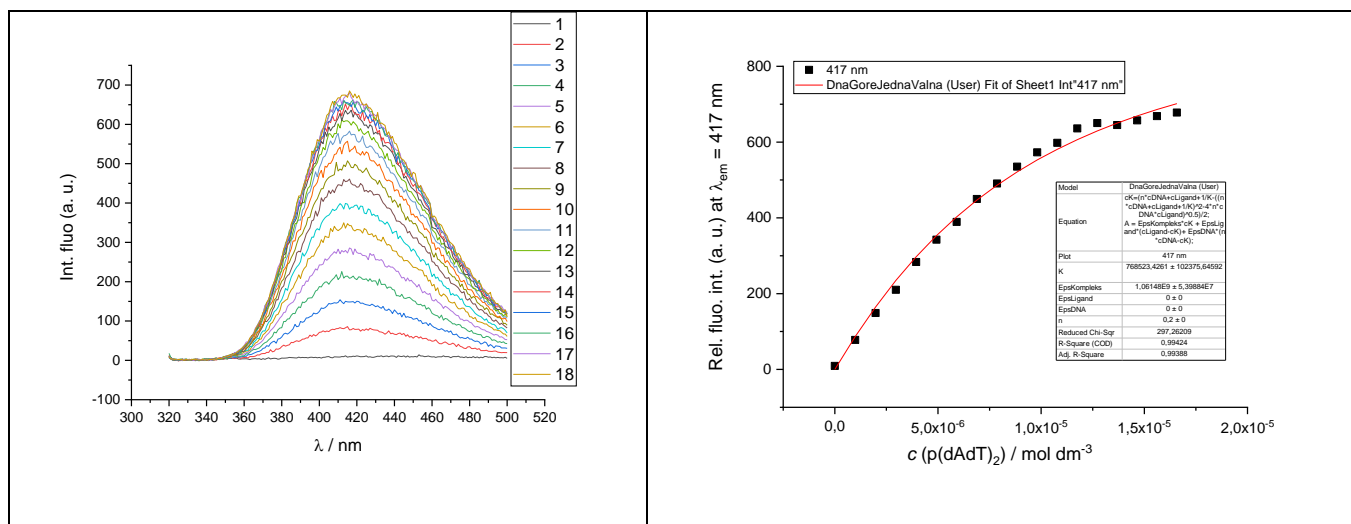


Figure S21. a) Changes in fluorescence spectrum of **16c** ( $c = 1 \times 10^{-6} \text{ mol dm}^{-3}$ ,  $\lambda_{\text{exc}} = 317 \text{ nm}$ ) upon titration with  $p(\text{dAdT})_2$  ( $c = 1.0 \times 10^{-6} - 1.7 \times 10^{-5} \text{ mol dm}^{-3}$ ); b) Dependence of **16c** absorbance at  $\lambda = 417 \text{ nm}$  on  $c(p(\text{dAdT})_2)$ , at pH=7, sodium cacodylate buffer,  $l = 0.05 \text{ mol dm}^{-3}$ .

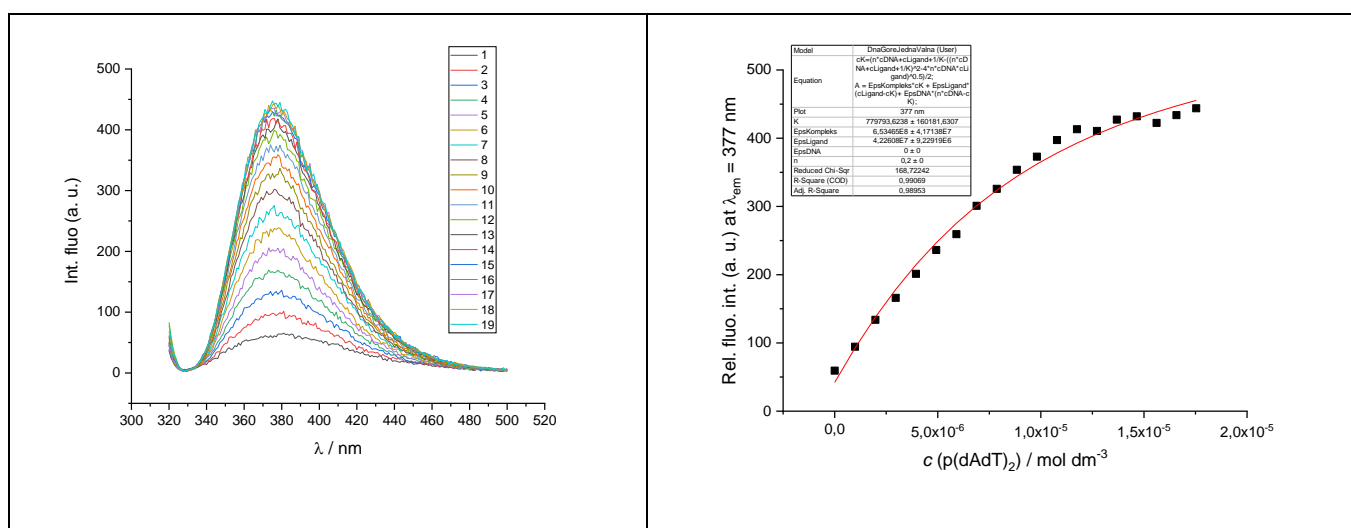


Figure S22. a) Changes in fluorescence spectrum of **15b** ( $c = 1 \times 10^{-6} \text{ mol dm}^{-3}$ ,  $\lambda_{\text{exc}} = 312 \text{ nm}$ ) upon titration with  $p(\text{dAdT})_2$  ( $c = 1.0 \times 10^{-6} - 1.7 \times 10^{-5} \text{ mol dm}^{-3}$ ); b) Dependence of **15b** absorbance at  $\lambda = 377 \text{ nm}$  on  $c(p(\text{dAdT})_2)$ , at pH=7, sodium cacodylate buffer,  $l = 0.05 \text{ mol dm}^{-3}$ .

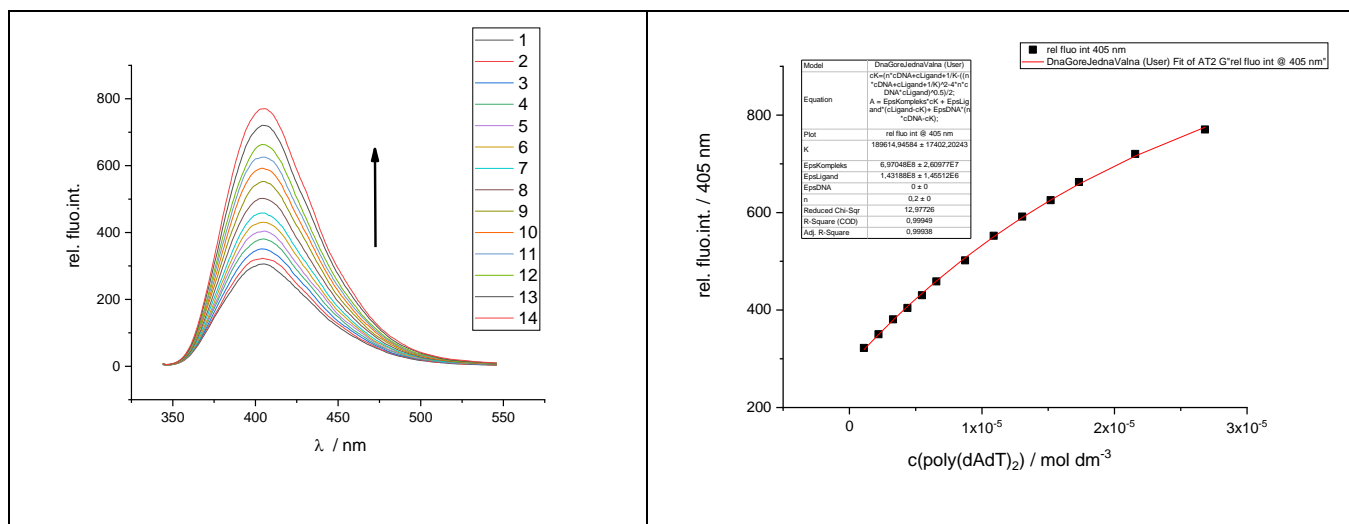


Figure S23. a) Changes in fluorescence spectrum of **21a** ( $c = 2 \times 10^{-6} \text{ mol dm}^{-3}$ ,  $\lambda_{\text{exc}} = 324 \text{ nm}$ ) upon titration with  $p(\text{dAdT})_2$  ( $c = 2.5 \times 10^{-6} - 8.5 \times 10^{-5} \text{ mol dm}^{-3}$ ); b) Dependence of **21a** absorbance at  $\lambda = 405 \text{ nm}$  on  $c(p(\text{dAdT})_2)$ , at  $\text{pH} = 7$ , sodium cacodylate buffer,  $l = 0.05 \text{ mol dm}^{-3}$ .

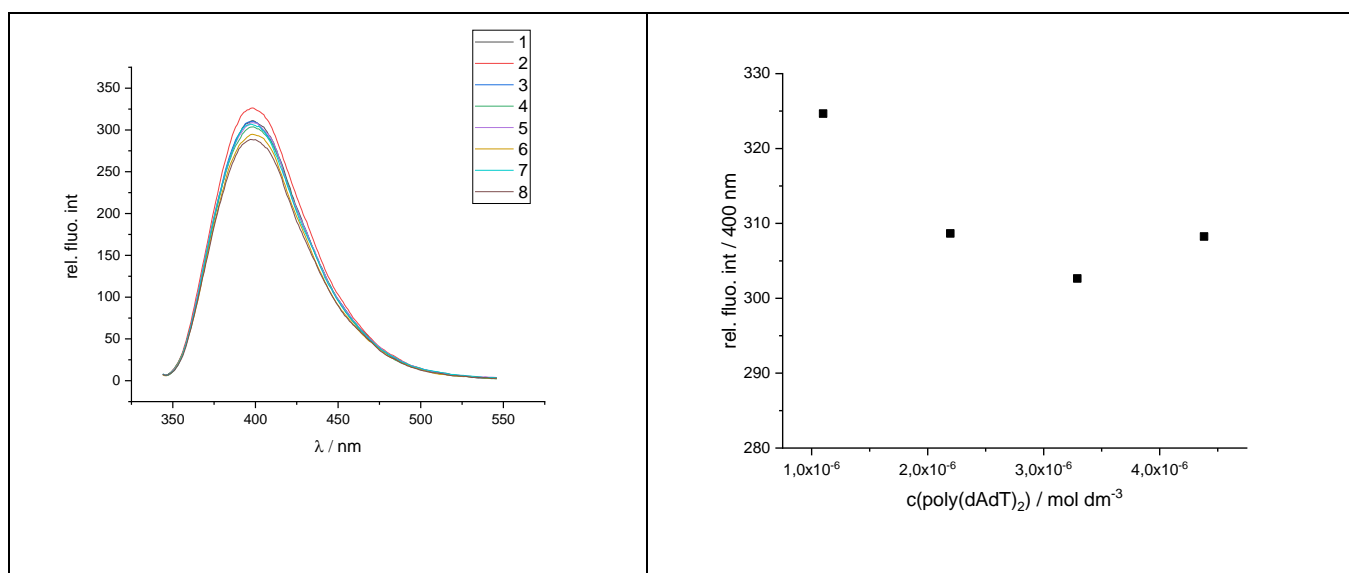


Figure S24. a) Changes in fluorescence spectrum of **21b** ( $c = 2 \times 10^{-6} \text{ mol dm}^{-3}$ ,  $\lambda_{\text{exc}} = 321 \text{ nm}$ ) upon titration with  $p(\text{dAdT})_2$  ( $c = 2.1 \times 10^{-6} - 4.4 \times 10^{-6} \text{ mol dm}^{-3}$ ); b) Dependence of **21b** absorbance at  $\lambda = 400 \text{ nm}$  on  $c(p(\text{dAdT})_2)$ , at  $\text{pH} = 7$ , sodium cacodylate buffer,  $l = 0.05 \text{ mol dm}^{-3}$ .

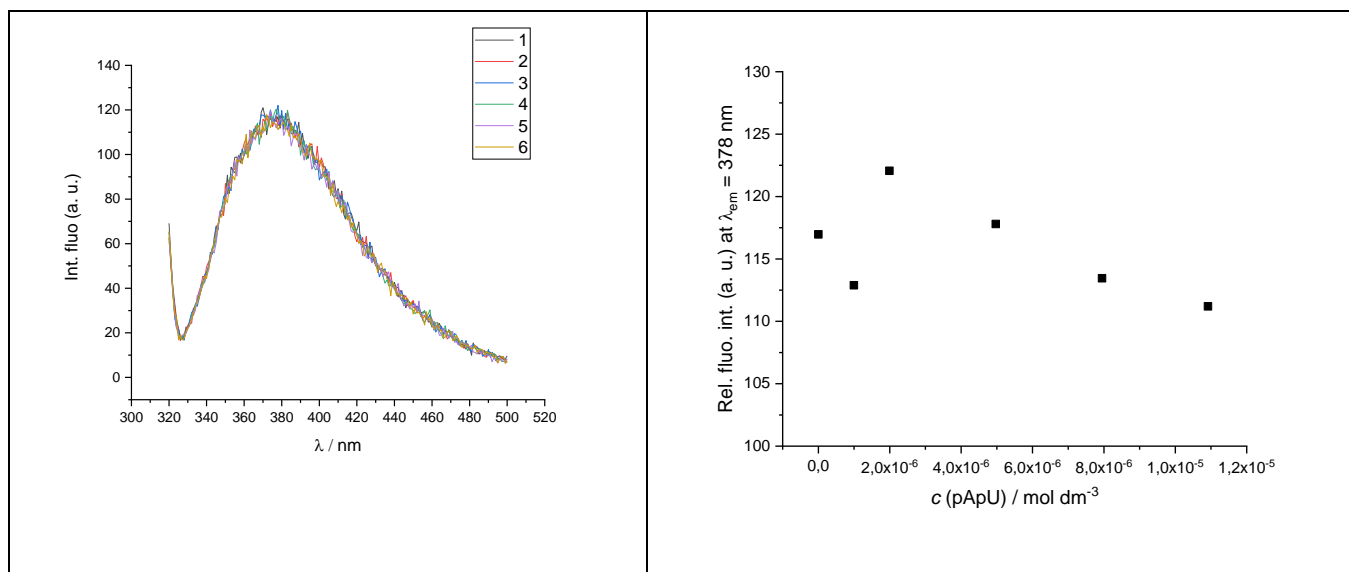


Figure S25. a) Changes in fluorescence spectrum of **15a** ( $c = 1 \times 10^{-6} \text{ mol dm}^{-3}$ ,  $\lambda_{\text{exc}} = 312 \text{ nm}$ ) upon titration with poly A-poly U ( $c = 1.0 \times 10^{-6} - 1.0 \times 10^{-5} \text{ mol dm}^{-3}$ ); b) Dependence of **15a** absorbance at  $\lambda = 378 \text{ nm}$  on  $c(\text{poly A-poly U})$ , at  $\text{pH} = 7$ , sodium cacodylate buffer,  $I = 0.05 \text{ mol dm}^{-3}$ .

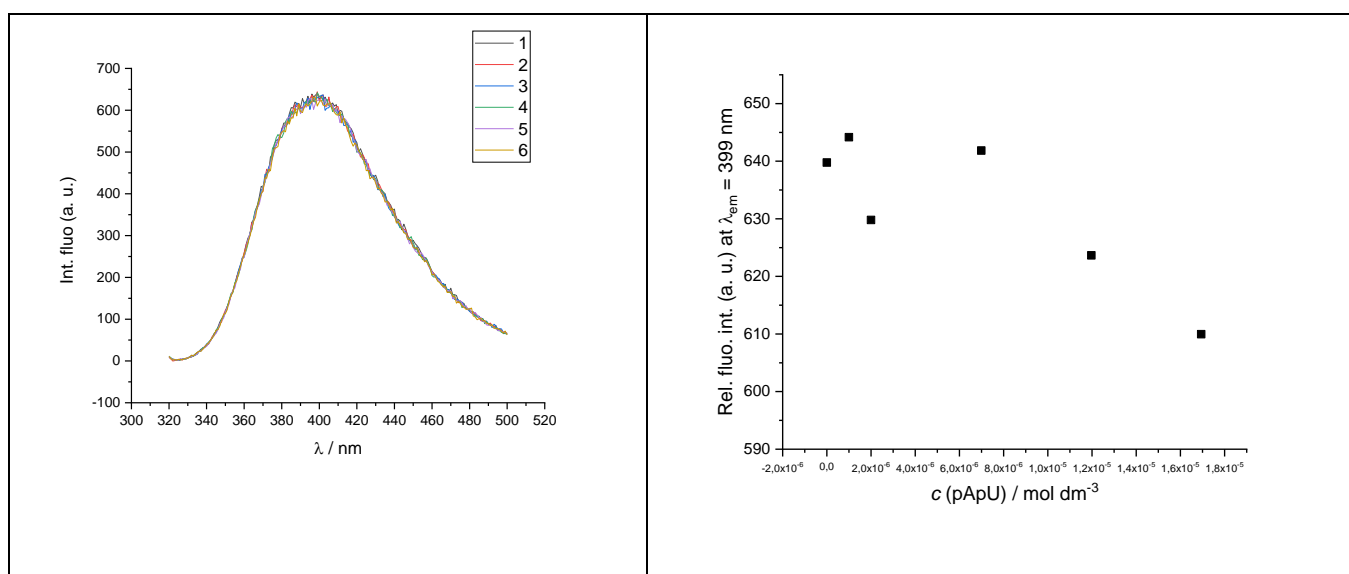


Figure S26. a) Changes in fluorescence spectrum of **17a** ( $c = 1 \times 10^{-6} \text{ mol dm}^{-3}$ ,  $\lambda_{\text{exc}} = 312 \text{ nm}$ ) upon titration with poly A-poly U ( $c = 1.0 \times 10^{-6} - 1.7 \times 10^{-5} \text{ mol dm}^{-3}$ ); b) Dependence of **17a** absorbance at  $\lambda = 399 \text{ nm}$  on  $c(\text{poly A-poly U})$ , at  $\text{pH} = 7$ , sodium cacodylate buffer,  $I = 0.05 \text{ mol dm}^{-3}$ .

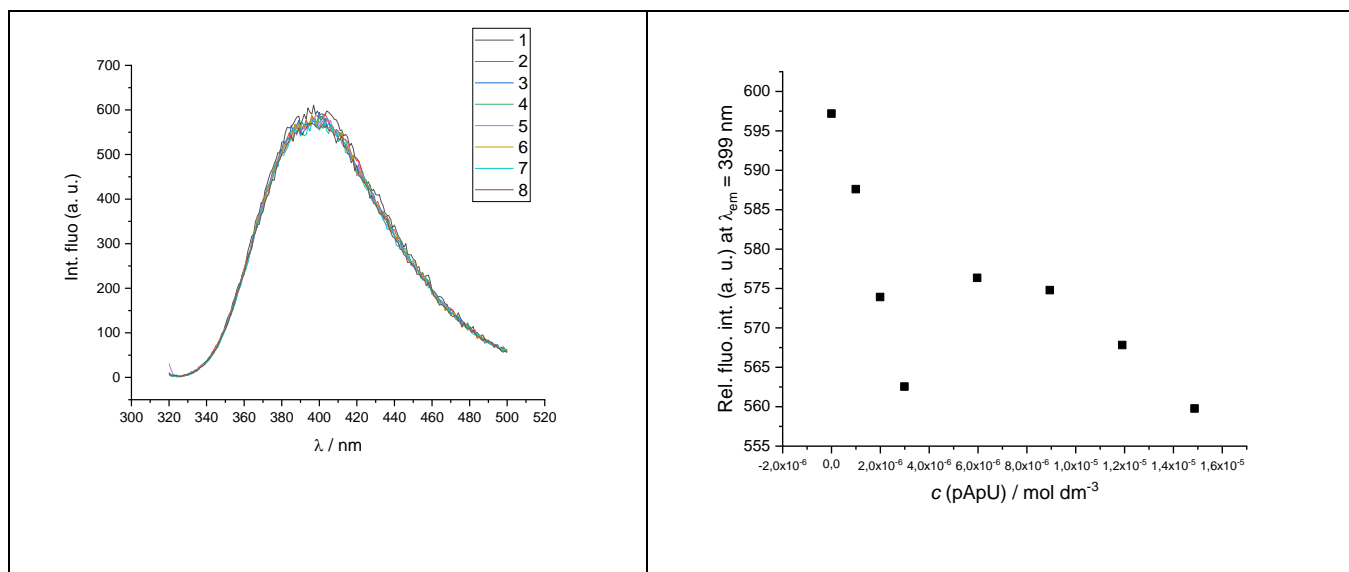


Figure S27. a) Changes in fluorescence spectrum of **16a** ( $c = 1 \times 10^{-6} \text{ mol dm}^{-3}$ ,  $\lambda_{\text{exc}} = 313 \text{ nm}$ ) upon titration with poly A-poly U ( $c = 1.0 \times 10^{-6} - 1.5 \times 10^{-5} \text{ mol dm}^{-3}$ ); b) Dependence of **16a** absorbance at  $\lambda = 399 \text{ nm}$  on  $c$  (poly A-poly U), at pH=7, sodium cacodylate buffer,  $I = 0.05 \text{ mol dm}^{-3}$ .

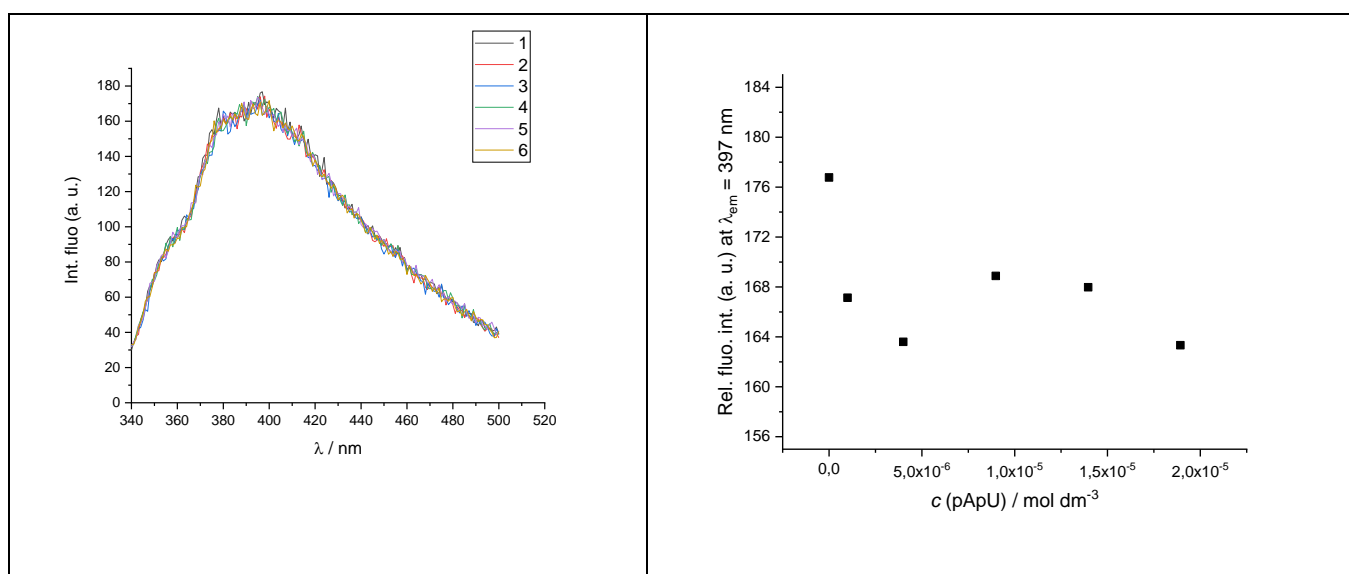


Figure S28. a) Changes in fluorescence spectrum of **15c** ( $c = 1 \times 10^{-6} \text{ mol dm}^{-3}$ ,  $\lambda_{\text{exc}} = 317 \text{ nm}$ ) upon titration with poly A-poly U ( $c = 1.0 \times 10^{-6} - 1.9 \times 10^{-5} \text{ mol dm}^{-3}$ ); b) Dependence of **15c** absorbance at  $\lambda = 397 \text{ nm}$  on  $c$  (poly A-poly U), at pH=7, sodium cacodylate buffer,  $I = 0.05 \text{ mol dm}^{-3}$ .



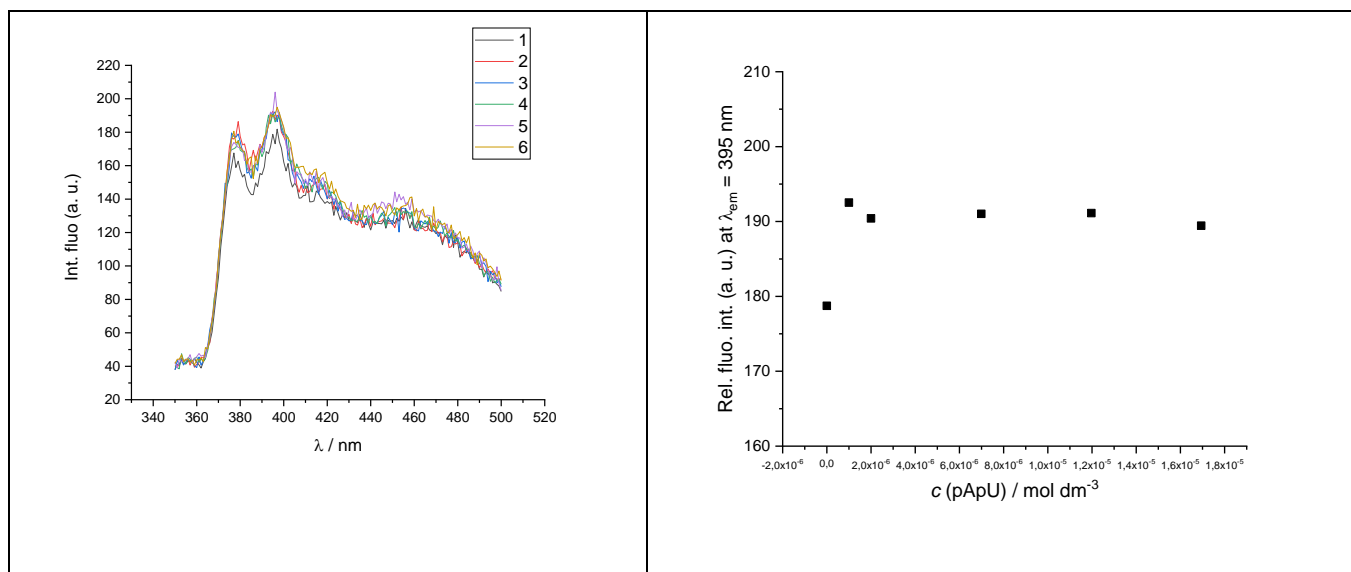


Figure S29. a) Changes in fluorescence spectrum of **16c** ( $c = 1 \times 10^{-6}$  mol dm<sup>-3</sup>,  $\lambda_{exc} = 317$  nm) upon titration with poly A-poly U ( $c = 1.0 \times 10^{-6} - 1.7 \times 10^{-5}$  mol dm<sup>-3</sup>); b) Dependence of **16c** absorbance at  $\lambda = 395$  nm on  $c$ (poly A-poly U), at pH=7, sodium cacodylate buffer,  $l = 0.05$  mol dm<sup>-3</sup>.

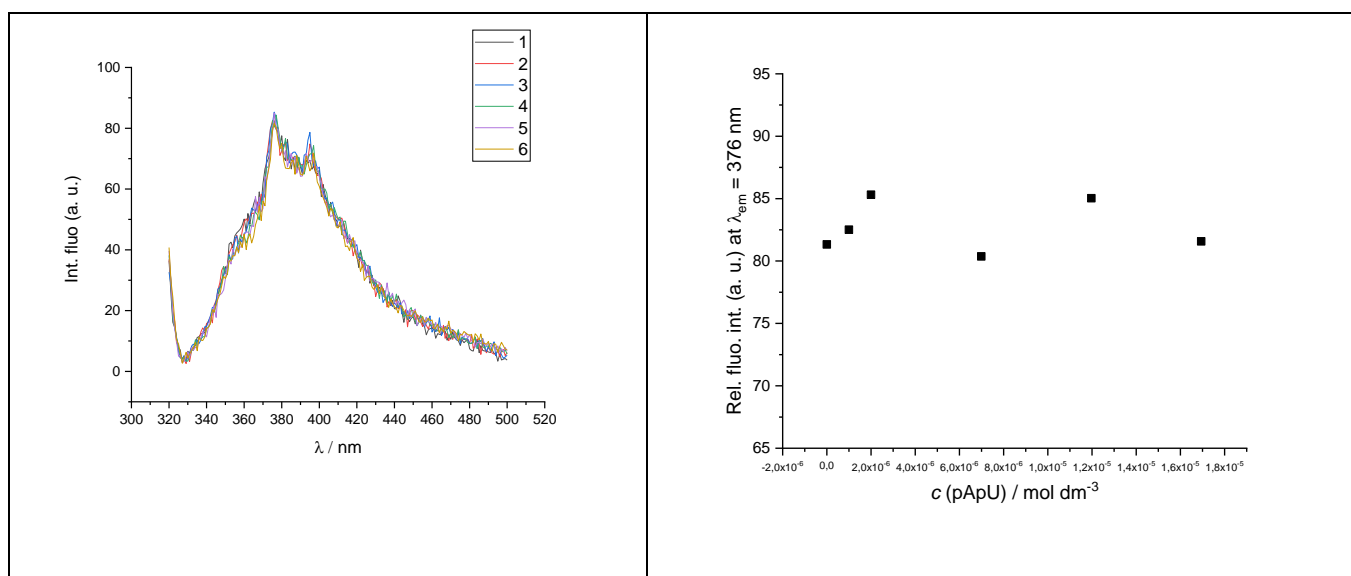


Figure S30. a) Changes in fluorescence spectrum of **15b** ( $c = 1 \times 10^{-6}$  mol dm<sup>-3</sup>,  $\lambda_{exc} = 312$  nm) upon titration with poly A-poly U ( $c = 1.0 \times 10^{-6} - 1.7 \times 10^{-5}$  mol dm<sup>-3</sup>); b) Dependence of **15b** absorbance at  $\lambda = 376$  nm on  $c$ (poly A-poly U), at pH=7, sodium cacodylate buffer,  $l = 0.05$  mol dm<sup>-3</sup>.

### 3.2. Thermal melting experiments

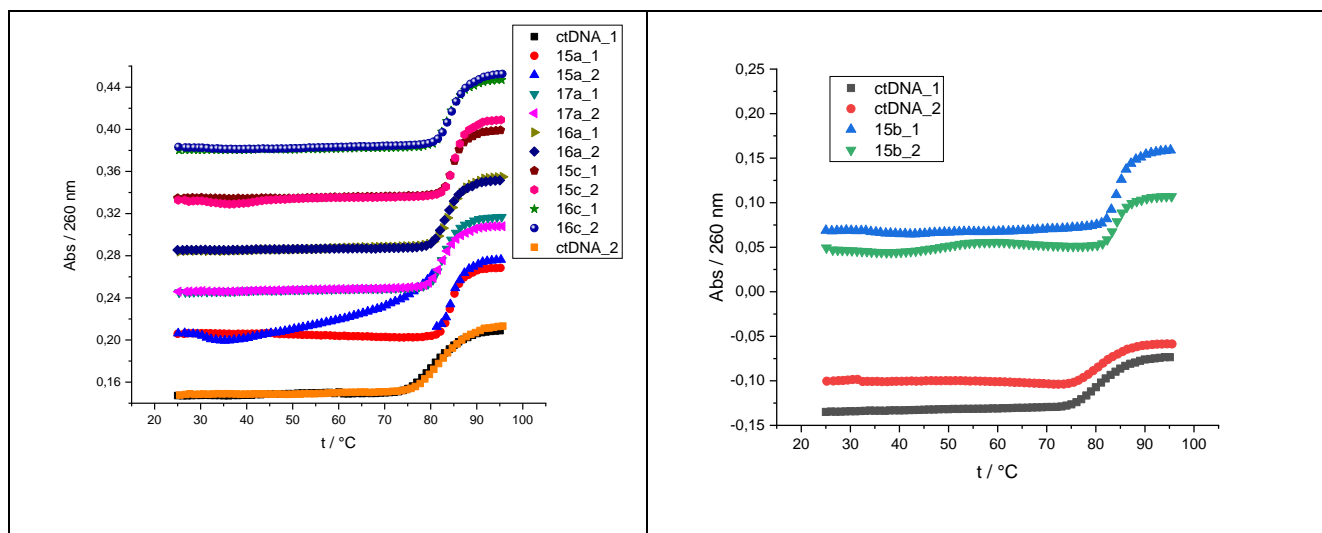


Figure S31. Melting curve of ctDNA upon addition of ratio,  $r$  ( [compound/ [polynucleotide]])=0.3 of **15a-c, 16a, 16c, 17a, 21a** and **21b** at pH = 7.0 (buffer sodium cacodylate,  $I = 0.05 \text{ mol dm}^{-3}$ ).

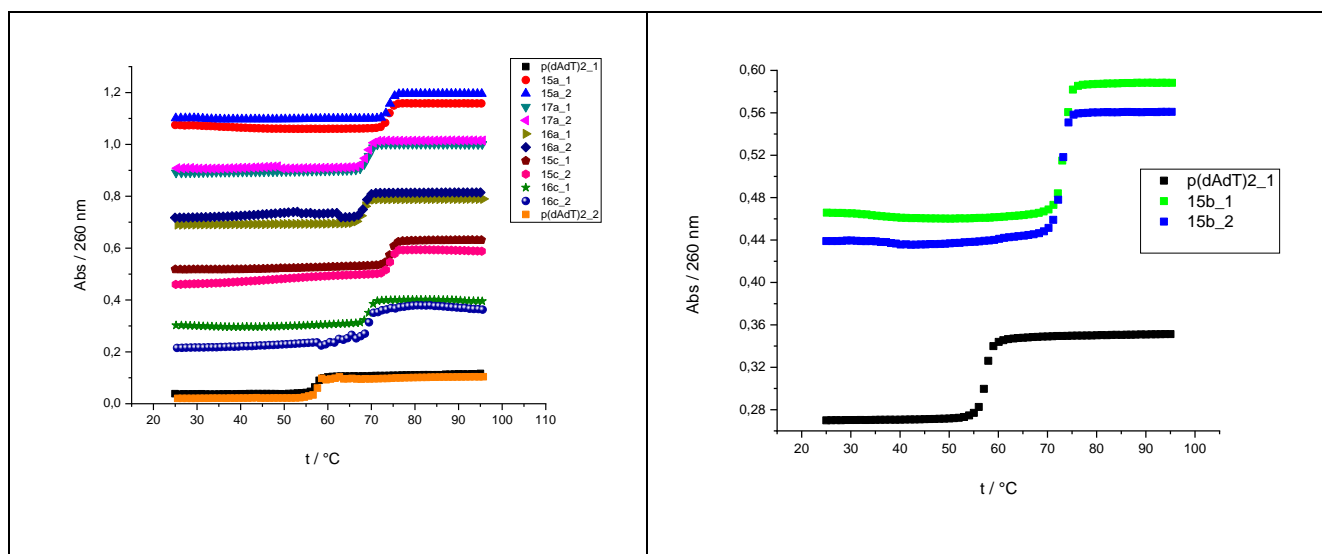


Figure S32. Melting curve of  $p(dAdT)_2$  upon addition of ratio,  $r$  ( [compound/ [polynucleotide]])=0.3 of **15a-c, 16a, 16c** and **17a** at pH = 7.0 (buffer sodium cacodylate,  $I = 0.05 \text{ mol dm}^{-3}$ ).

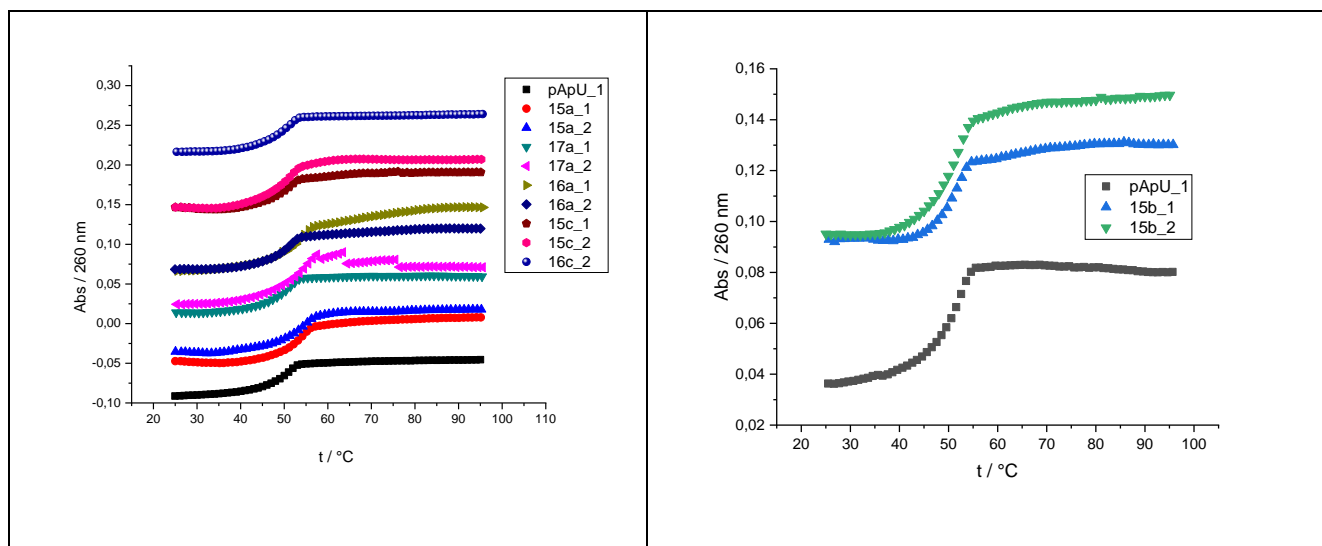


Figure S33. Melting curve of poly A – poly U upon addition of ratio,  $r$  ( [compound/ [polynucleotide] )=0.3 of **15a-c**, **16a**, **16c** and **17a** at pH = 7.0 (buffer sodium cacodylate,  $I = 0.05 \text{ mol dm}^{-3}$ ).

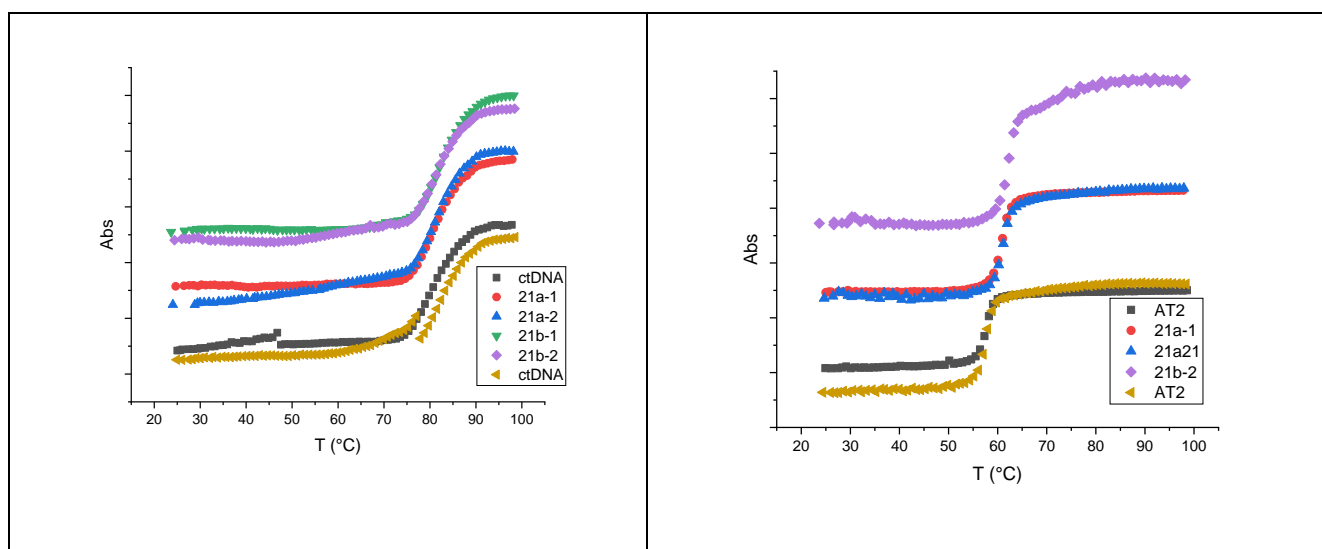
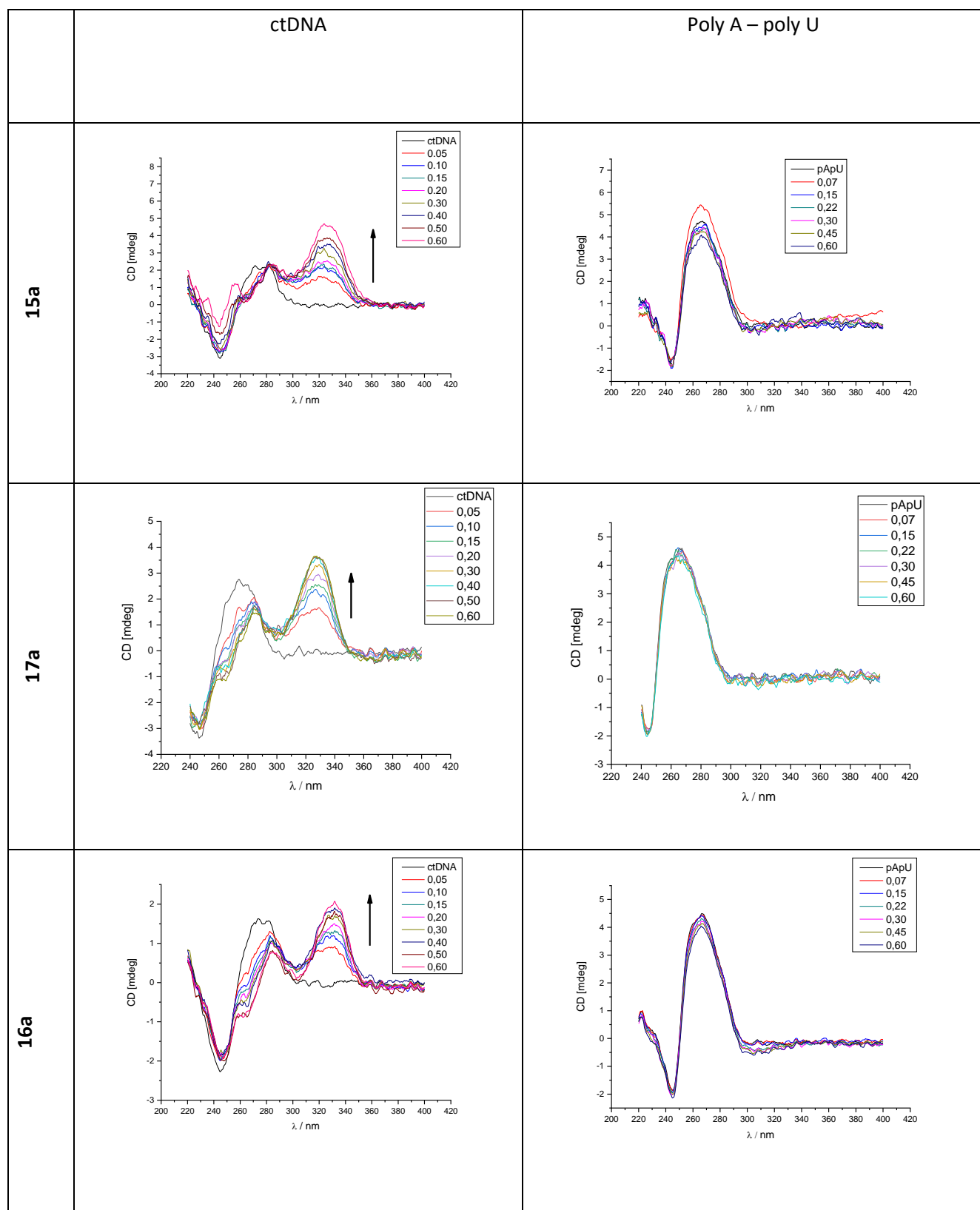
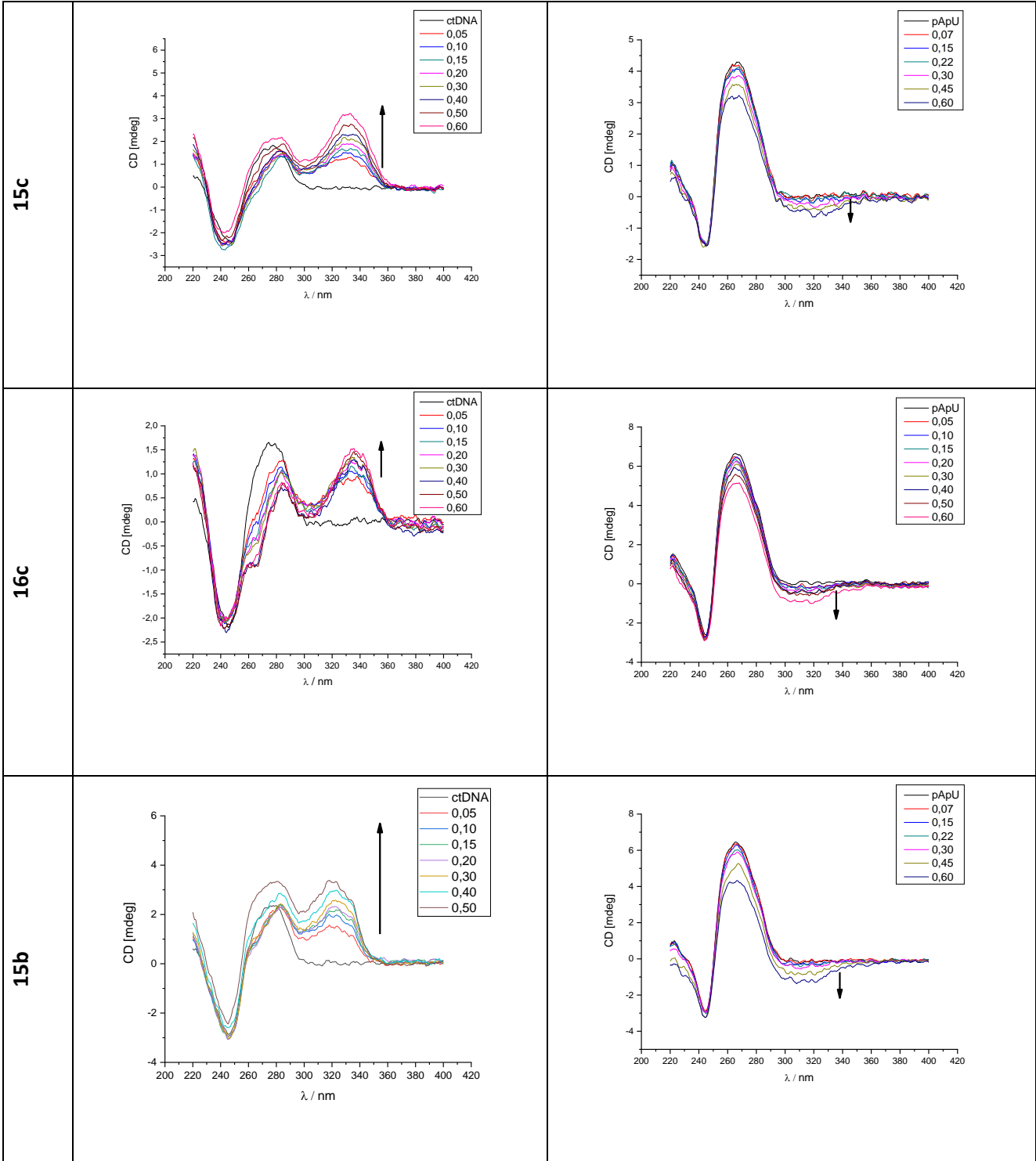


Figure S34. Melting curve of ctDNA and poly(dAdT)<sub>2</sub> upon addition of ratio,  $r$  ( [compound/ [polynucleotide] )=0.3 of **21a** and **21b** at pH = 7.0 (buffer sodium cacodylate,  $I = 0.05 \text{ mol dm}^{-3}$ ).

### 3.3. Circular dichroism (CD) titrations





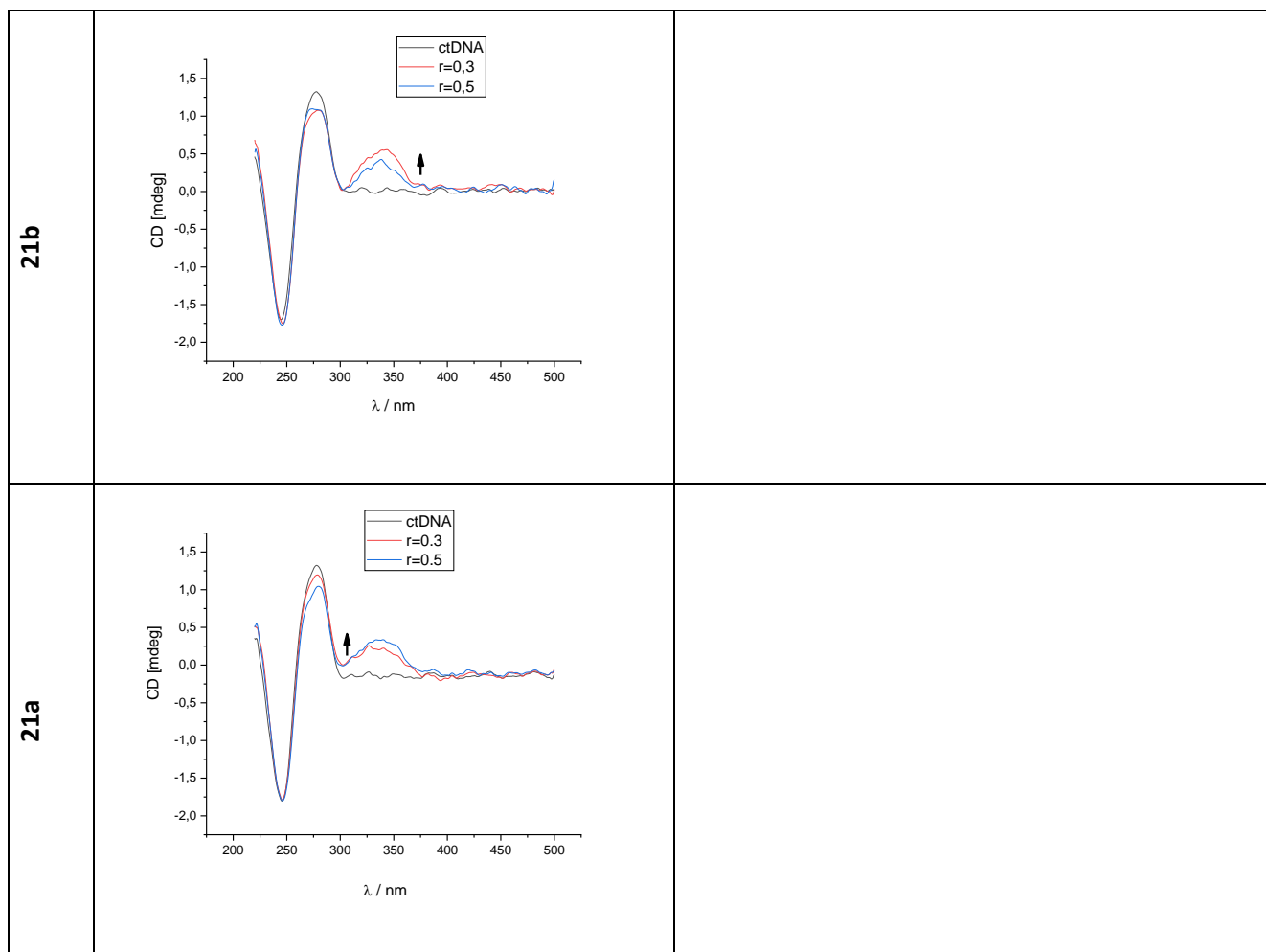
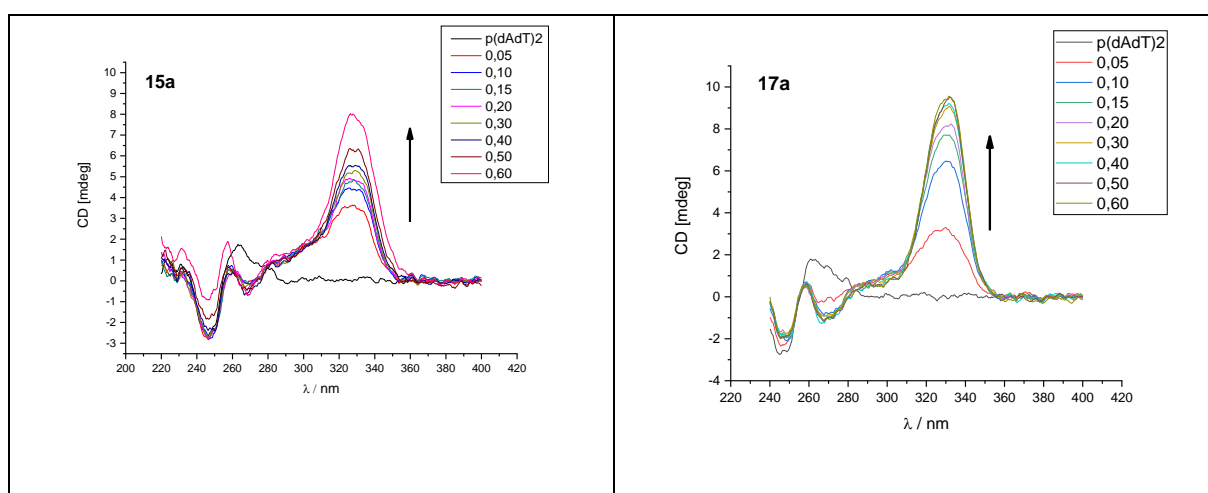


Figure S35. CD titration of ctDNA ( $c = 3.0 \times 10^{-5} \text{ mol dm}^{-3}$ ) and poly A-poly U ( $c = 3.0 \times 10^{-5} \text{ mol dm}^{-3}$ ) with **15a-c**, **16a**, **16c**, **17a**, **21a** and **21b** at molar ratios  $r = [\text{compound}] / [\text{polynucleotide}]$  (pH = 7.0, buffer sodium cacodylate,  $I = 0.05 \text{ mol dm}^{-3}$ ).



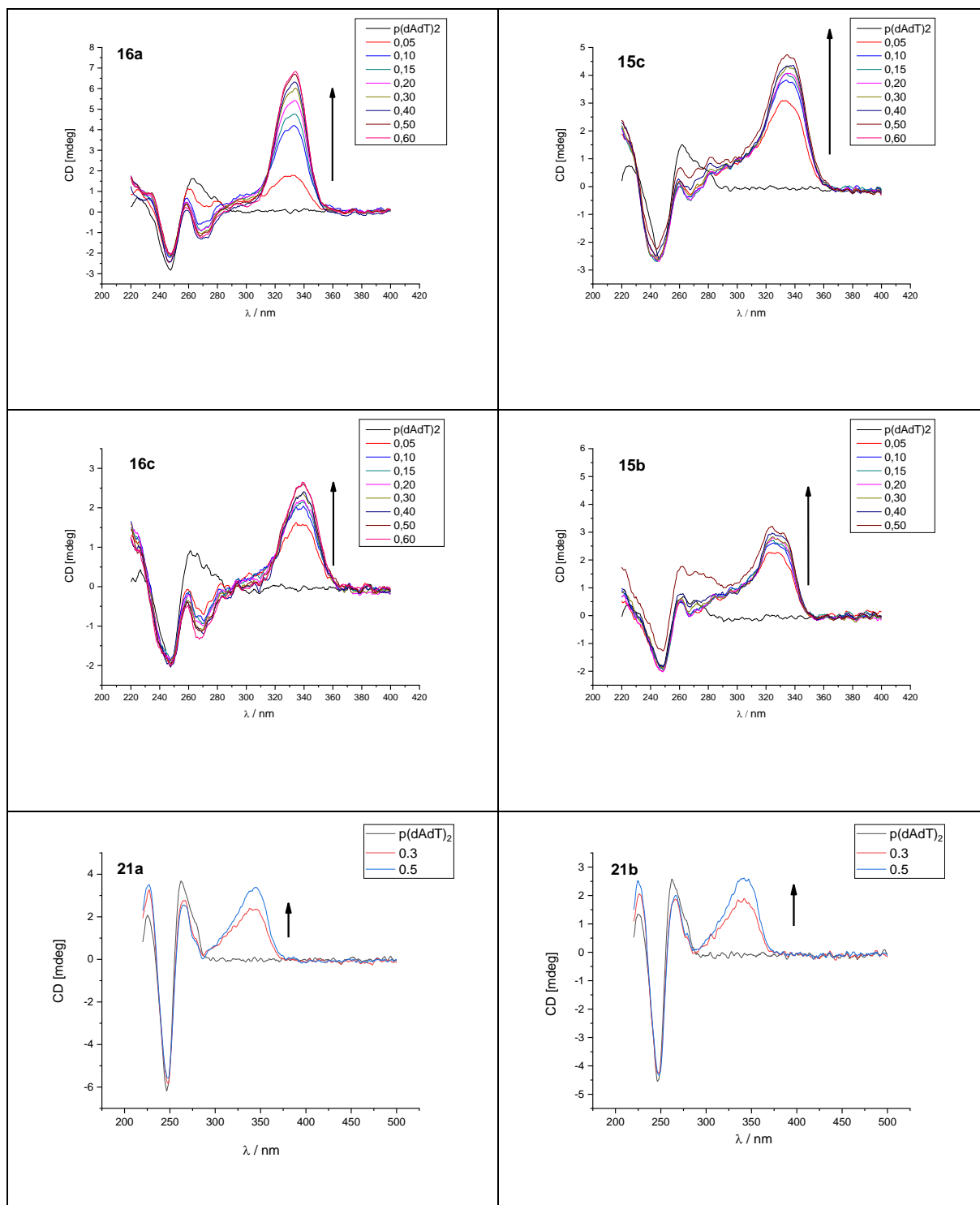
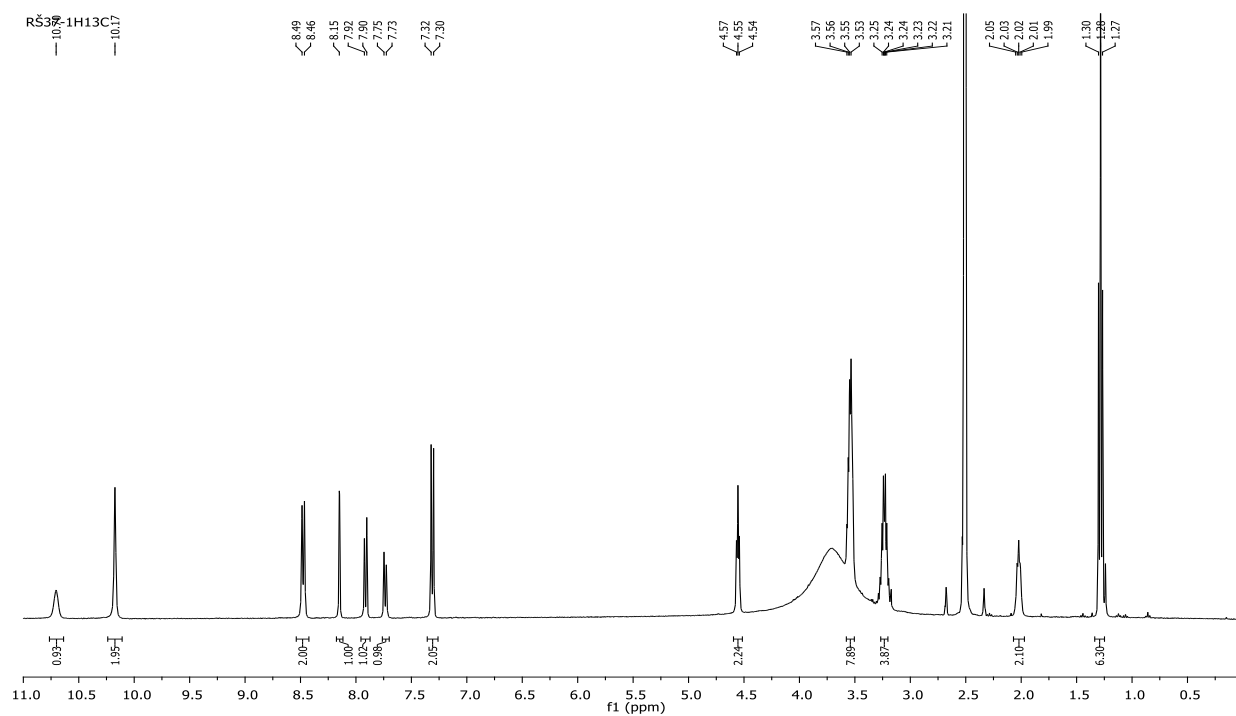
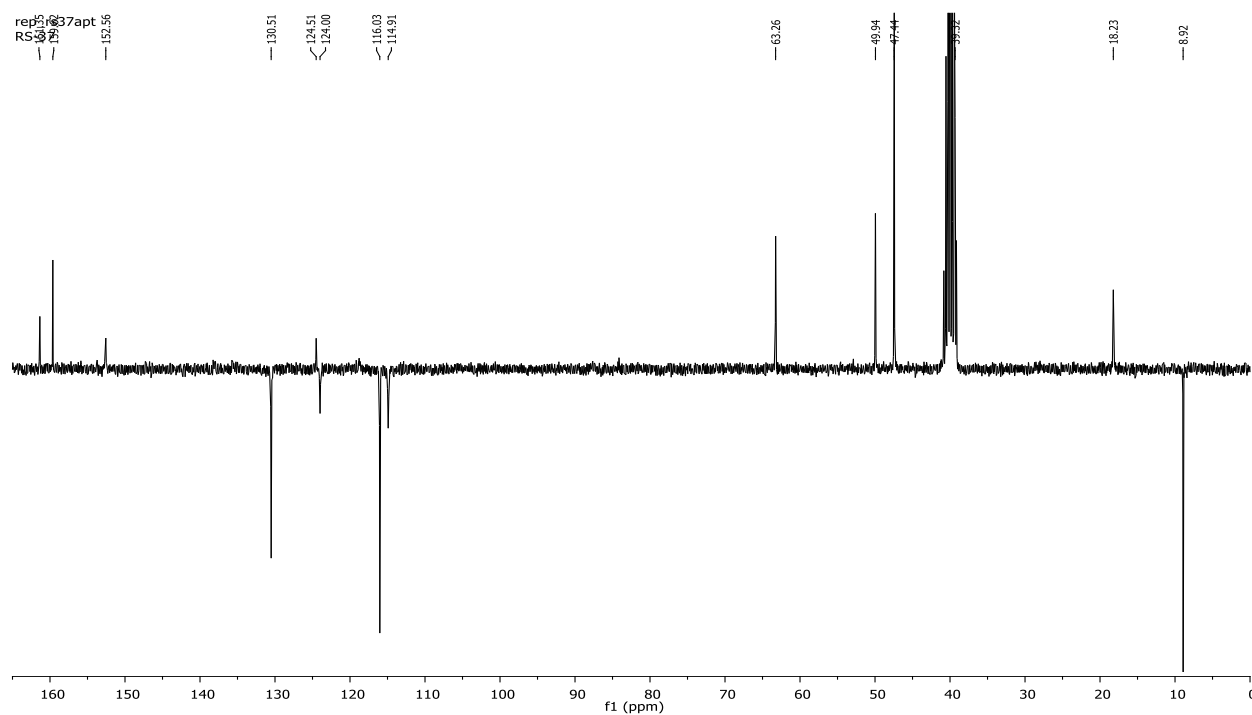


Figure S36. CD titration of poly(dAdT)<sub>2</sub> ( $c = 3.0 \times 10^{-5} \text{ mol dm}^{-3}$ ) with **15a-c**, **16a**, **16c**, **17a**, **21a** and **21b** at molar ratios  $r = [\text{compound}] / [\text{polynucleotide}]$  (pH = 7.0, buffer sodium cacodylate,  $I = 0.05 \text{ mol dm}^{-3}$ ).

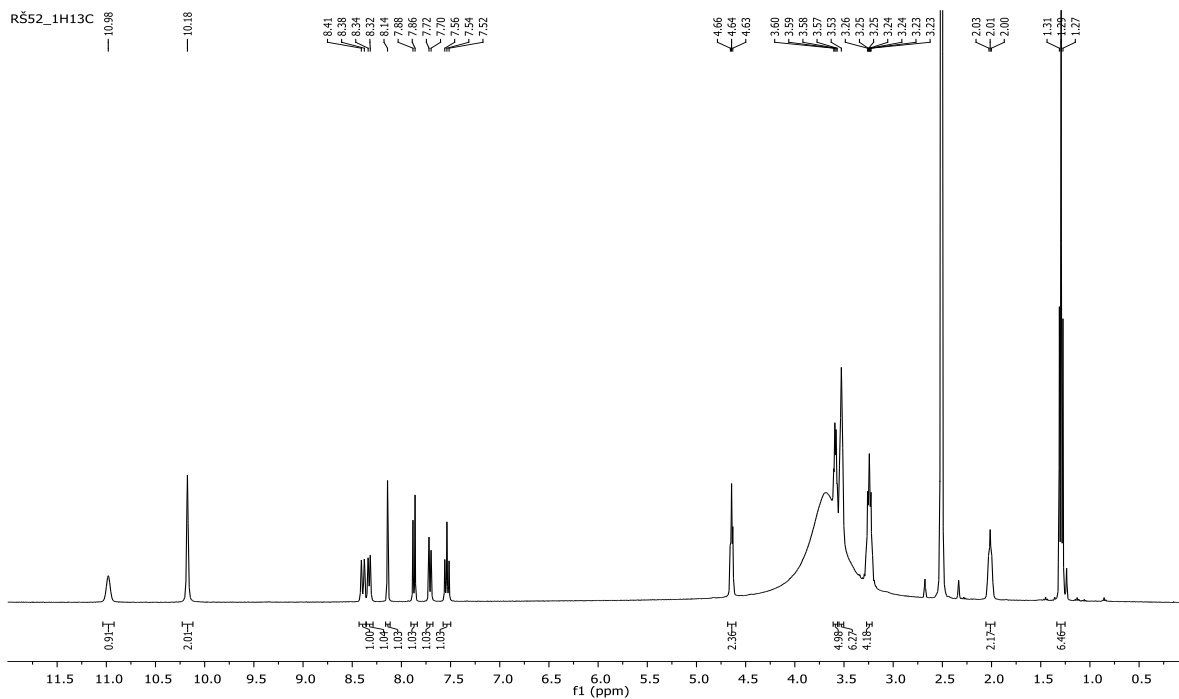


$^1\text{H}$  NMR (400 MHz, DMSO)  $\delta$  spectrum of 2-(4-(2-(Diethylamino)ethoxy)phenyl)-5(6)-(3,4,5,6-tetrahydropyrimidin-2-yl)-1H-benzimidazole dihydrochloride (**12a**)

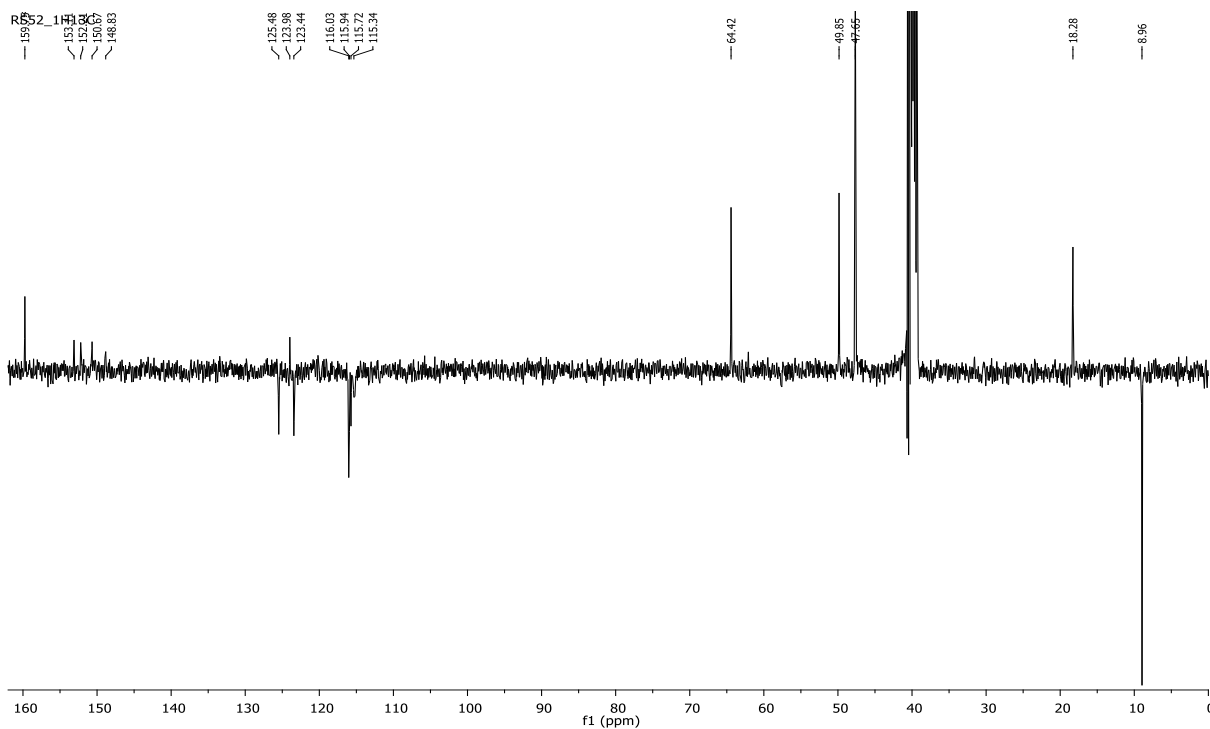


$^{13}\text{C}$  NMR (75 MHz, DMSO)  $\delta$  spectrum of 2-(4-(2-(Diethylamino)ethoxy)phenyl)-5(6)-(3,4,5,6-tetrahydropyrimidin-2-yl)-1H-benzimidazole dihydrochloride (**12a**)

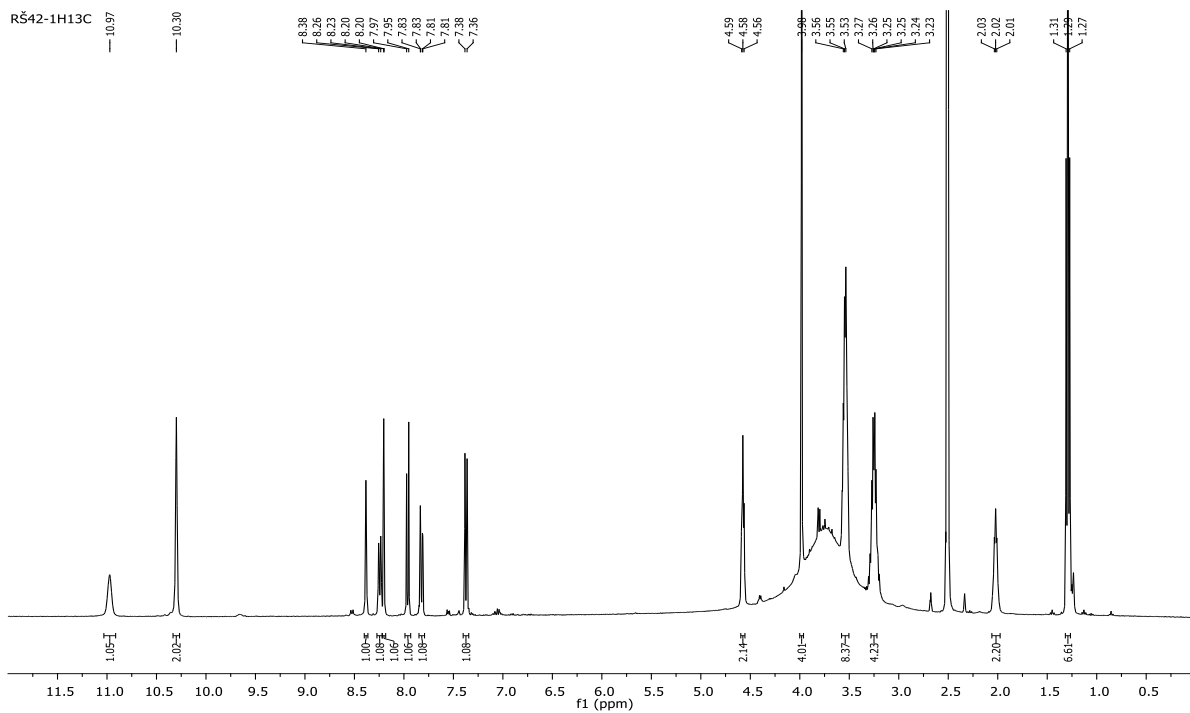




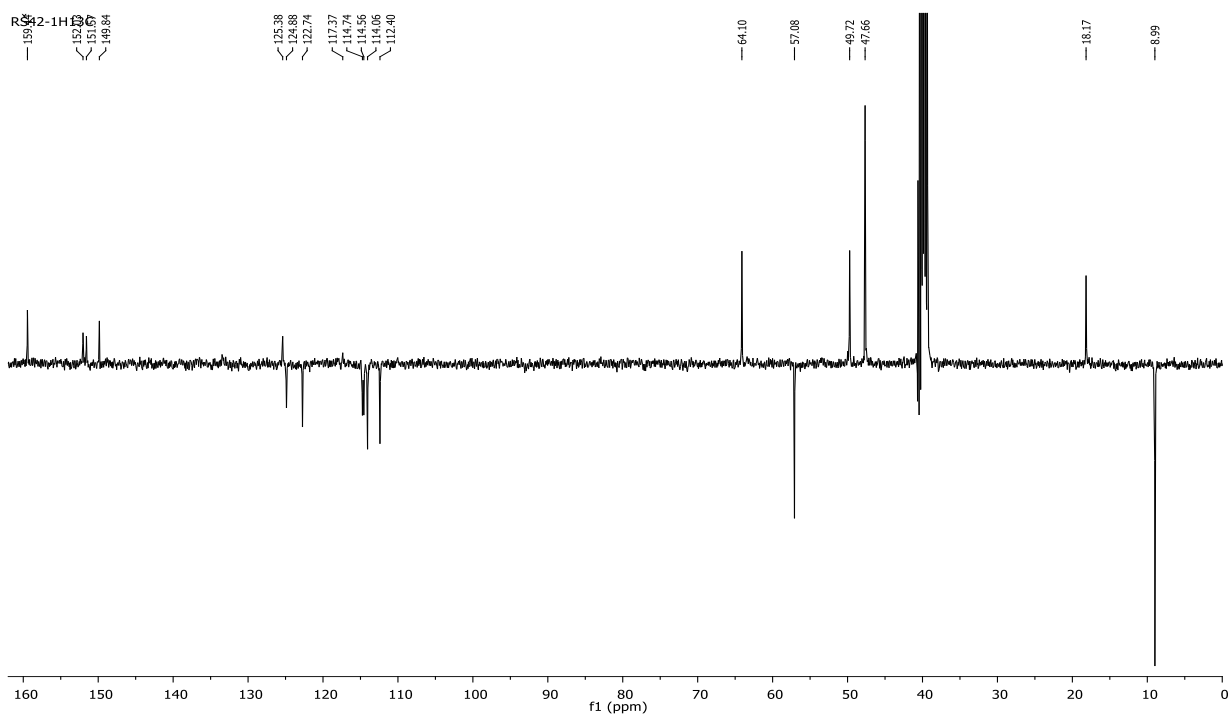
$^1\text{H}$  NMR (400 MHz, DMSO)  $\delta$  spectrum of 2-(4-(2-(Diethylamino)ethoxy)-3-fluorophenyl)-5(6)-(3,4,5,6-tetrahydropyrimidin-2-yl)-1H-benzimidazole dihydrochloride (**12b**)



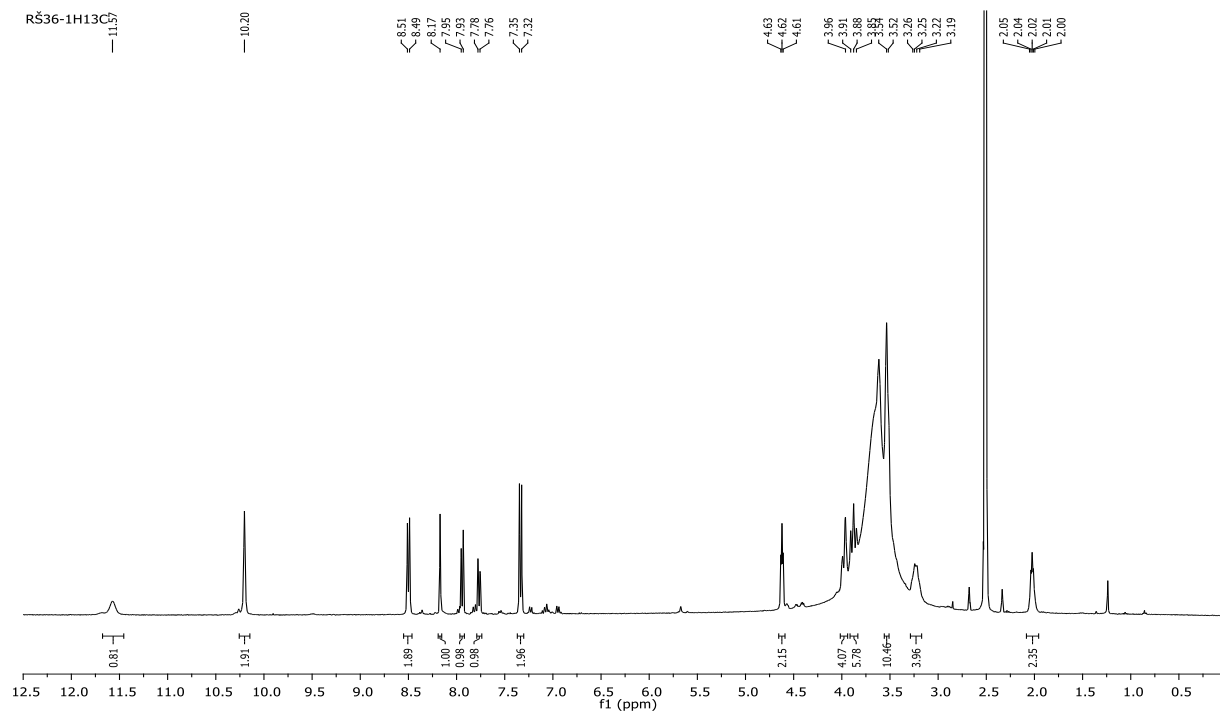
$^{13}\text{C}$  NMR (101 MHz, DMSO)  $\delta$  spectrum of 2-(4-(2-(Diethylamino)ethoxy)-3-fluorophenyl)-5(6)-(3,4,5,6-tetrahydropyrimidin-2-yl)-1H-benzimidazole dihydrochloride (**12b**)



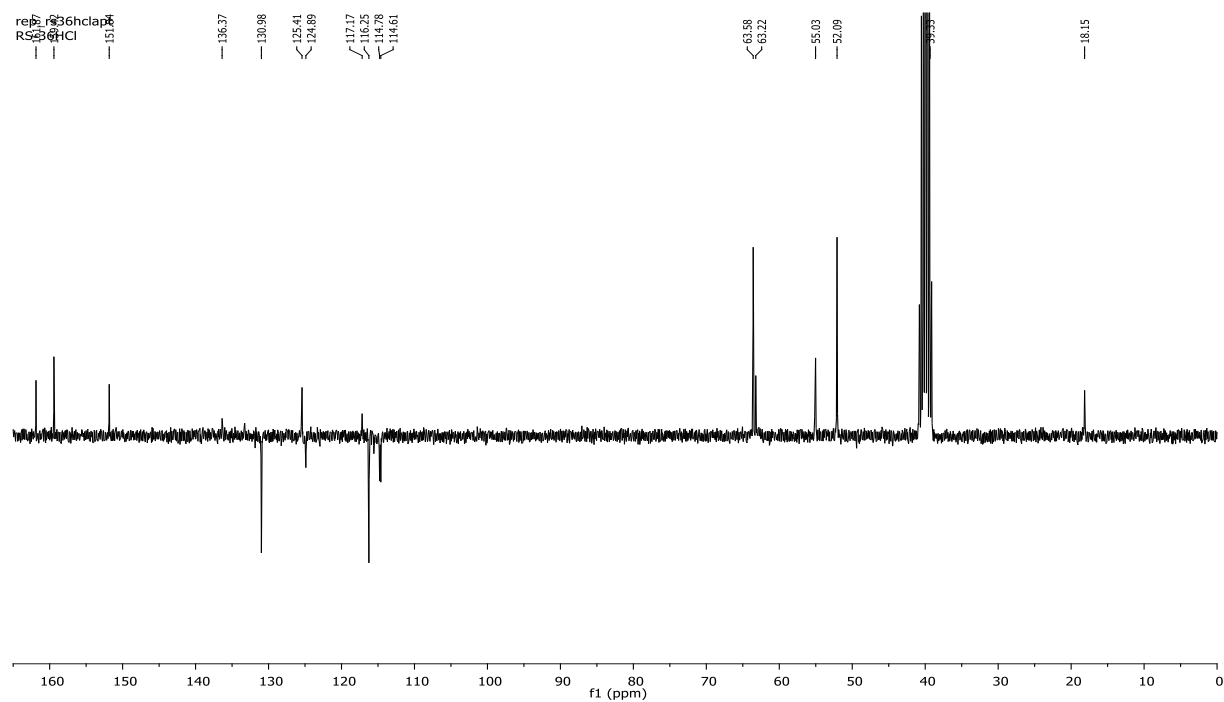
$^1\text{H}$  NMR (400 MHz, DMSO)  $\delta$  spectrum of 2-(4-(2-(Diethylamino)ethoxy)-3-methoxyphenyl)-5(6)-(3,4,5,6-tetrahydropyrimidin-2-yl)-1H-benzimidazole dihydrochloride (**12c**)



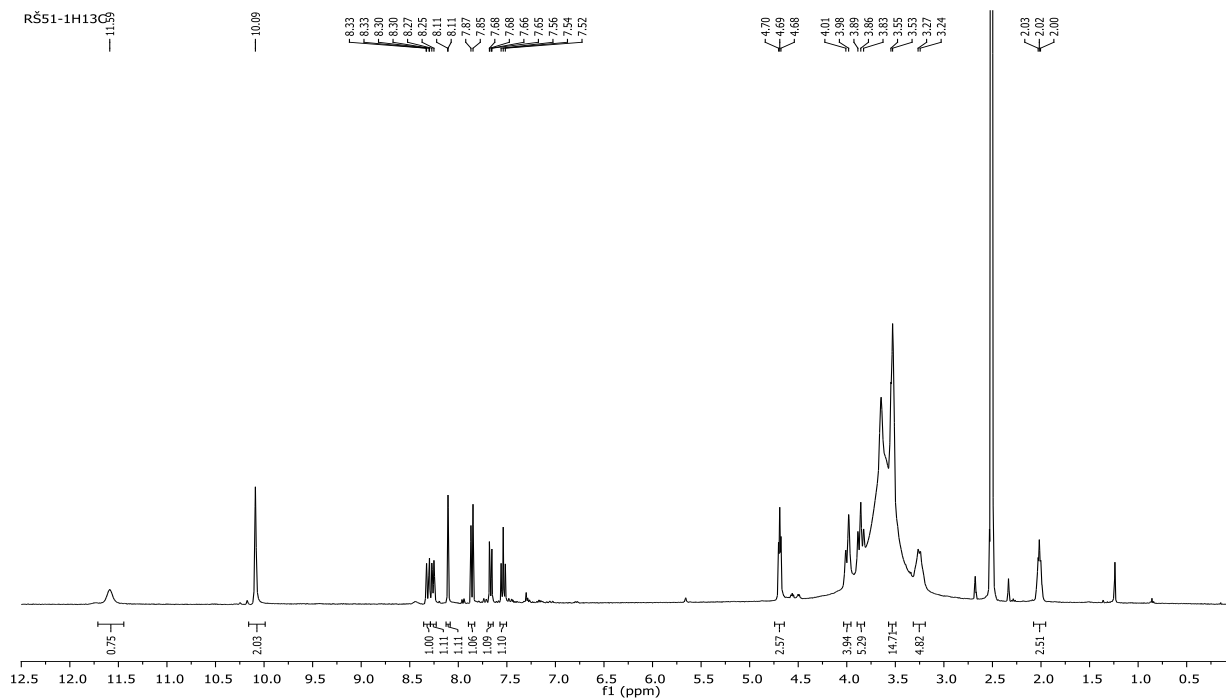
$^{13}\text{C}$  NMR (75 MHz, DMSO)  $\delta$  spectrum of 2-(4-(2-(Diethylamino)ethoxy)-3-methoxyphenyl)-5(6)-(3,4,5,6-tetrahydropyrimidin-2-yl)-1H-benzimidazole dihydrochloride (**12c**)



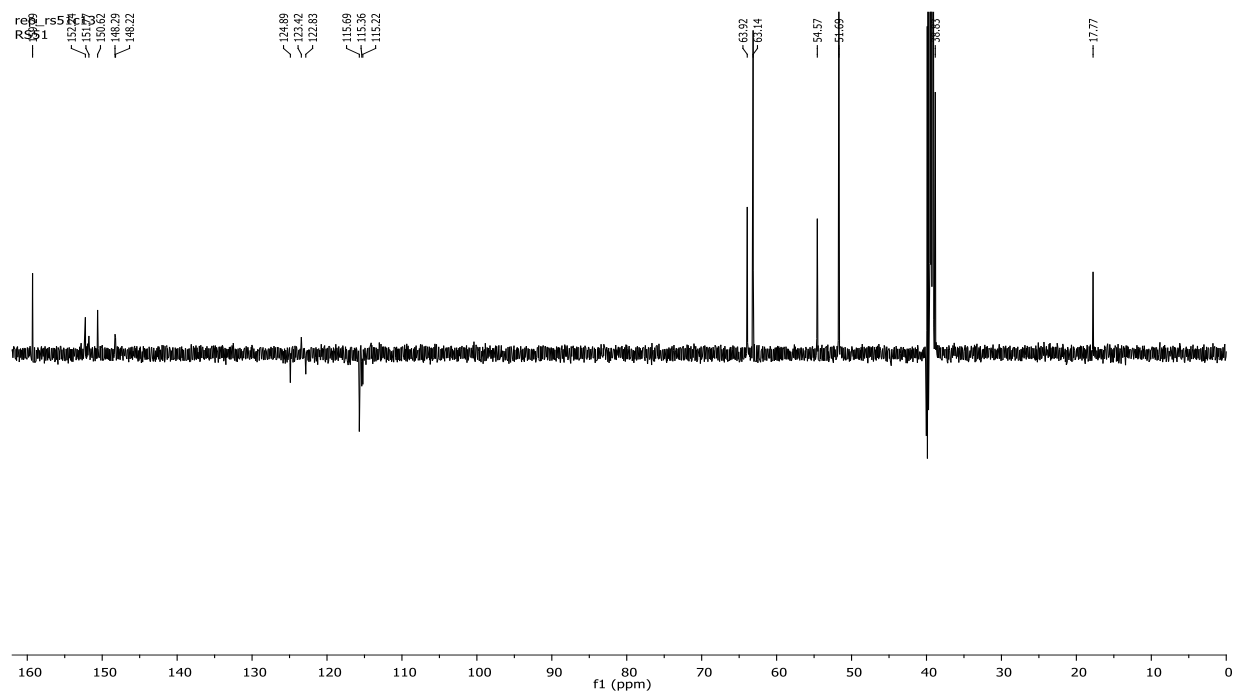
$^1\text{H}$  NMR (400 MHz, DMSO)  $\delta$  spectrum of 2-(4-(2-Morpholinoethoxy)phenyl)-5(6)-(3,4,5,6-tetrahydropyrimidin-2-yl)-1H-benzimidazole dihydrochloride (**13a**)



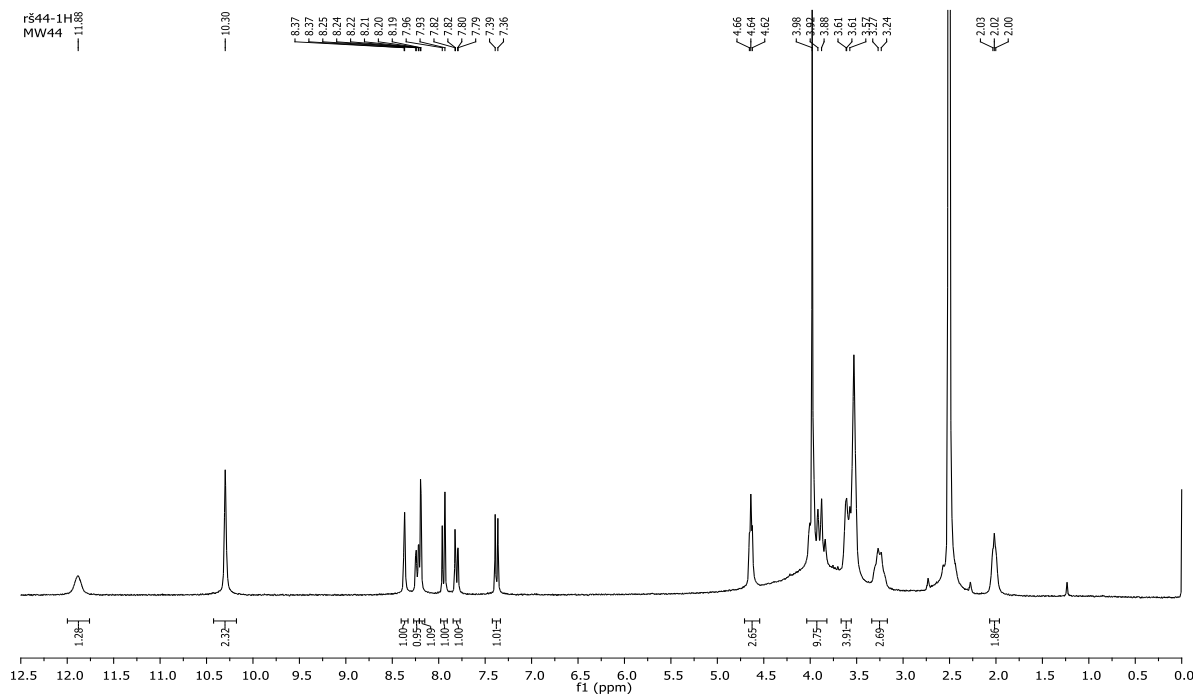
$^{13}\text{C}$  NMR (75 MHz, DMSO)  $\delta$  spectrum of 2-(4-(2-Morpholinoethoxy)phenyl)-5(6)-(3,4,5,6-tetrahydropyrimidin-2-yl)-1H-benzimidazole dihydrochloride (**13a**)



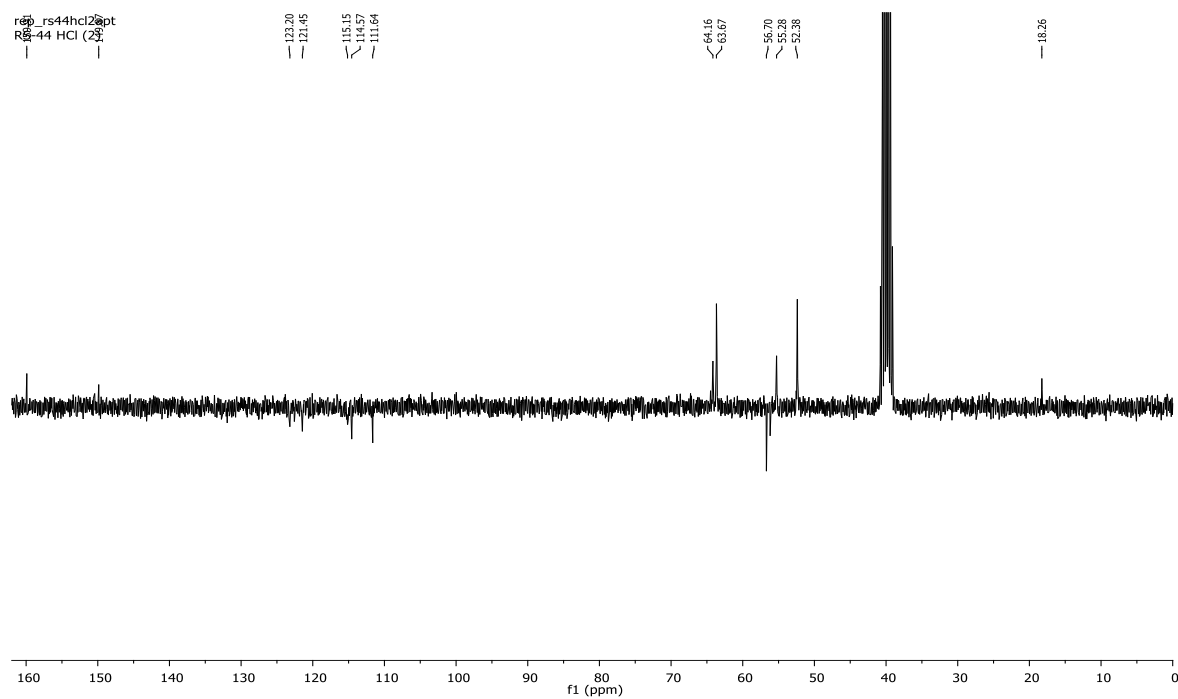
$^1\text{H}$  NMR (400 MHz, DMSO)  $\delta$  spectrum of 2-(3-Fluoro-4-(2-morpholinoethoxy)phenyl)-5(6)-(3,4,5,6-tetrahydropyrimidin-2-yl)-1H-benzimidazole dihydrochloride (**13b**)



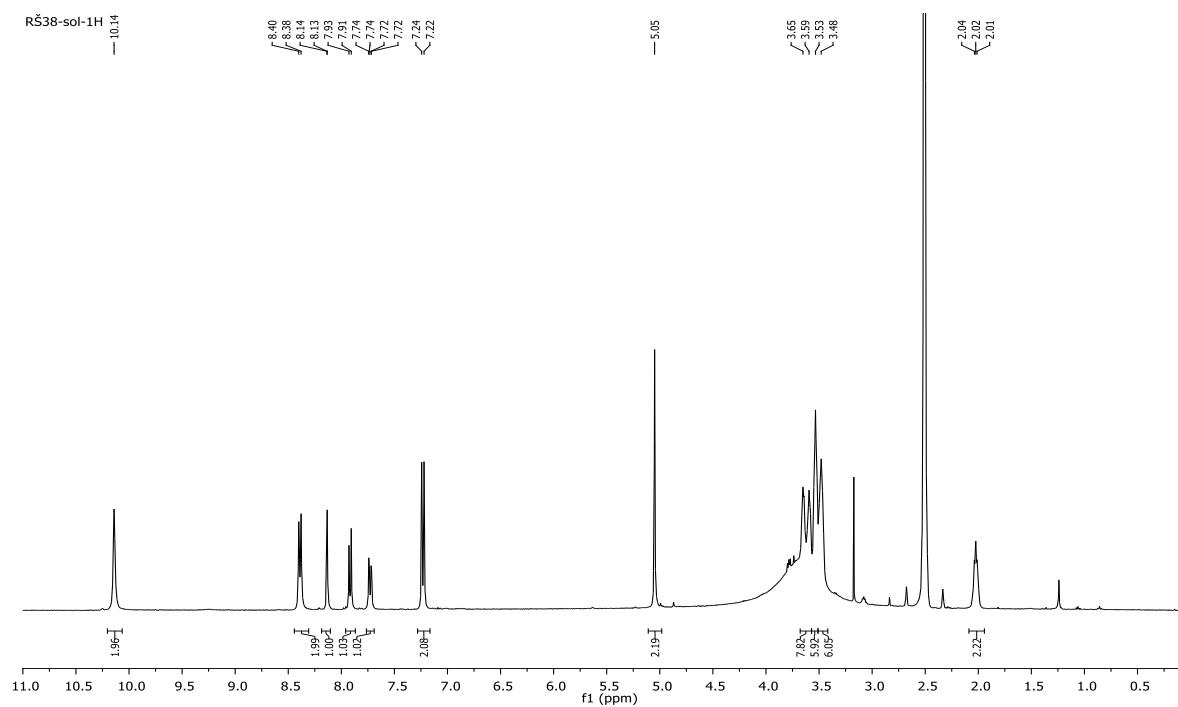
$^{13}\text{C}$  NMR (151 MHz, DMSO)  $\delta$  spectrum of 2-(3-Fluoro-4-(2-morpholinoethoxy)phenyl)-5(6)-(3,4,5,6-tetrahydropyrimidin-2-yl)-1H-benzimidazole dihydrochloride (**13b**)



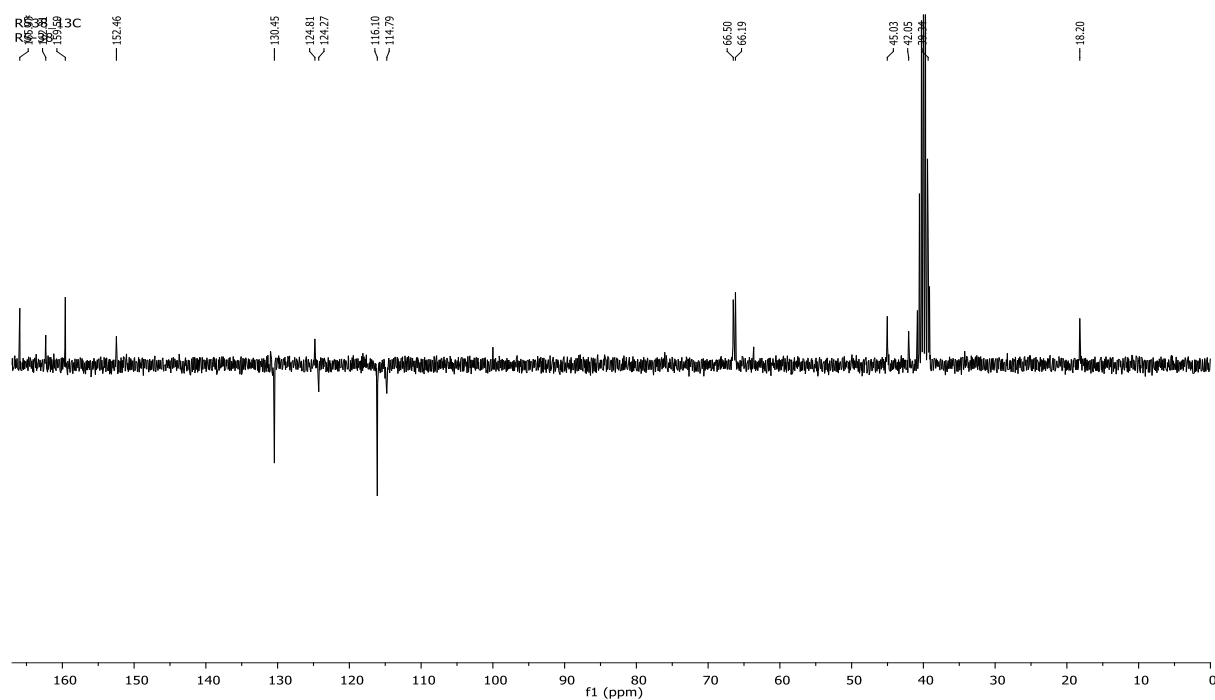
$^1\text{H}$  NMR (300 MHz, DMSO)  $\delta$  spectrum of 2-(3-Methoxy-4-(2-morpholinoethoxy)phenyl)-5(6)-(3,4,5,6-tetrahydropyrimidin-2-yl)-1H-benzimidazole dihydrochloride (**13c**)



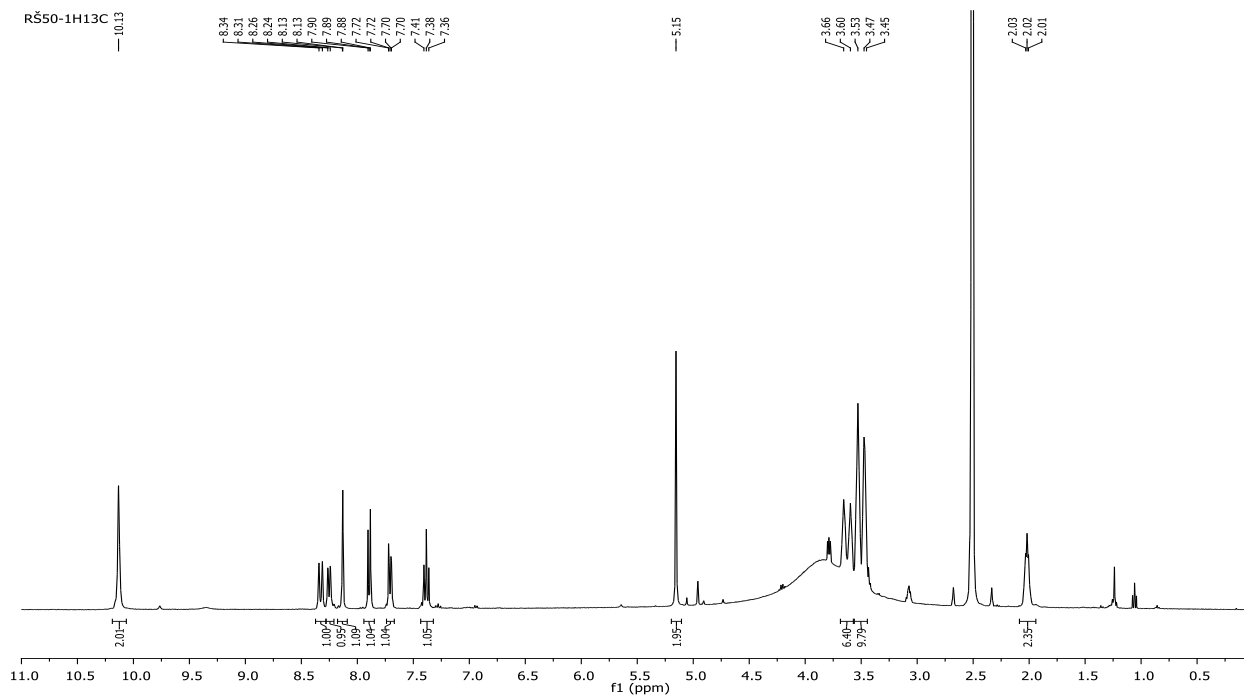
$^{13}\text{C}$  NMR (75 MHz, DMSO)  $\delta$  spectrum of 2-(3-Methoxy-4-(2-morpholinoethoxy)phenyl)-5(6)-(3,4,5,6-tetrahydropyrimidin-2-yl)-1H-benzimidazole dihydrochloride (**13c**)



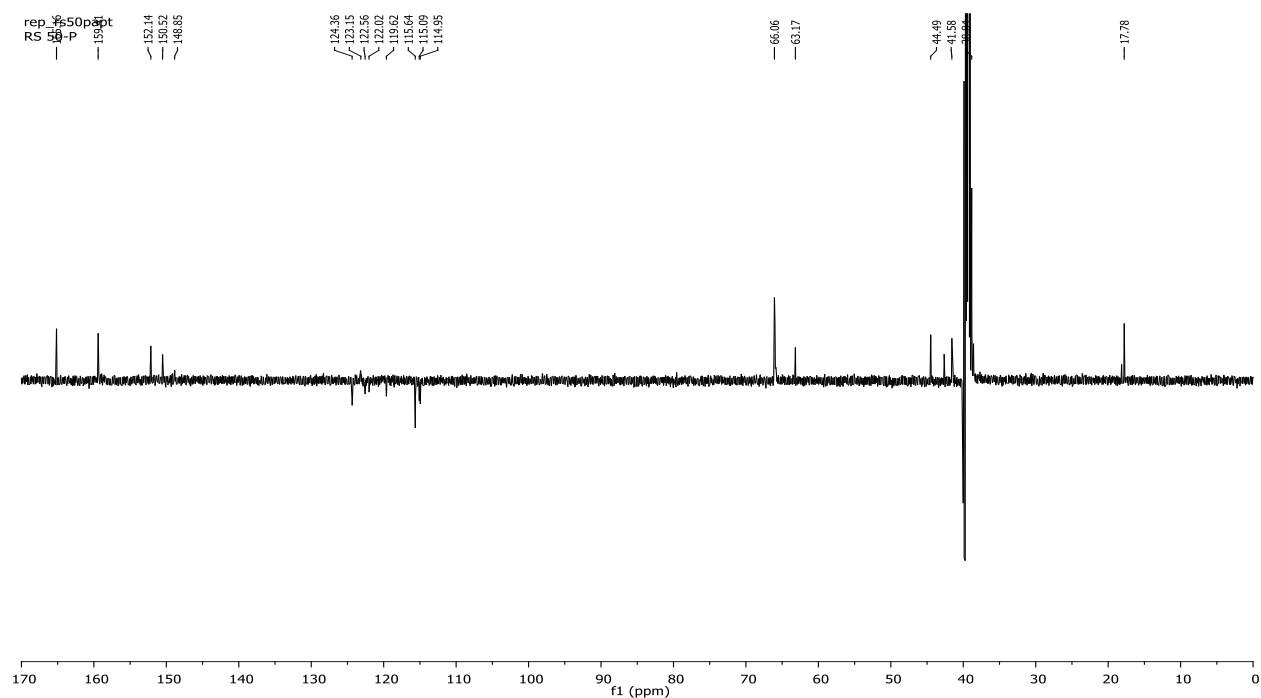
$^1\text{H}$  NMR (400 MHz, DMSO)  $\delta$  spectrum of 2-(4-(2-Morpholino-2-oxoethoxy)phenyl)-5(6)-(3,4,5,6-tetrahydropyrimidin-2-yl)-1H- benzimidazole hydrochloride (**14a**)



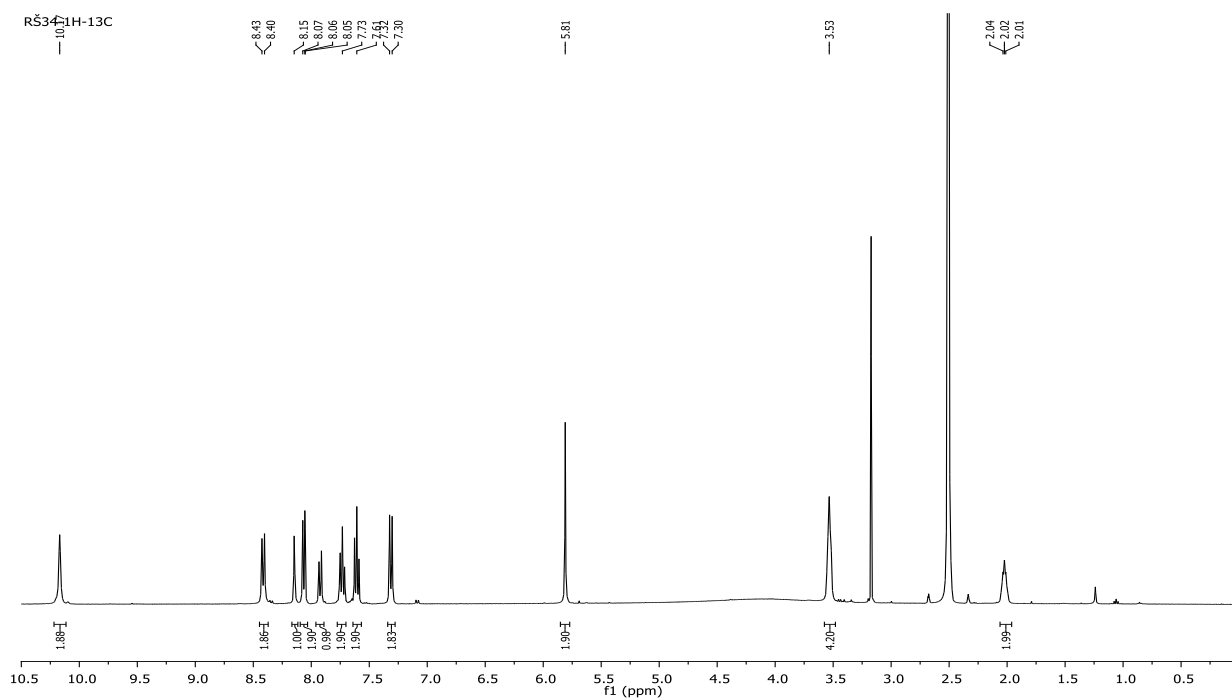
$^{13}\text{C}$  NMR (75 MHz, DMSO)  $\delta$  spectrum of 2-(4-(2-Morpholino-2-oxoethoxy)phenyl)-5(6)-(3,4,5,6-tetrahydropyrimidin-2-yl)-1H- benzimidazole hydrochloride (**14a**)



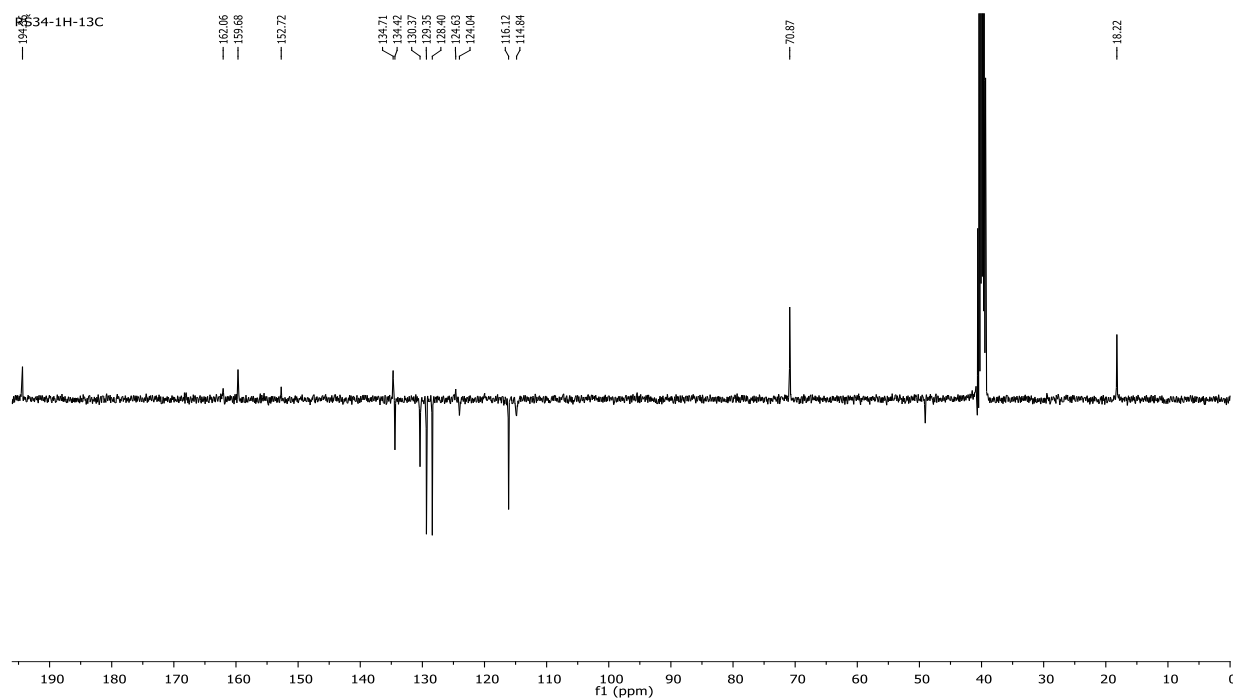
$^1\text{H}$  NMR (400 MHz, DMSO)  $\delta$  spectrum of 2-(3-Fluoro-4-(2-morpholino-2-oxoethoxy)phenyl)-5(6)-(3,4,5,6-tetrahydropyrimidin-2-yl)-1H-benzimidazole hydrochloride (**14b**)



$^{13}\text{C}$  NMR (151 MHz, DMSO)  $\delta$  spectrum of 2-(3-Fluoro-4-(2-morpholino-2-oxoethoxy)phenyl)-5(6)-(3,4,5,6-tetrahydropyrimidin-2-yl)-1H-benzimidazole hydrochloride (**14b**)

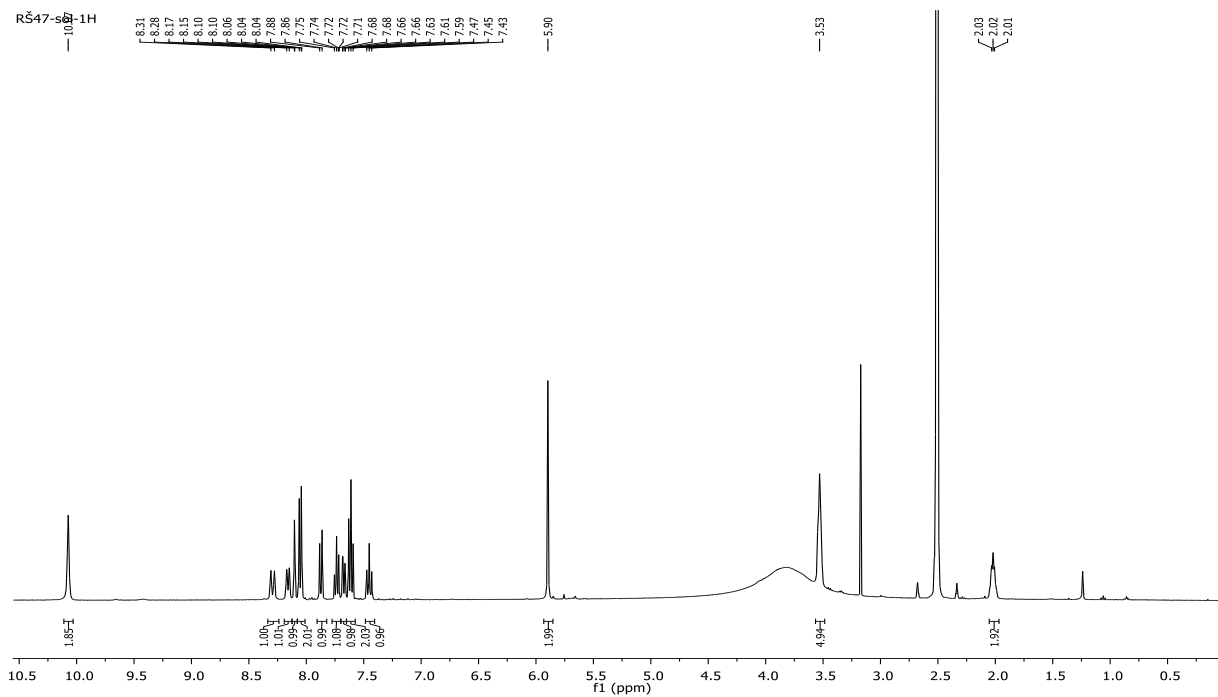


$^1\text{H}$  NMR (400 MHz, DMSO)  $\delta$  spectrum of 2-(4-(2-Oxo-2-phenylethoxy)phenyl)-5(6)-(3,4,5,6-tetrahydropyrimidin-2-yl)-1H-benzimidazole hydrochloride (**15a**)

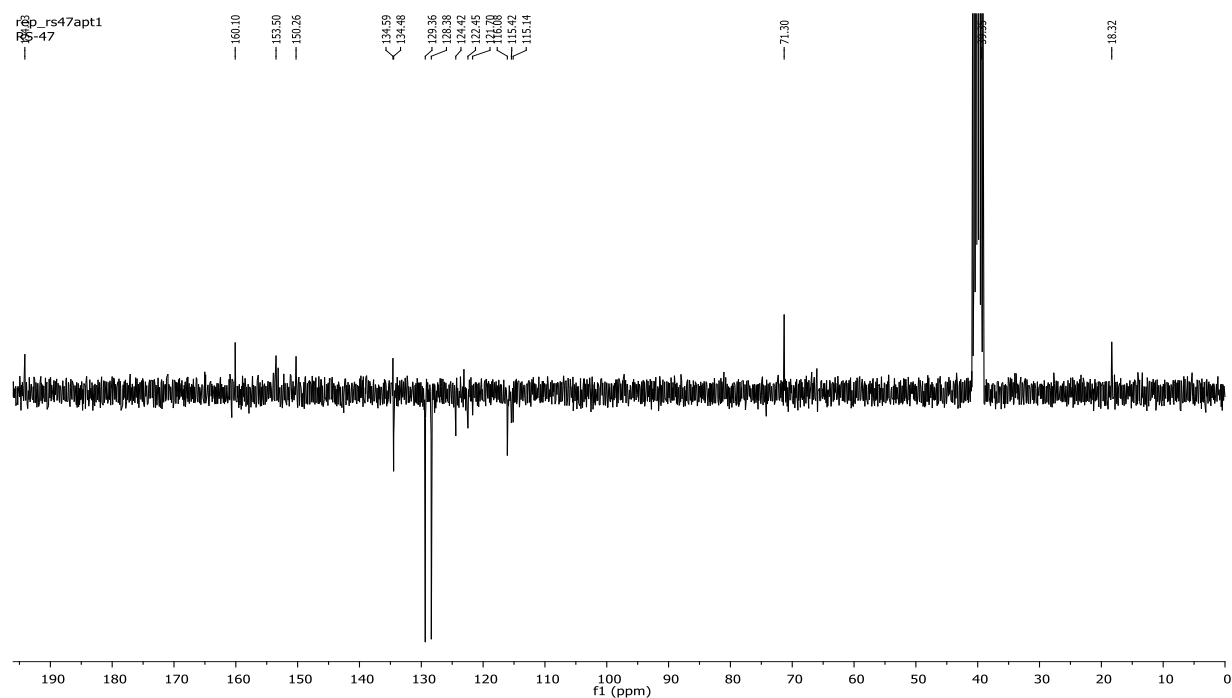


$^{13}\text{C}$  NMR (101 MHz, DMSO)  $\delta$  spectrum of 2-(4-(2-Oxo-2-phenylethoxy)phenyl)-5(6)-(3,4,5,6-tetrahydropyrimidin-2-yl)-1H-benzimidazole hydrochloride (**15a**)

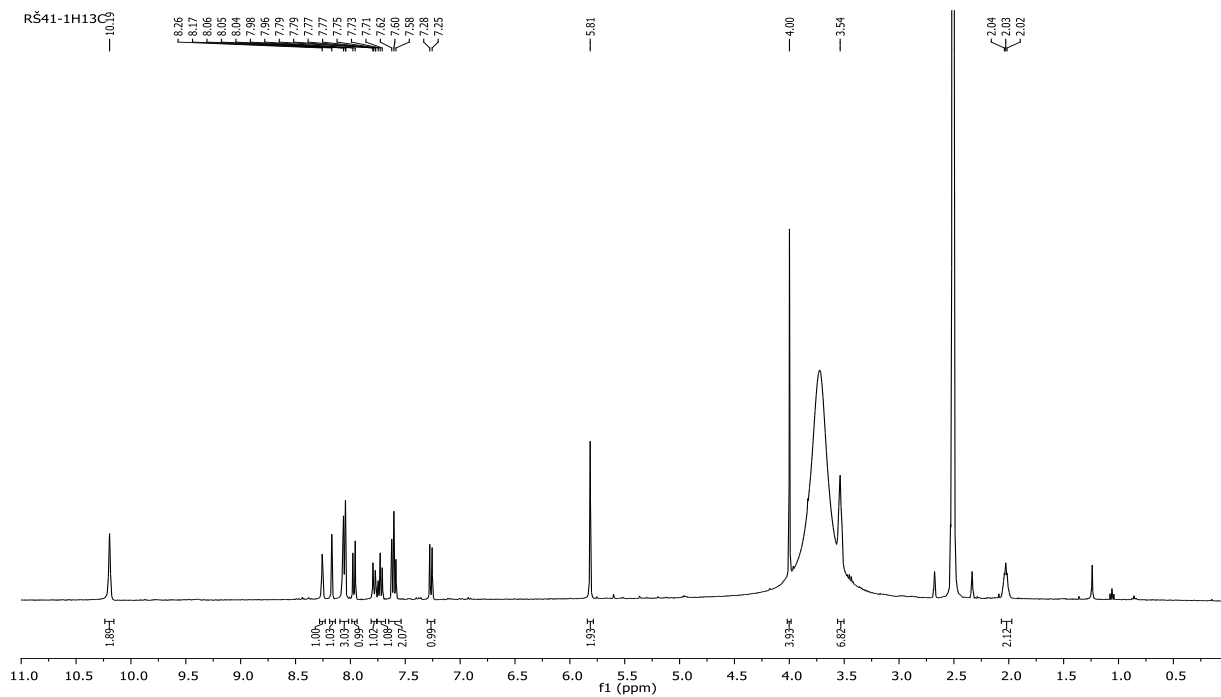




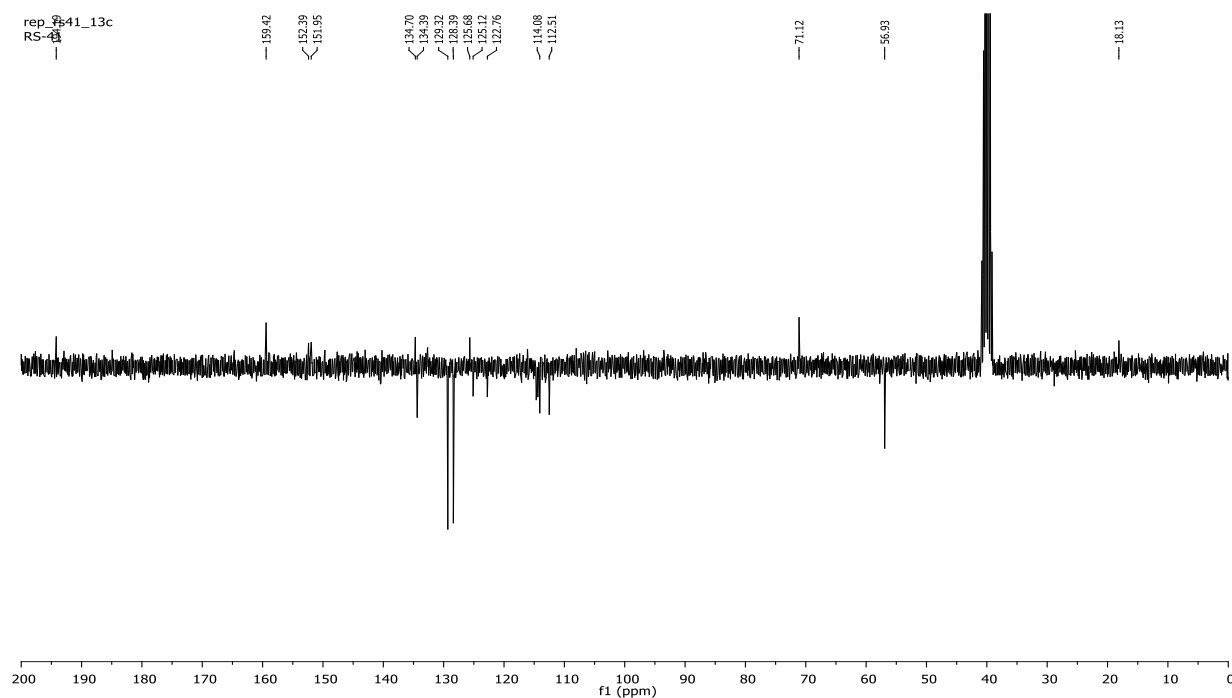
$^1\text{H}$  NMR (400 MHz, DMSO)  $\delta$  spectrum of 2-(3-Fluoro-4-(2-oxo-2-phenylethoxy)phenyl)-5(6)-(3,4,5,6-tetrahydropyrimidin-2-yl)-1H- benzimidazole hydrochloride (**15b**)



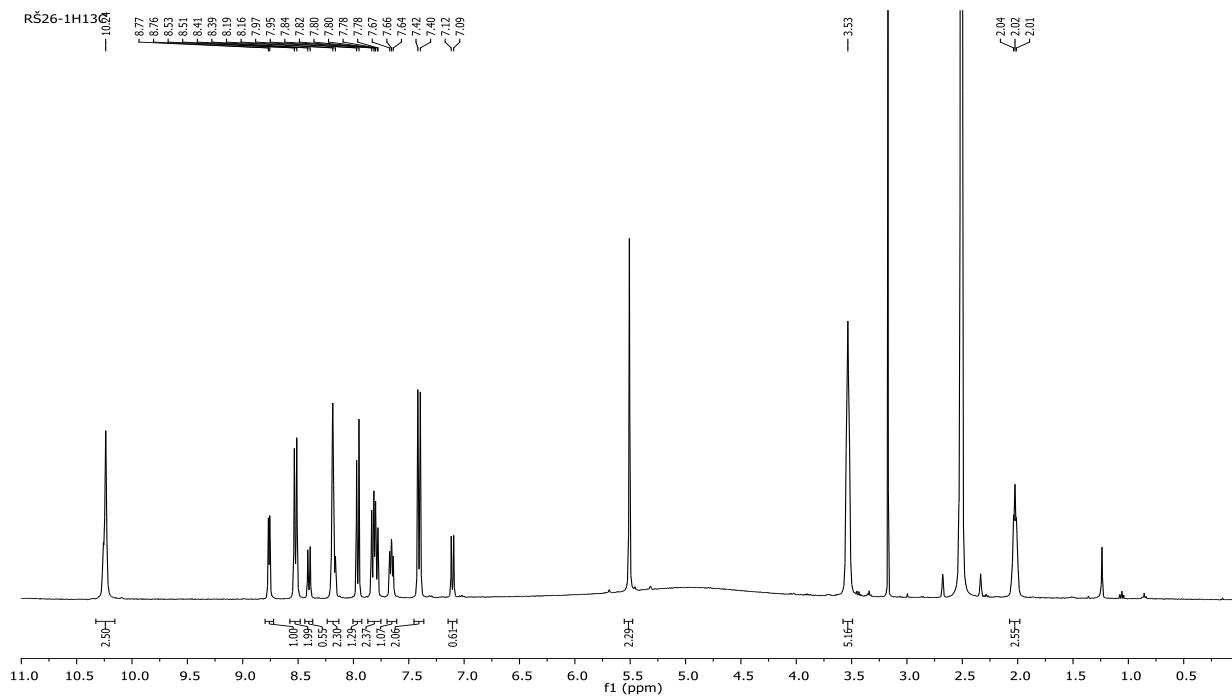
$^{13}\text{C}$  NMR (75 MHz, DMSO)  $\delta$  spectrum of 2-(3-Fluoro-4-(2-oxo-2-phenylethoxy)phenyl)-5(6)-(3,4,5,6-tetrahydropyrimidin-2-yl)-1H- benzimidazole hydrochloride (**15b**)



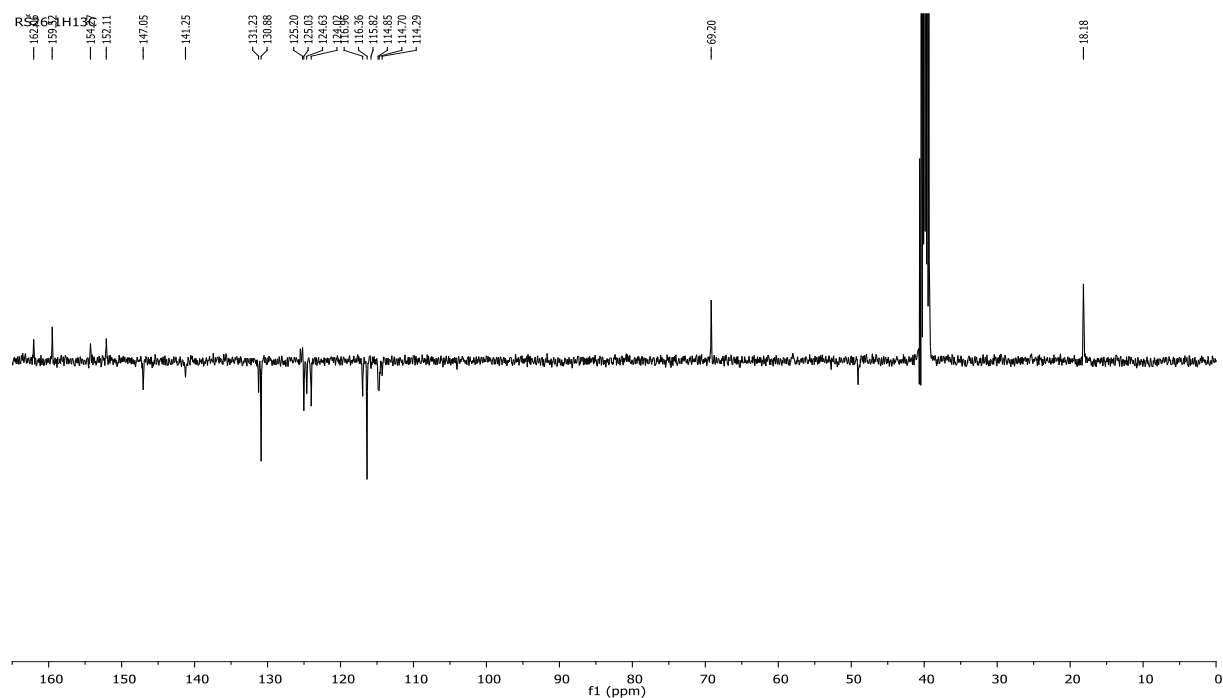
$^1\text{H}$  NMR (400 MHz, DMSO)  $\delta$  spectrum of 2-(3-Methoxy-4-(2-oxo-2-phenylethoxy)phenyl)-5(6)-(3,4,5,6-tetrahydropyrimidin-2-yl)-1H-benzimidazole hydrochloride (**15c**)



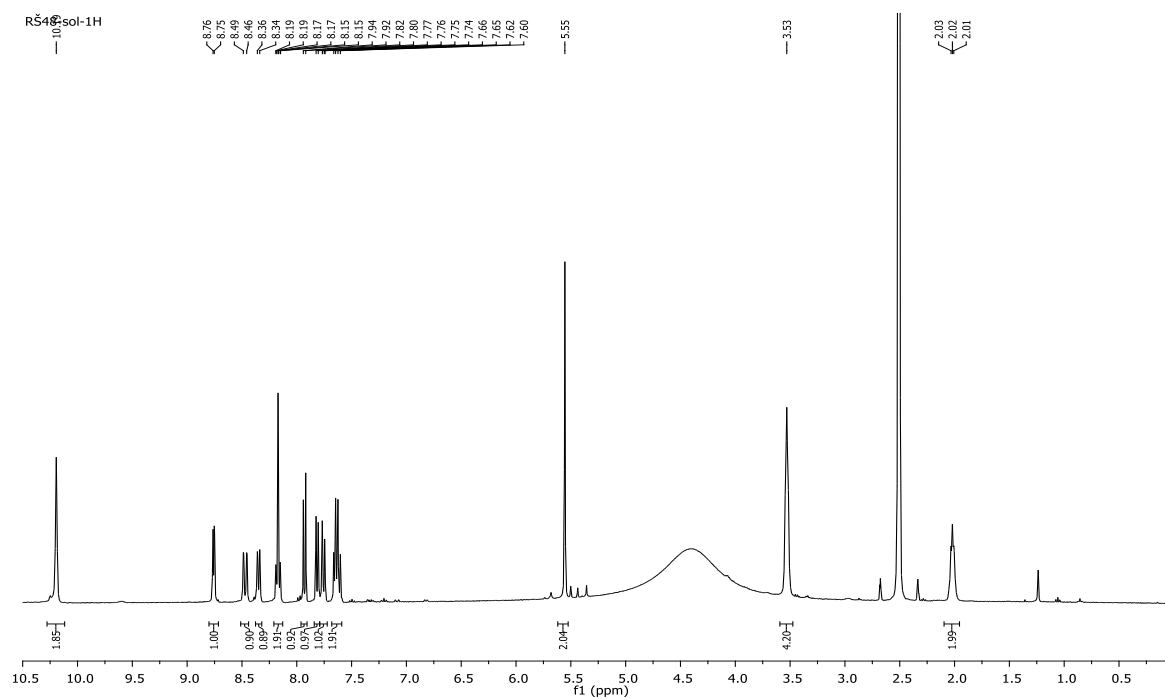
$^{13}\text{C}$  NMR (75 MHz, DMSO)  $\delta$  spectrum of 2-(3-Methoxy-4-(2-oxo-2-phenylethoxy)phenyl)-5(6)-(3,4,5,6-tetrahydropyrimidin-2-yl)-1H-benzimidazole hydrochloride (**15c**)



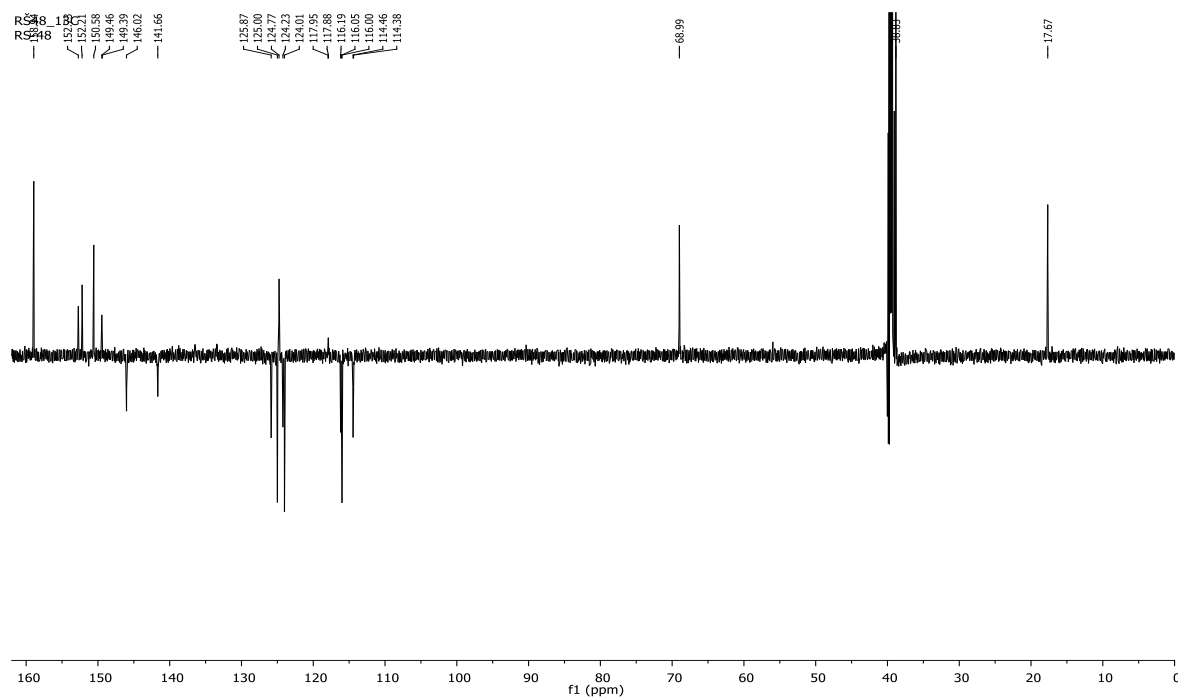
$^1\text{H}$  NMR (400 MHz, DMSO)  $\delta$  spectrum of 2-(4-(Pyridin-2-ylmethoxy)phenyl)-5(6)-(3,4,5,6-tetrahydropyrimidin-2-yl)-1H-benzimidazole hydrochloride (**16a**)



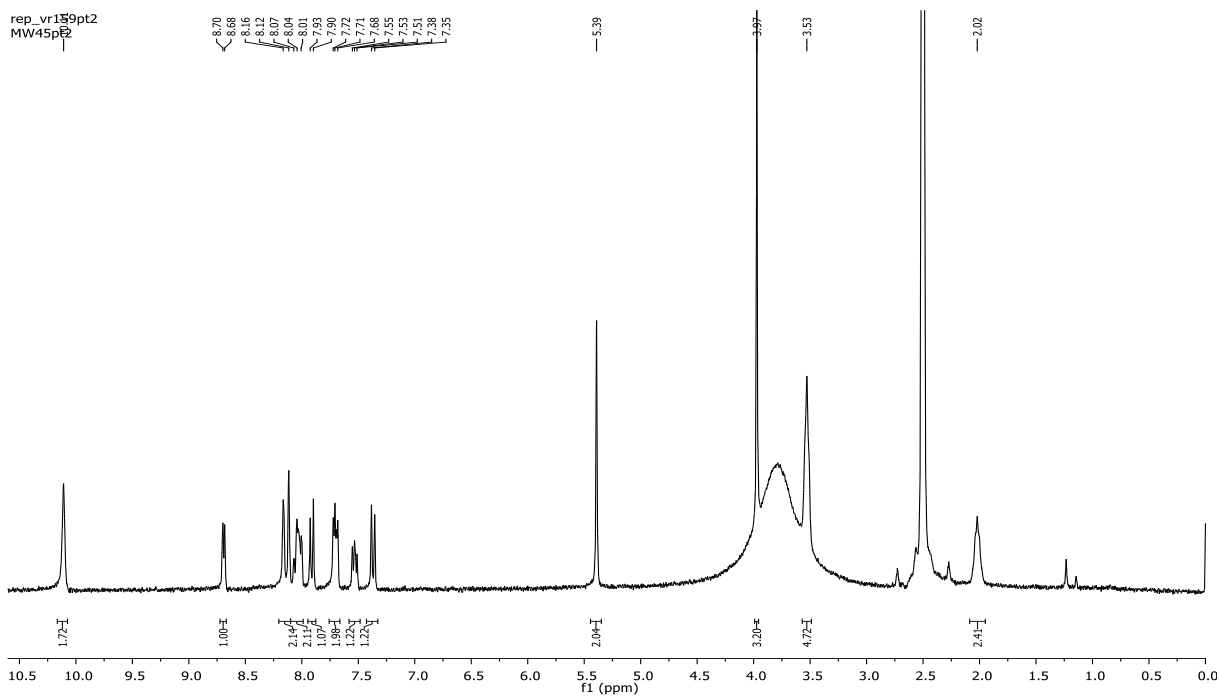
$^{13}\text{C}$  NMR (101 MHz, DMSO)  $\delta$  spectrum of 2-(4-(Pyridin-2-ylmethoxy)phenyl)-5(6)-(3,4,5,6-tetrahydropyrimidin-2-yl)-1H-benzimidazole hydrochloride (**16a**)



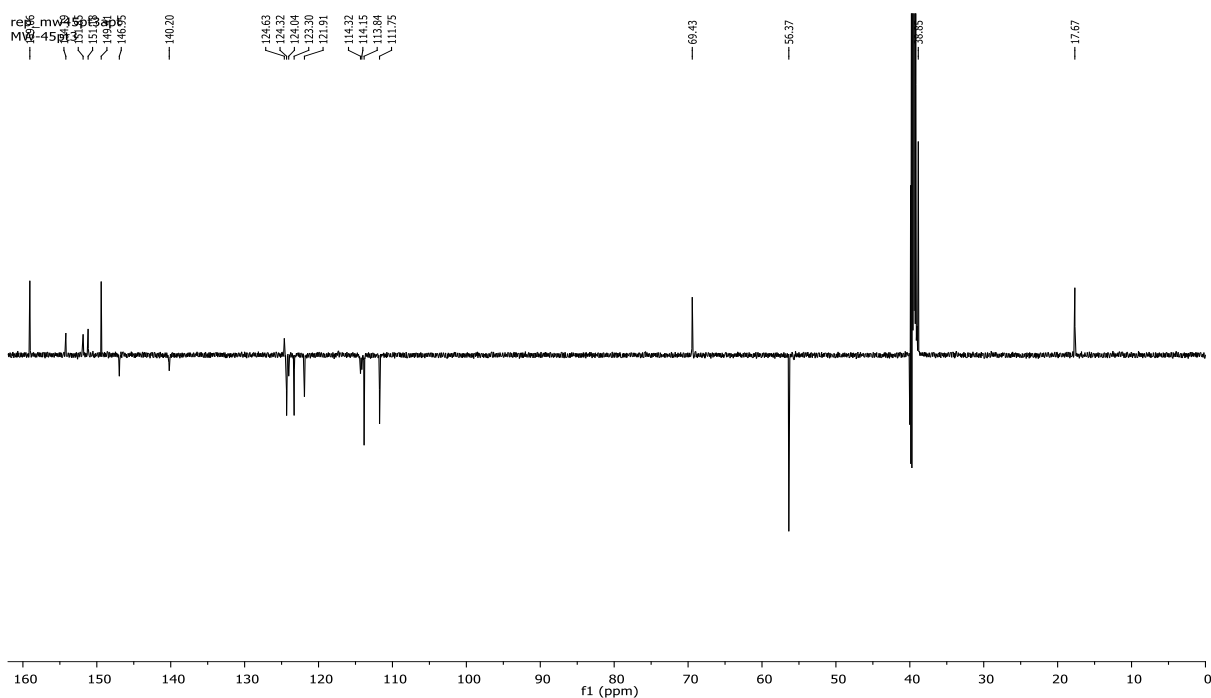
$^1\text{H}$  NMR (400 MHz, DMSO)  $\delta$  spectrum of 2-(3-Fluoro-4-(pyridin-2-ylmethoxy)phenyl)-5(6)-(3,4,5,6-tetrahydropyrimidin-2-yl)-1H-benzimidazole hydrochloride (**16b**)



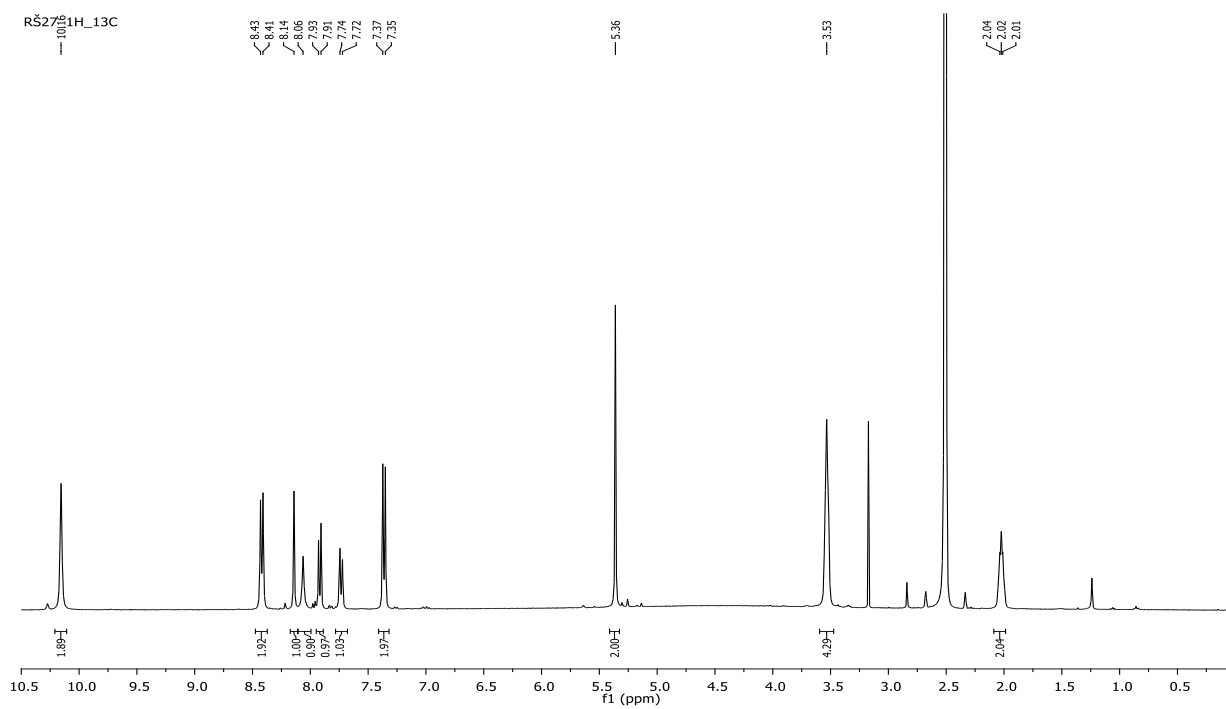
$^{13}\text{C}$  NMR (151 MHz, DMSO)  $\delta$  spectrum of 2-(3-Fluoro-4-(pyridin-2-ylmethoxy)phenyl)-5(6)-(3,4,5,6-tetrahydropyrimidin-2-yl)-1H-benzimidazole hydrochloride (**16b**)



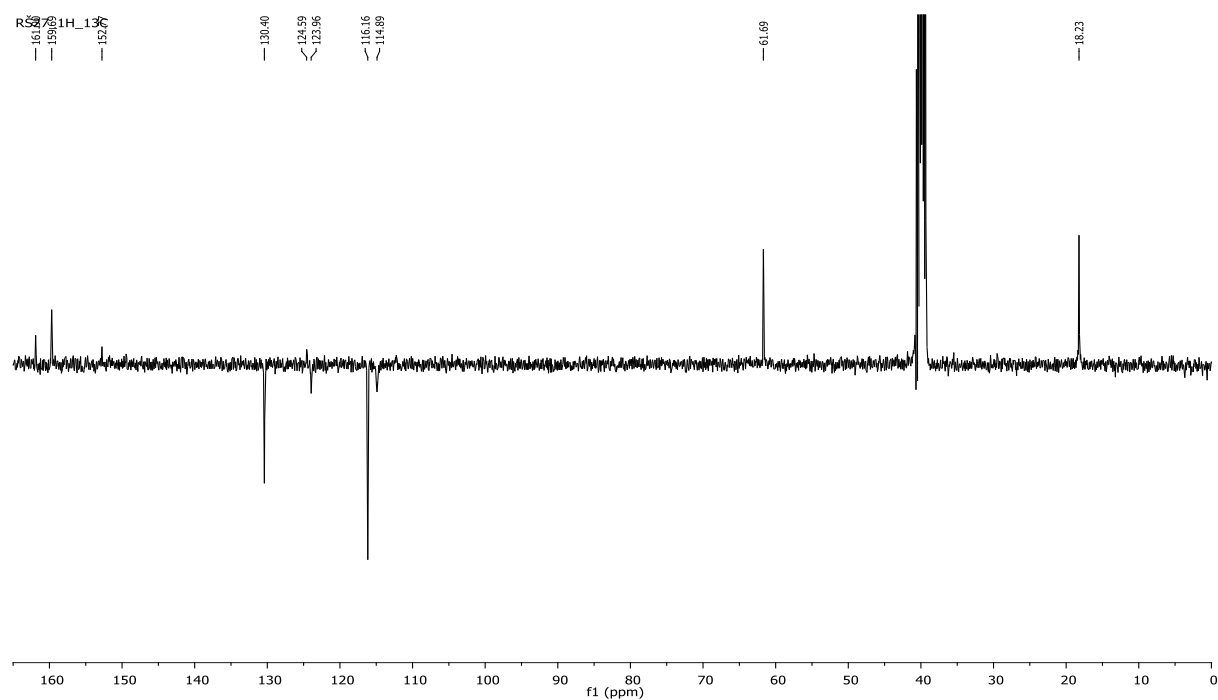
$^1\text{H}$  NMR (300 MHz, DMSO)  $\delta$  spectrum of 2-(3-Methoxy-4-(pyridin-2-ylmethoxy)phenyl)-5(6)-(3,4,5,6-tetrahydropyrimidin-2-yl)-1H-benzimidazole hydrochloride (**16c**)



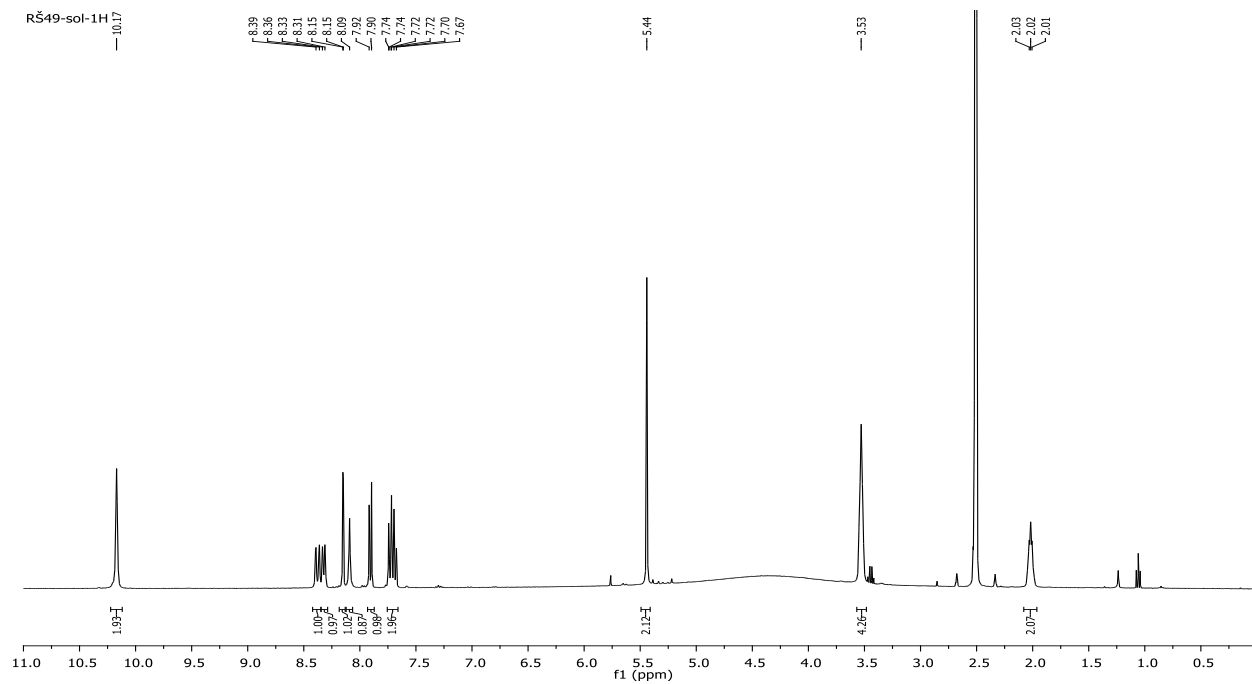
$^{13}\text{C}$  NMR (151 MHz, DMSO)  $\delta$  spectrum of 2-(3-Methoxy-4-(pyridin-2-ylmethoxy)phenyl)-5(6)-(3,4,5,6-tetrahydropyrimidin-2-yl)-1H-benzimidazole hydrochloride (**16c**)



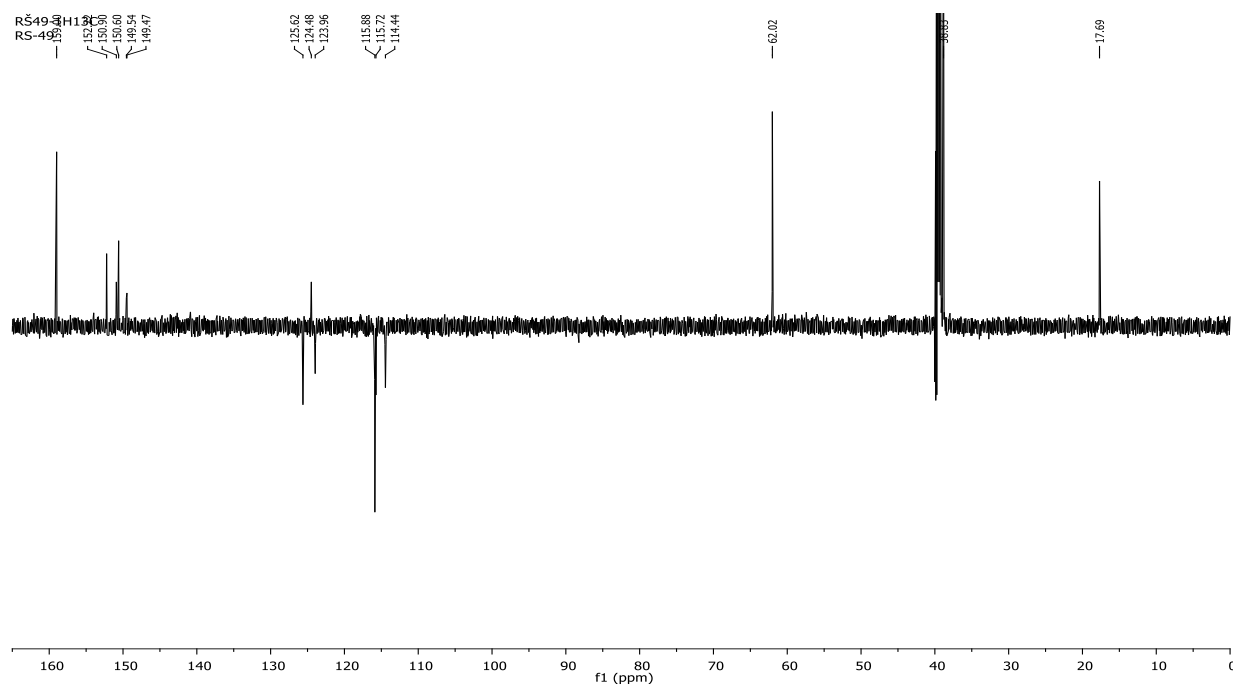
$^1\text{H}$  NMR (400 MHz, DMSO)  $\delta$  spectrum of 2-(4-((1H-1,2,3-triazol-4-yl)methoxy)phenyl)-5(6)-(3,4,5,6-tetrahydropyrimidin-2-yl)-1H-benzimidazole hydrochloride (**17a**)



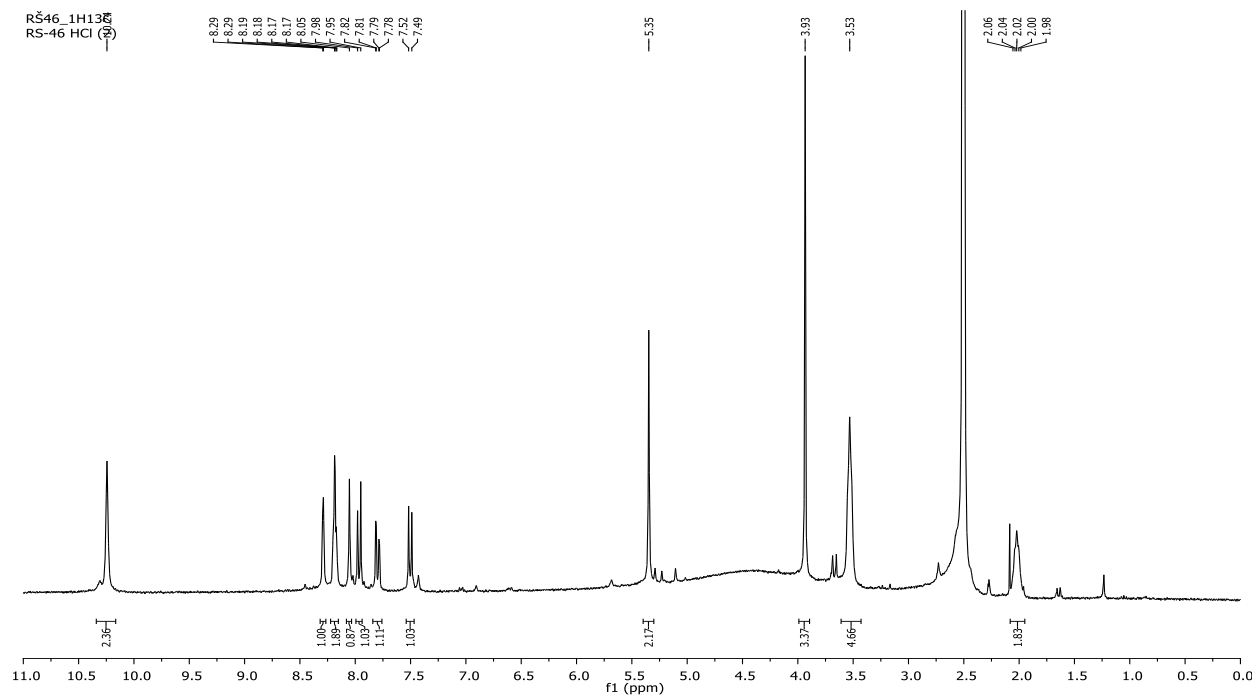
$^{13}\text{C}$  NMR (101 MHz, DMSO)  $\delta$  spectrum of 2-(4-((1H-1,2,3-triazol-4-yl)methoxy)phenyl)-5(6)-(3,4,5,6-tetrahydropyrimidin-2-yl)-1H-benzimidazole hydrochloride (**17a**)



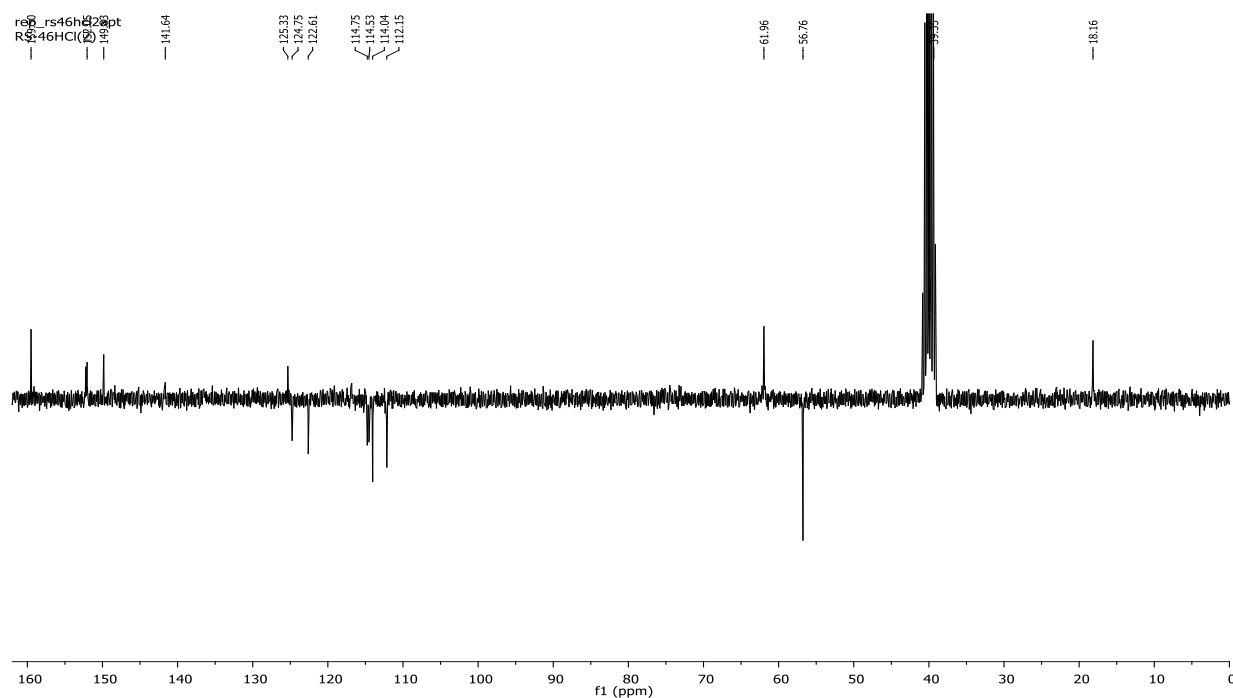
$^1\text{H}$  NMR (400 MHz, DMSO)  $\delta$  spectrum of 2-(4-((1H-1,2,3-triazol-4-yl)methoxy)-3-fluorophenyl)-5(6)-(3,4,5,6-tetrahydropyrimidin-2-yl)-1H-benzimidazole hydrochloride (**17b**)



$^{13}\text{C}$  NMR (151 MHz, DMSO)  $\delta$  spectrum of 2-(4-((1H-1,2,3-triazol-4-yl)methoxy)-3-fluorophenyl)-5(6)-(3,4,5,6-tetrahydropyrimidin-2-yl)-1H-benzimidazole hydrochloride (**17b**)

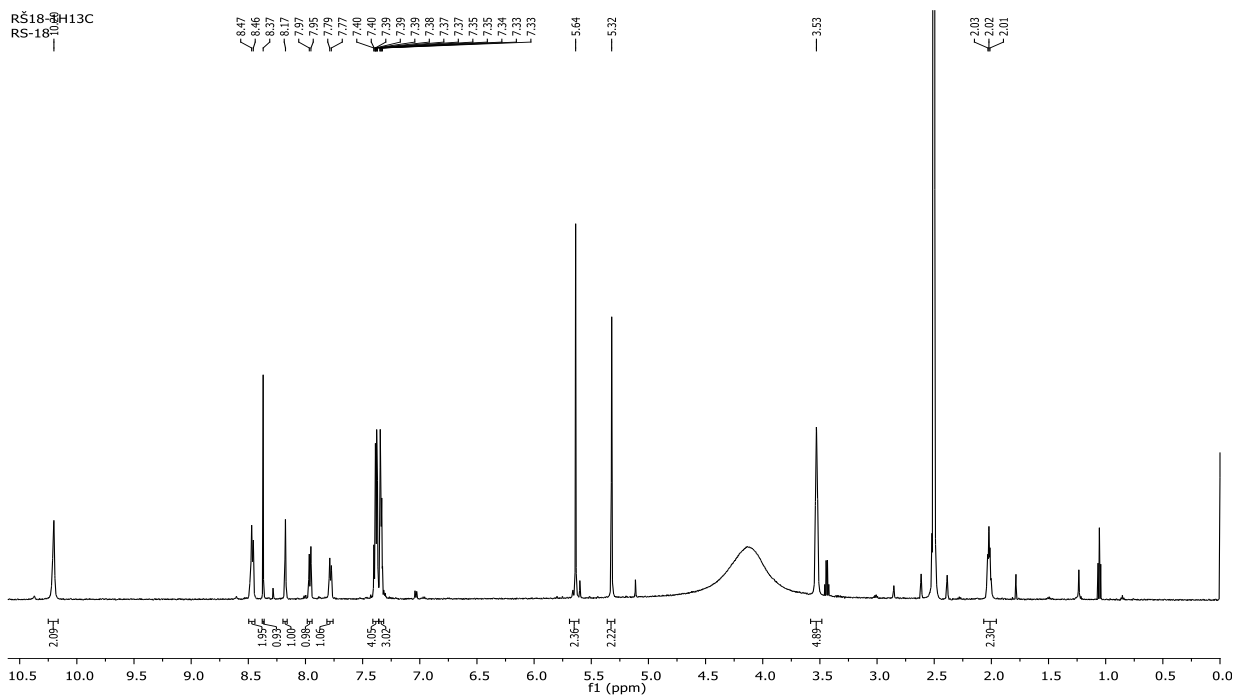


$^1\text{H}$  NMR (300 MHz, DMSO)  $\delta$  spectrum of 2-(4-((1H-1,2,3-triazol-4-yl)methoxy)-3-methoxyphenyl)-5(6)-(3,4,5,6-tetrahydropyrimidin-2-yl)-1H-benzimidazole hydrochloride (**17c**)

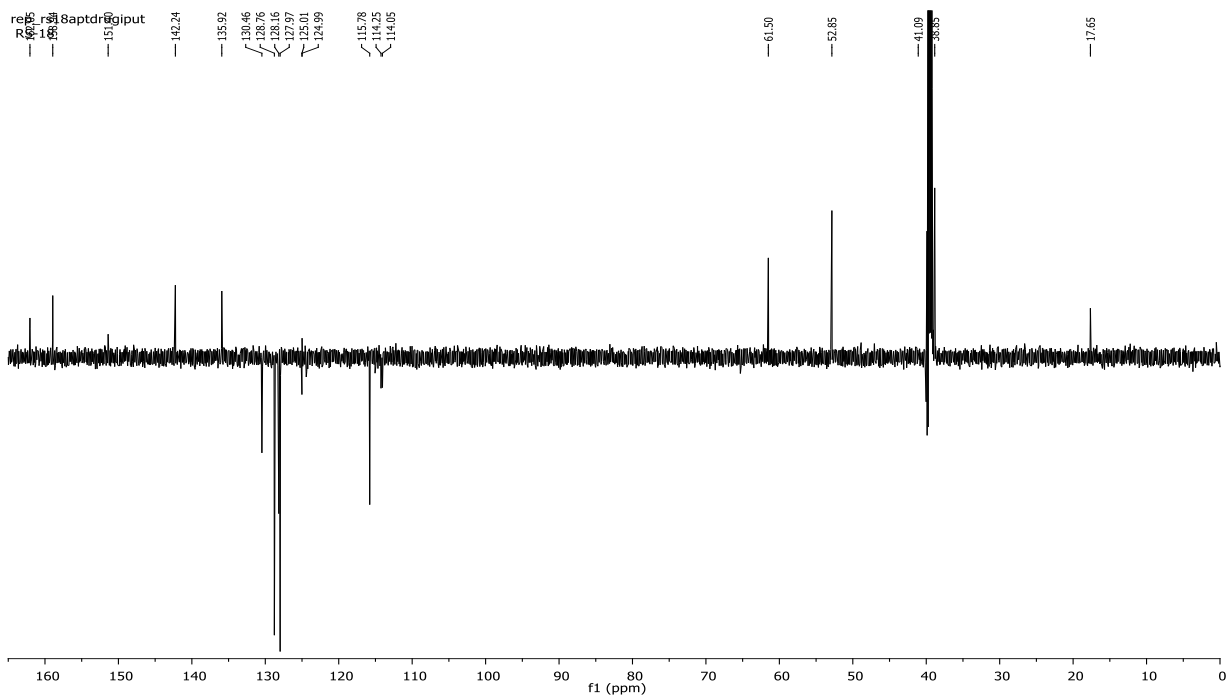


$^{13}\text{C}$  NMR (75 MHz, DMSO)  $\delta$  spectrum of 2-(4-((1H-1,2,3-triazol-4-yl)methoxy)-3-methoxyphenyl)-5(6)-(3,4,5,6-tetrahydropyrimidin-2-yl)-1H-benzimidazole hydrochloride (**17c**)

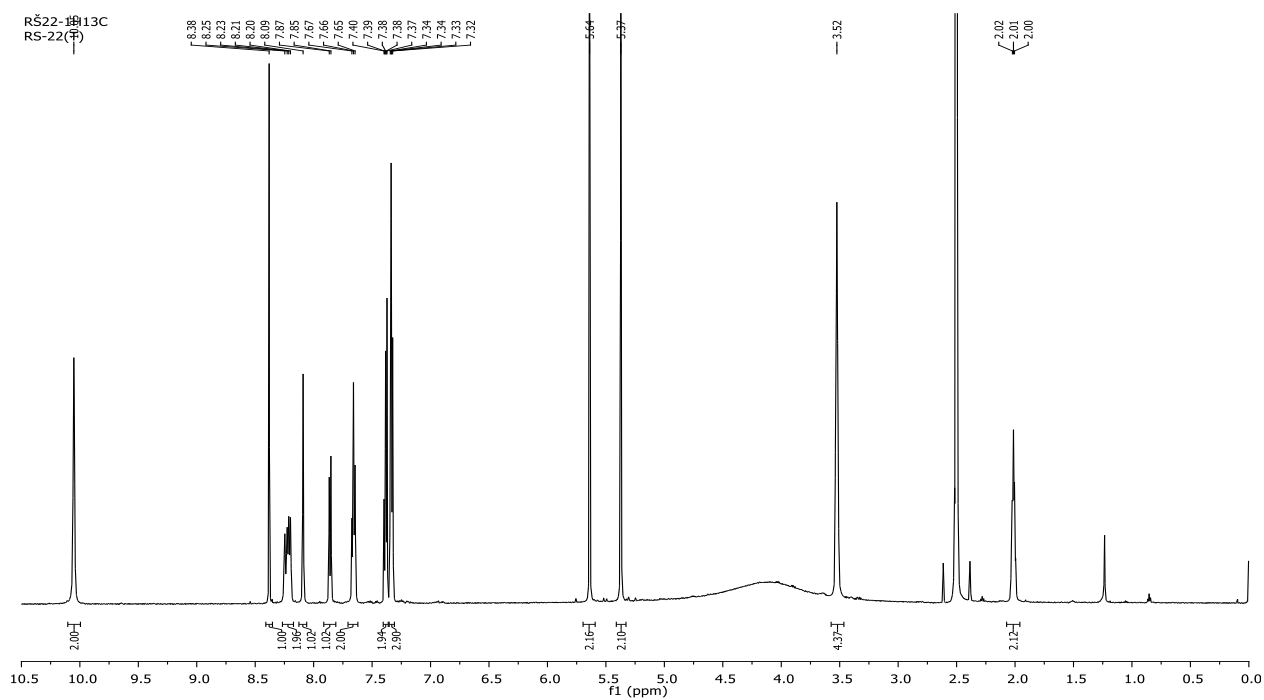




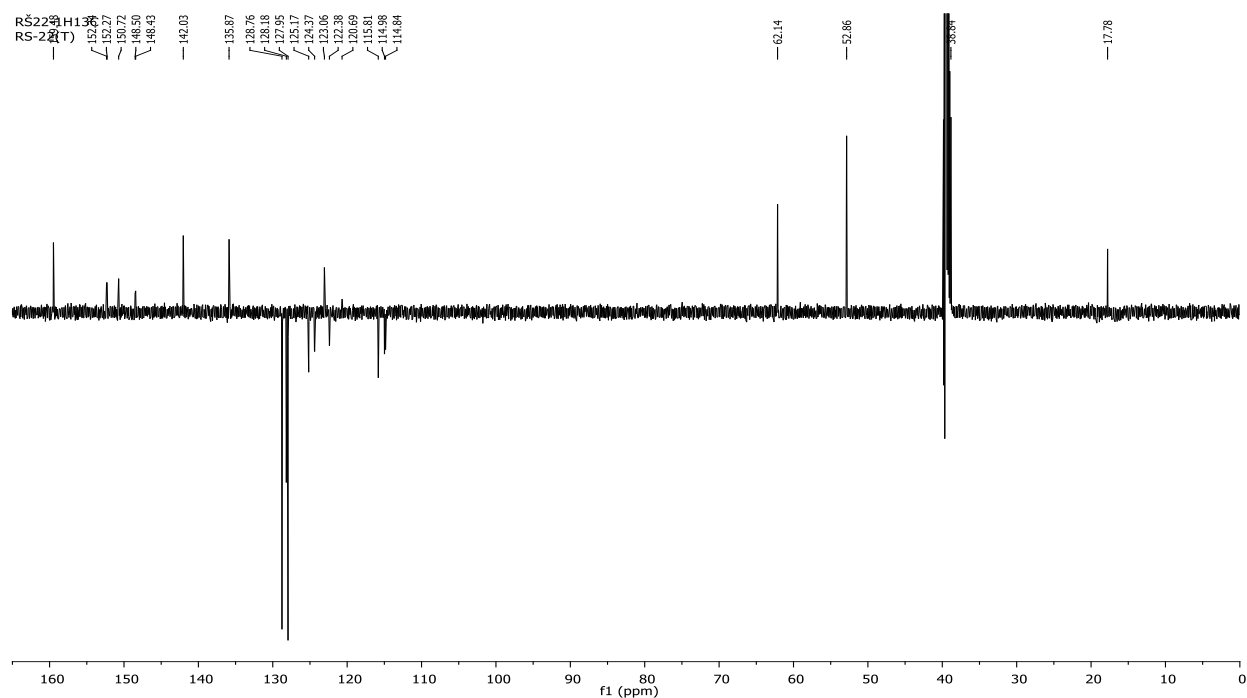
<sup>1</sup>H NMR (600 MHz, DMSO)  $\delta$  spectrum of 2-(4-((1-Benzyl-1H-1,2,3-triazol-4-yl)methoxy)phenyl)-5(6)-(3,4,5,6-tetrahydropyrimidin-2-yl)-1H-benzimidazole hydrochloride (**18a**)



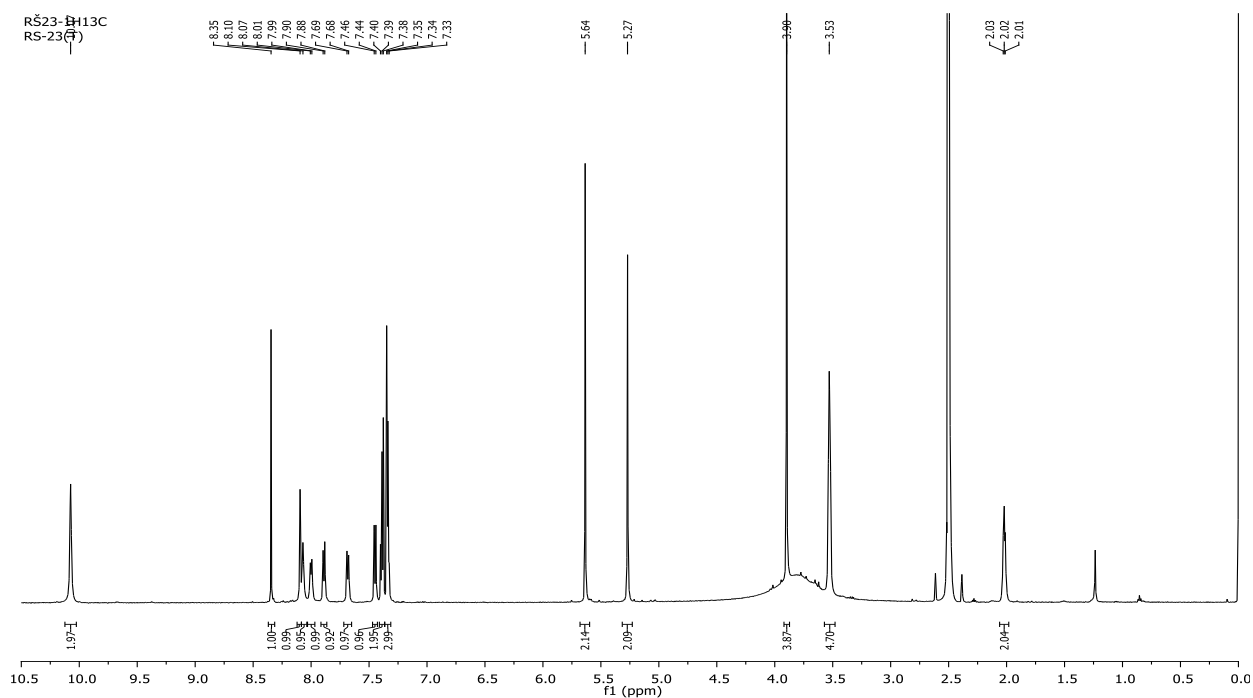
<sup>13</sup>C NMR (151 MHz, DMSO)  $\delta$  spectrum of 2-(4-((1-Benzyl-1H-1,2,3-triazol-4-yl)methoxy)phenyl)-5(6)-(3,4,5,6-tetrahydropyrimidin-2-yl)-1H-benzimidazole hydrochloride (**18a**)



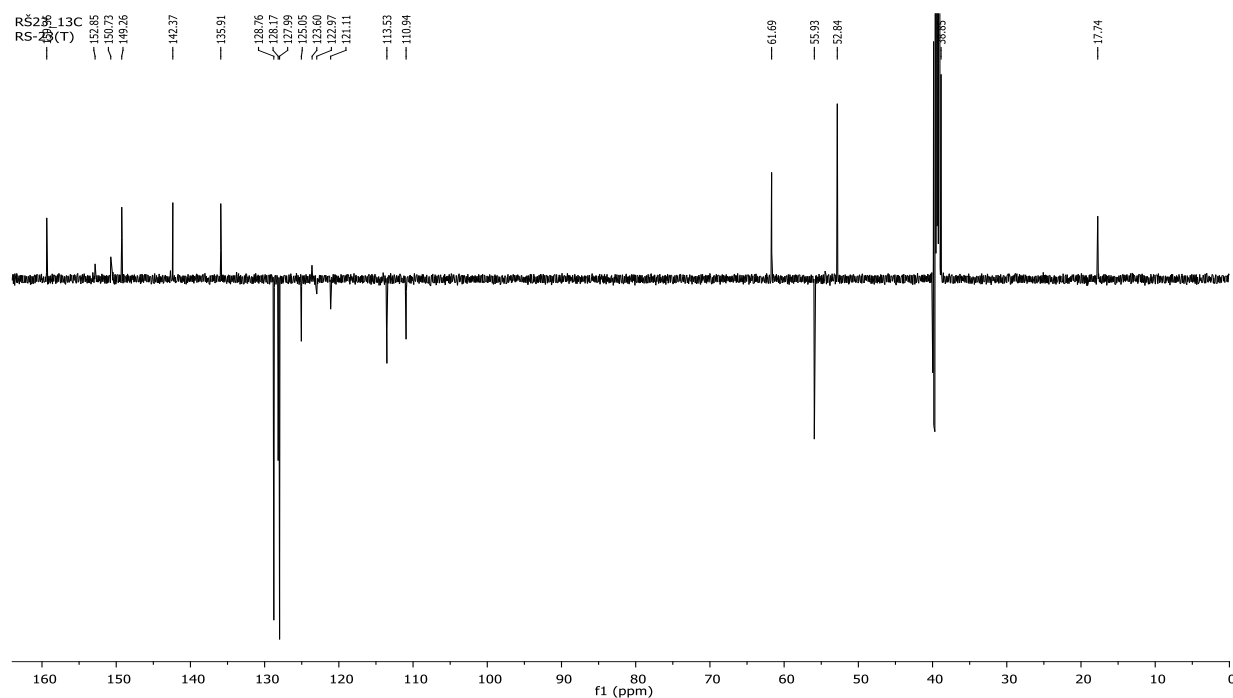
$^1\text{H}$  NMR (600 MHz, DMSO)  $\delta$  spectrum of 2-(4-((1-Benzyl-1H-1,2,3-triazol-4-yl)methoxy)-3-fluorophenyl)-5(6)-(3,4,5,6-tetrahydropyrimidin-2-yl)-1H-benzimidazole hydrochloride (**18b**)



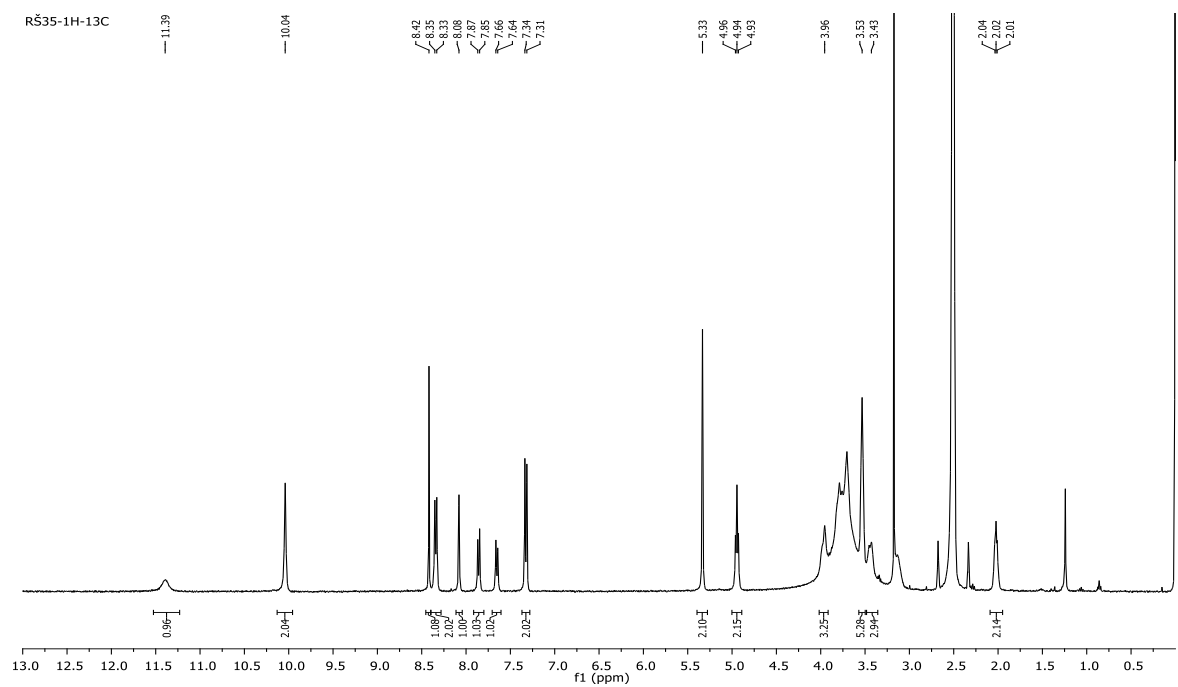
$^{13}\text{C}$  NMR (151 MHz, DMSO)  $\delta$  spectrum of 2-(4-((1-Benzyl-1H-1,2,3-triazol-4-yl)methoxy)-3-fluorophenyl)-5(6)-(3,4,5,6-tetrahydropyrimidin-2-yl)-1H-benzimidazole hydrochloride (**18b**)



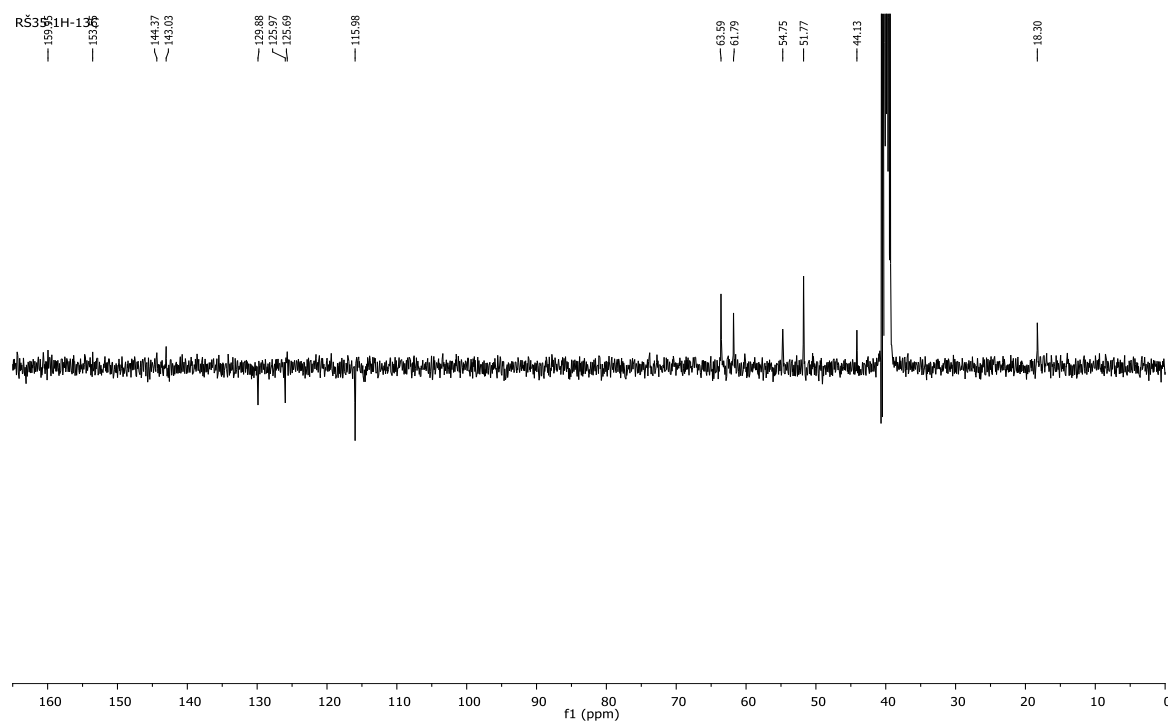
$^1\text{H}$  NMR (600 MHz, DMSO)  $\delta$  spectrum of 2-(4-((1-Benzyl-1H-1,2,3-triazol-4-yl)methoxy)-3-methoxyphenyl)-5(6)-(3,4,5,6-tetrahydropyrimidin-2-yl)-1H-benzimidazole hydrochloride (**18c**)



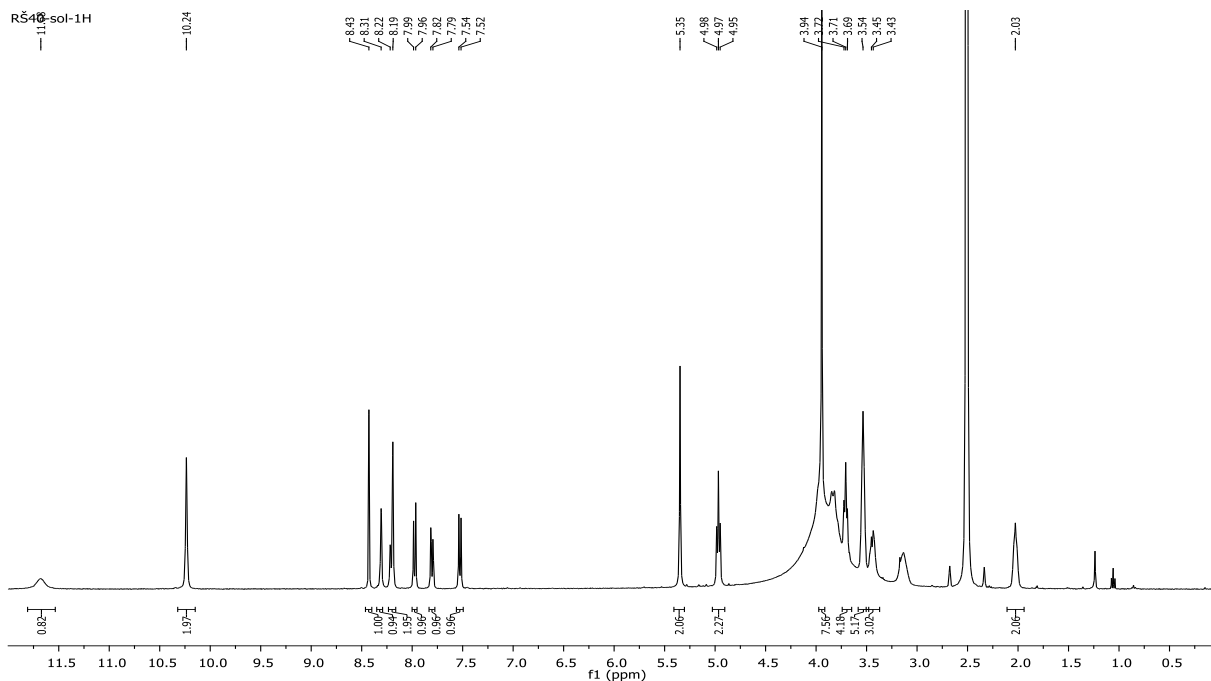
$^{13}\text{C}$  NMR (151 MHz, DMSO)  $\delta$  spectrum of 2-(4-((1-Benzyl-1H-1,2,3-triazol-4-yl)methoxy)-3-methoxyphenyl)-5(6)-(3,4,5,6-tetrahydropyrimidin-2-yl)-1H-benzimidazole hydrochloride (**18c**)



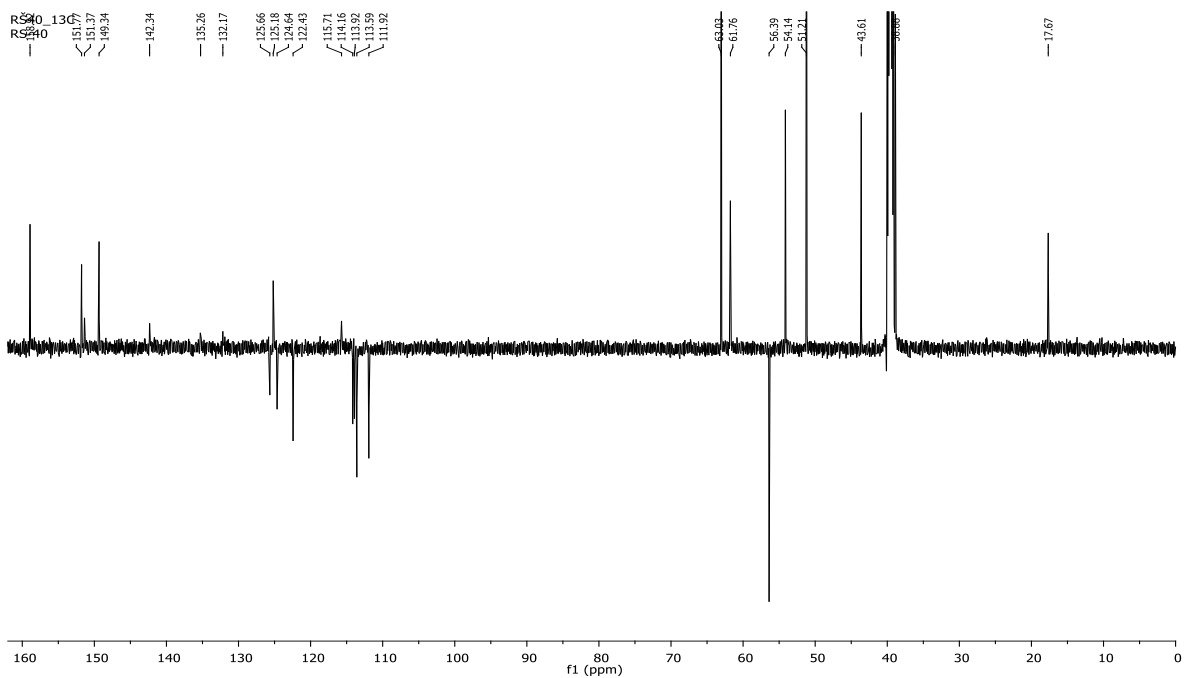
$^1\text{H}$  NMR (300 MHz, DMSO)  $\delta$  spectrum of 2-(4-((1-(2-Morpholinoethyl)-1H-1,2,3-triazol-4-yl)methoxy)phenyl)-5(6)-(3,4,5,6-tetrahydropyrimidin-2-yl)-1H-benzimidazole dihydrochloride (**19a**)



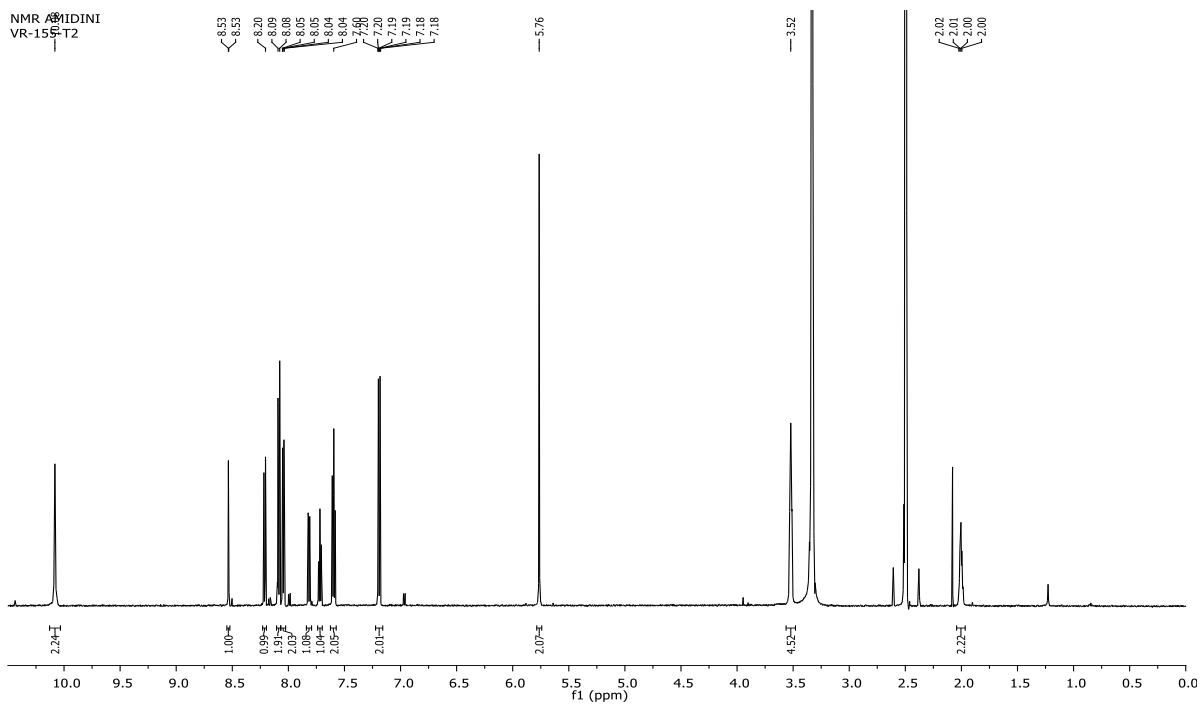
$^{13}\text{C}$  NMR (101 MHz, DMSO)  $\delta$  spectrum of 2-(4-((1-(2-Morpholinoethyl)-1H-1,2,3-triazol-4-yl)methoxy)phenyl)-5(6)-(3,4,5,6-tetrahydropyrimidin-2-yl)-1H-benzimidazole dihydrochloride (**19a**)



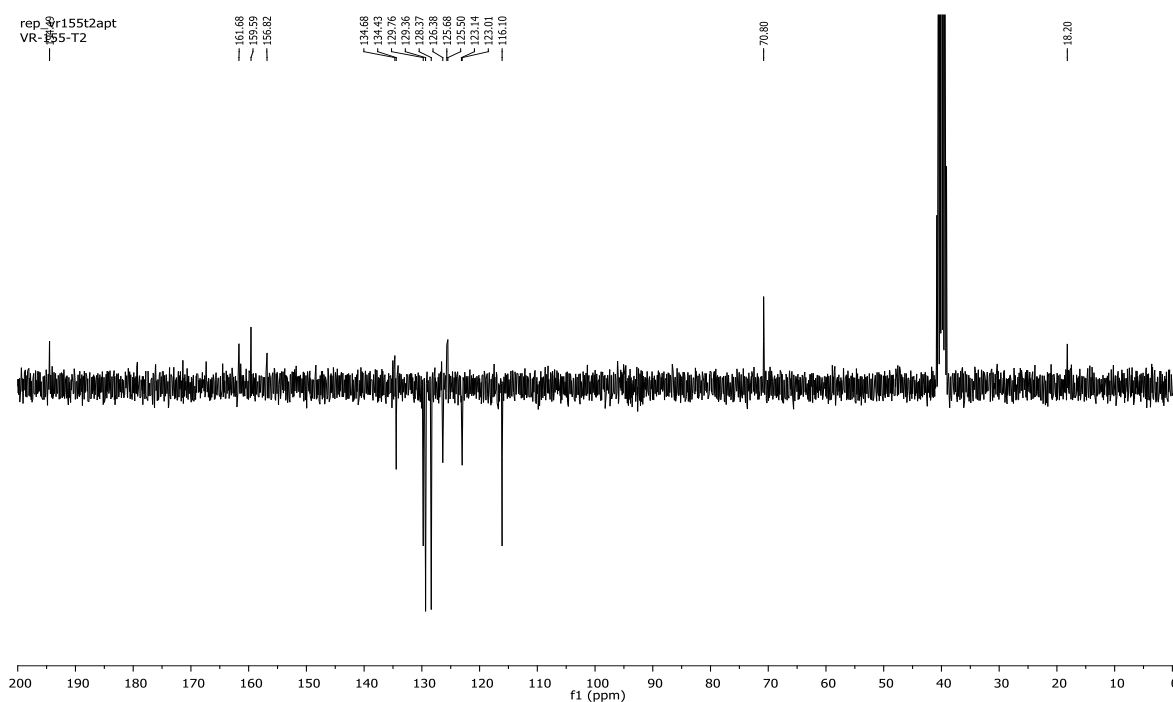
<sup>1</sup>H NMR (400 MHz, DMSO) δ spectrum of 2-(4-((1-(2-Morpholinoethyl)-1H-1,2,3-triazol-4-yl)methoxy)-3-methoxyphenyl)-5(6)-(3,4,5,6-tetrahydropyrimidin-2-yl)-1H-benzimidazole dihydrochloride (**19c**)



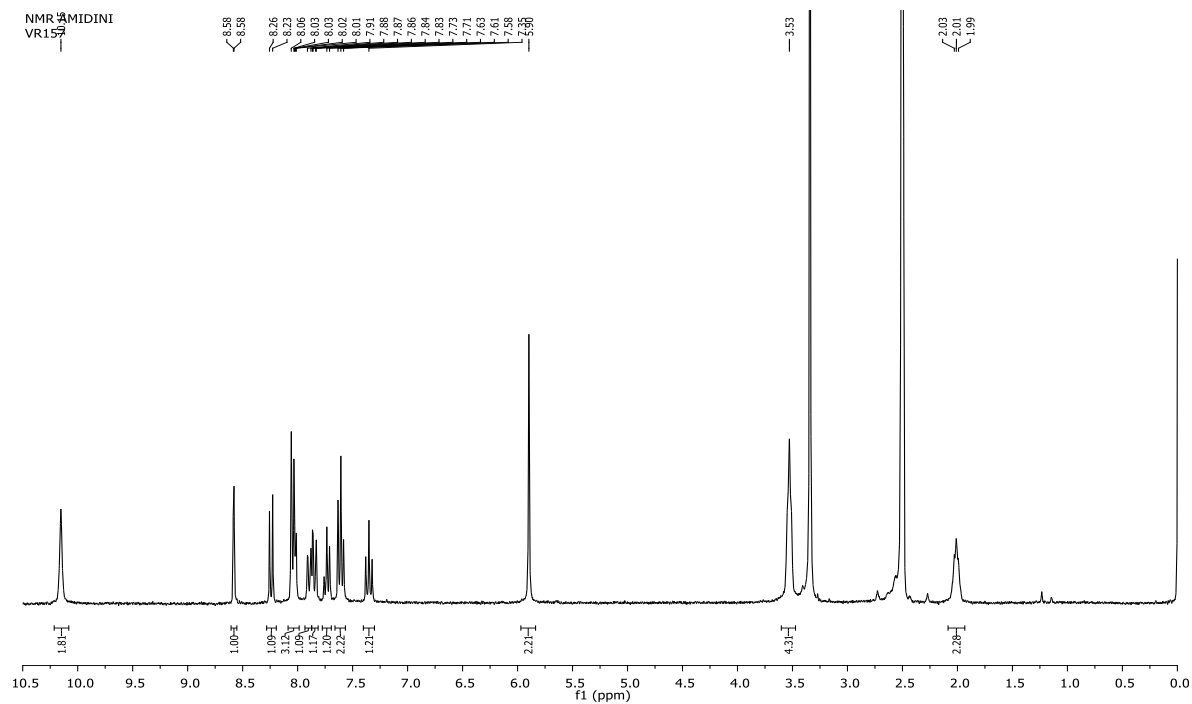
<sup>13</sup>C NMR (151 MHz, DMSO) δ spectrum of 2-(4-((1-(2-Morpholinoethyl)-1H-1,2,3-triazol-4-yl)methoxy)-3-methoxyphenyl)-5(6)-(3,4,5,6-tetrahydropyrimidin-2-yl)-1H-benzimidazole dihydrochloride (**19c**)



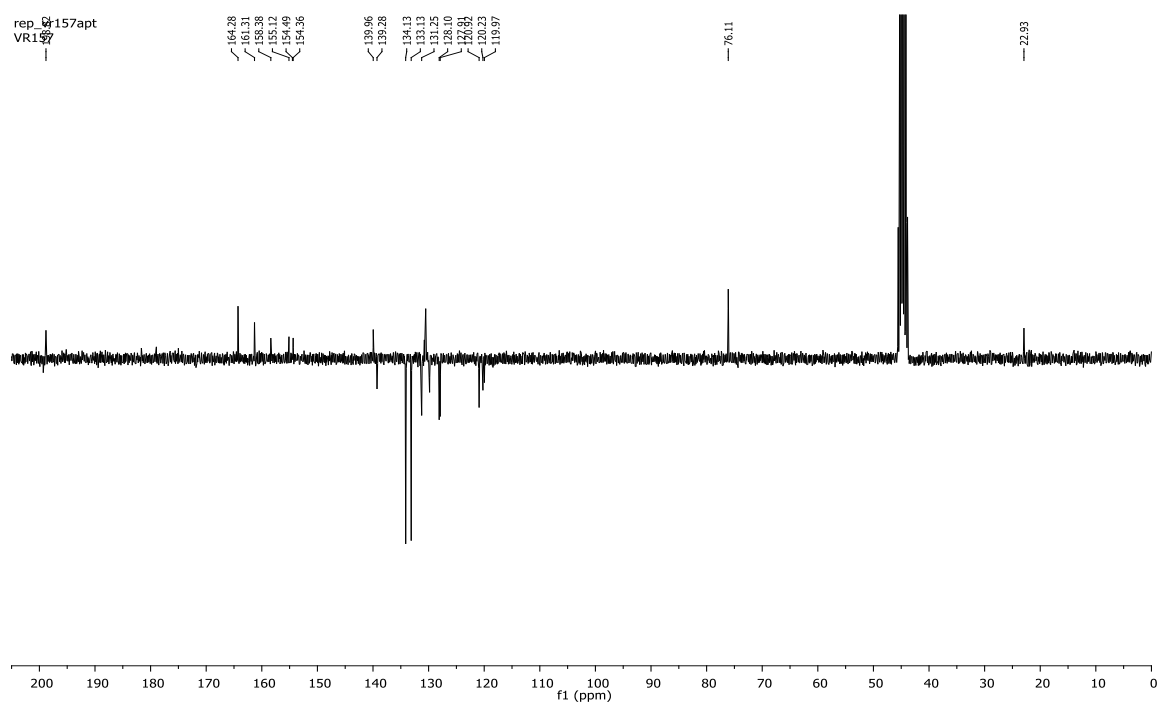
$^1\text{H}$  NMR (600 MHz, DMSO)  $\delta$  spectrum of 2-(4-(2-Oxo-2-phenylethoxy)phenyl)-6-(1,4,5,6-tetrahydropyrimidin-2-yl)benzothiazole hydrochloride (**21a**)



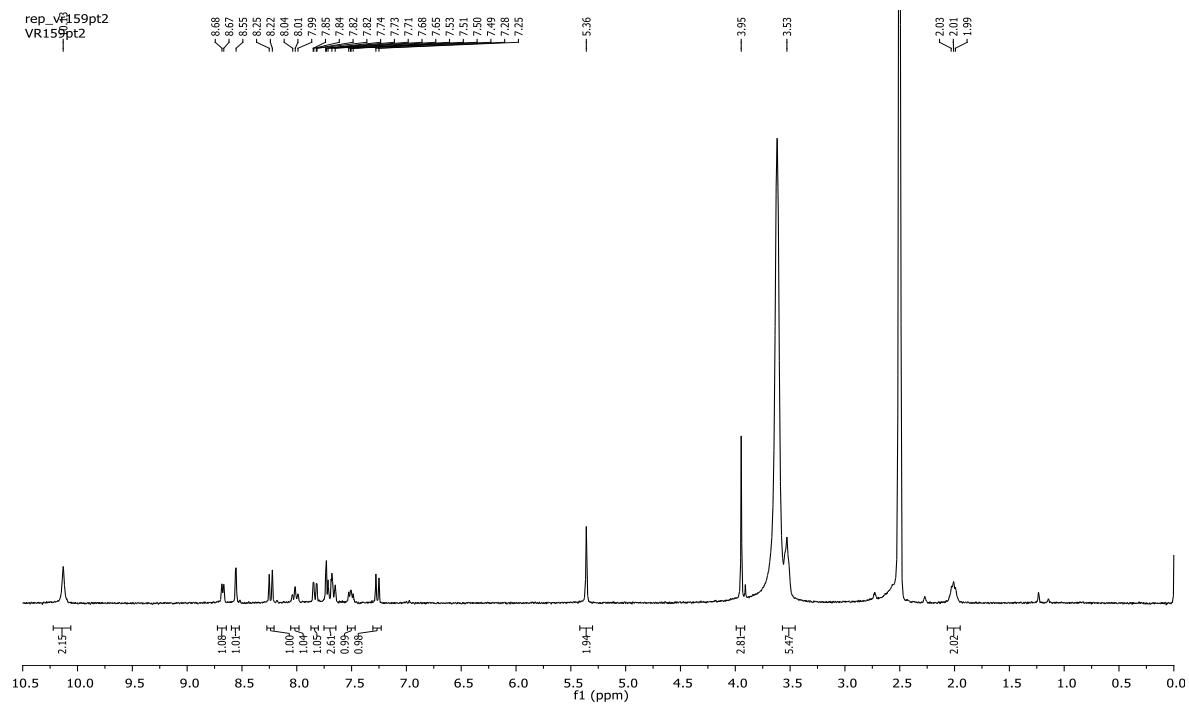
$^{13}\text{C}$  NMR (75 MHz, DMSO)  $\delta$  spectrum of 2-(4-(2-Oxo-2-phenylethoxy)phenyl)-6-(1,4,5,6-tetrahydropyrimidin-2-yl)benzothiazole hydrochloride (**21a**)



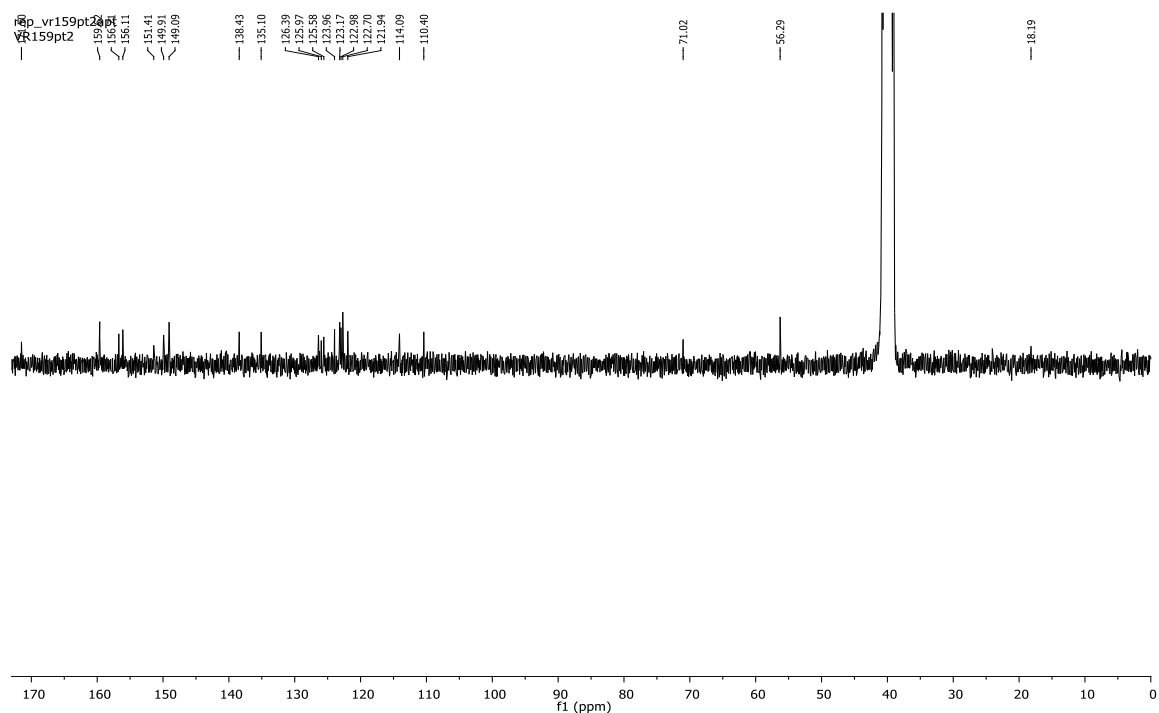
$^1\text{H}$  NMR (300 MHz, DMSO)  $\delta$  spectrum of 2-(3-Fluoro-4-(2-oxo-2-phenylethoxy)phenyl)-6-(1,4,5,6-tetrahydropyrimidin-2-yl)benzothiazole hydrochloride (**21b**)



$^{13}\text{C}$  NMR (75 MHz, DMSO)  $\delta$  spectrum of 2-(3-Fluoro-4-(2-oxo-2-phenylethoxy)phenyl)-6-(1,4,5,6-tetrahydropyrimidin-2-yl)benzothiazole hydrochloride (**21b**)

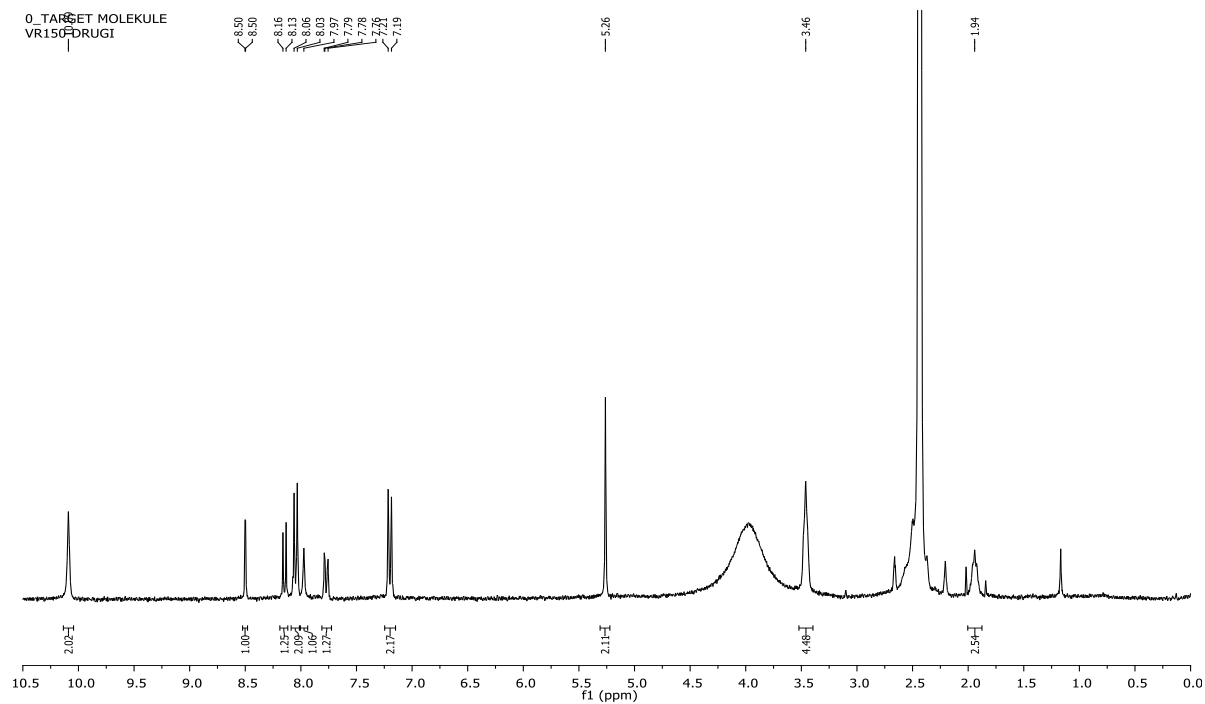


$^1\text{H}$  NMR (300 MHz, DMSO)  $\delta$  spectrum of 2-(3-Methoxy-4-(pyridin-2-ylmethoxy)phenyl)-6-(1,4,5,6-tetrahydropyrimidin-2-yl)benzothiazole hydrochloride (**22c**)

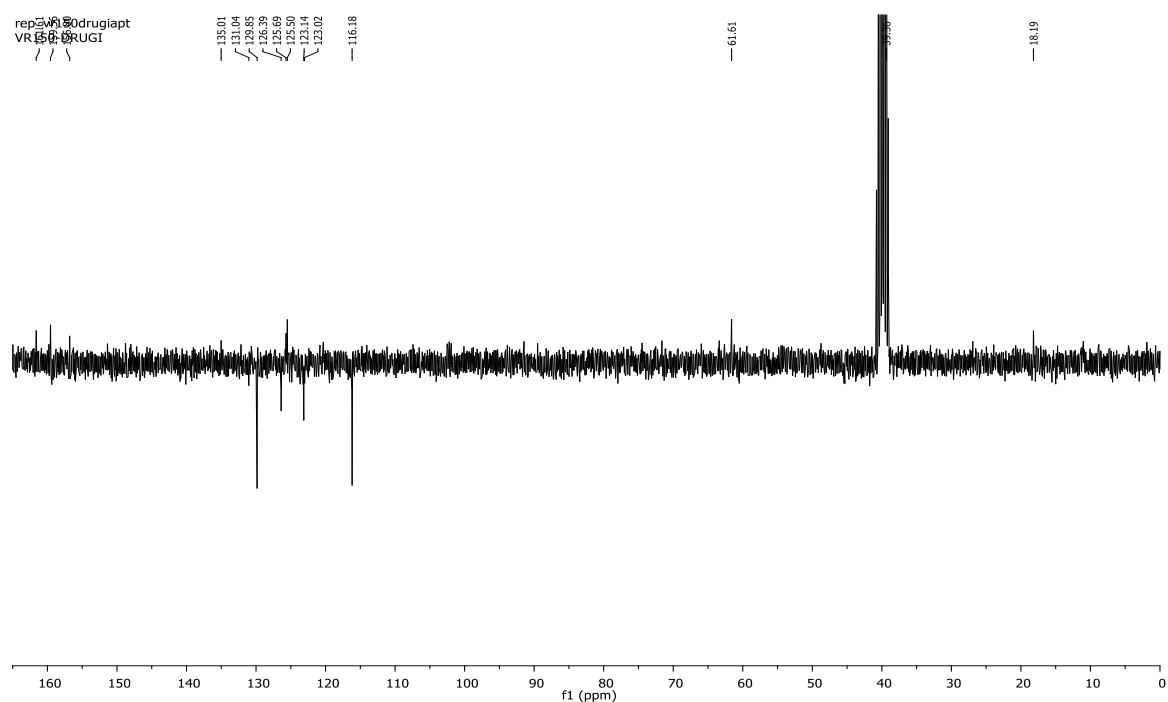


$^{13}\text{C}$  NMR (75 MHz, DMSO)  $\delta$  spectrum of 2-(3-Methoxy-4-(pyridin-2-ylmethoxy)phenyl)-6-(1,4,5,6-tetrahydropyrimidin-2-yl)benzothiazole hydrochloride (**22c**)

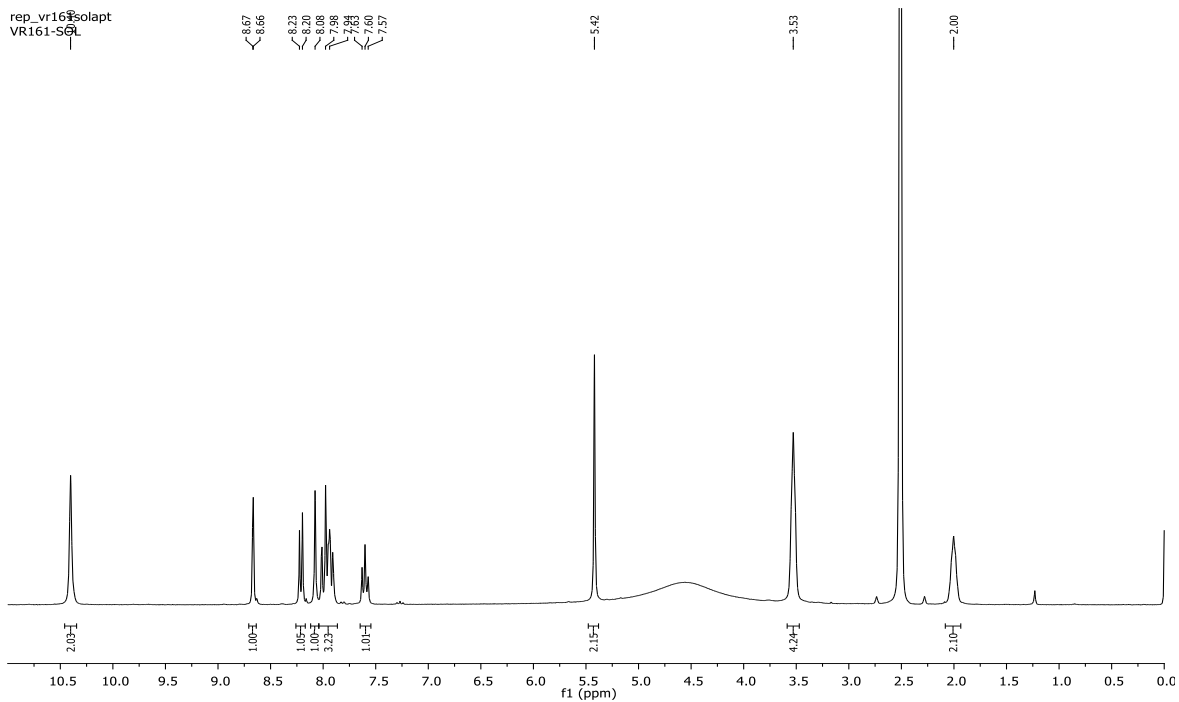




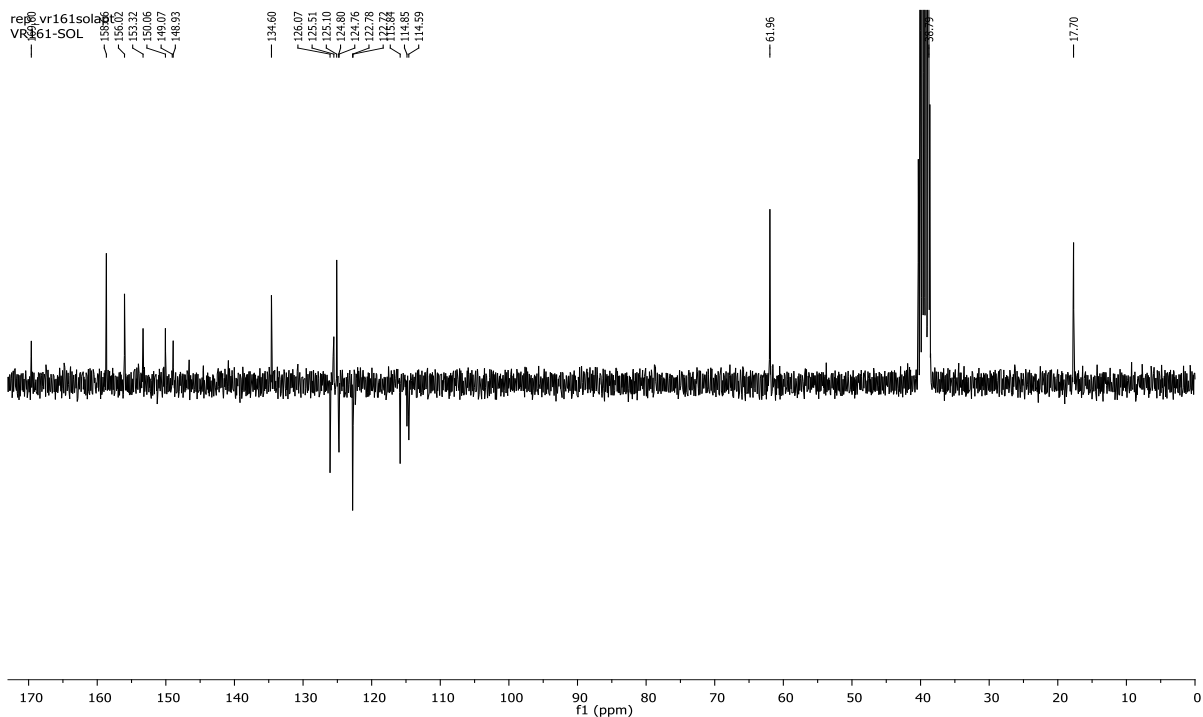
$^1\text{H}$  NMR (300 MHz, DMSO)  $\delta$  spectrum of 2-(4-((1H-1,2,3-triazol-4-yl)methoxy)phenyl)-6-(1,4,5,6-tetrahydropyrimidin-2-yl)benzothiazole hydrochloride (**23a**)



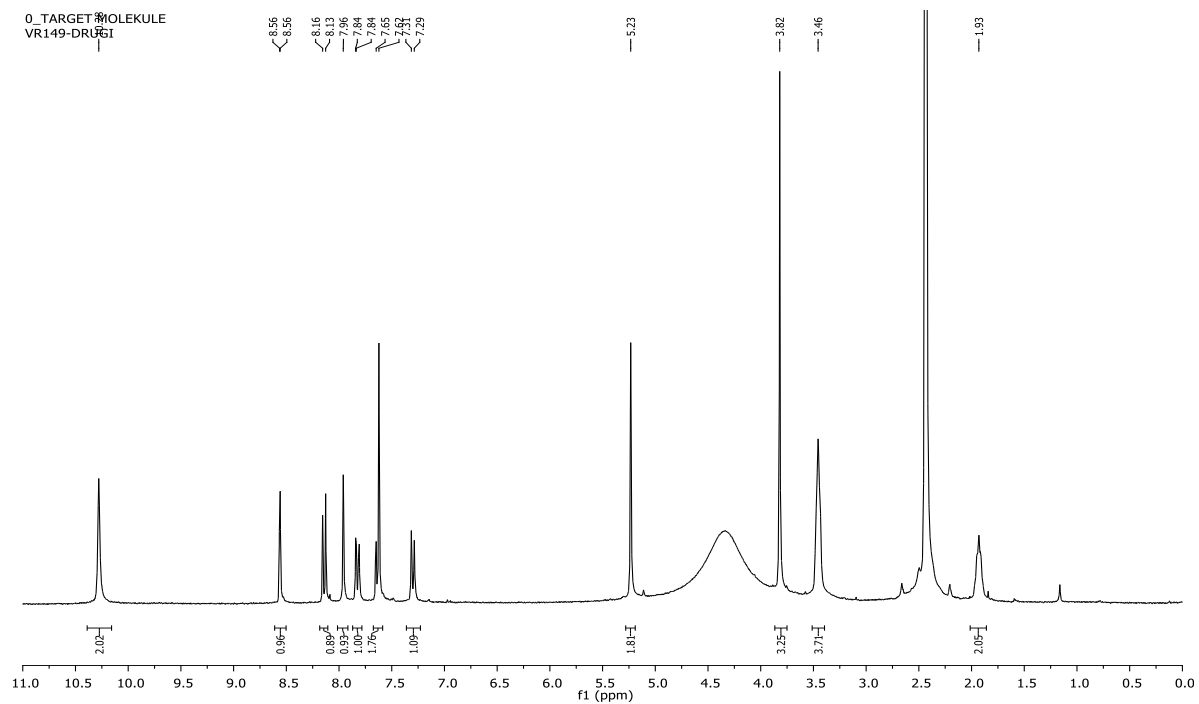
$^{13}\text{C}$  NMR (75 MHz, DMSO)  $\delta$  spectrum of 2-(4-((1H-1,2,3-triazol-4-yl)methoxy)phenyl)-6-(1,4,5,6-tetrahydropyrimidin-2-yl)benzothiazole hydrochloride (**23a**)



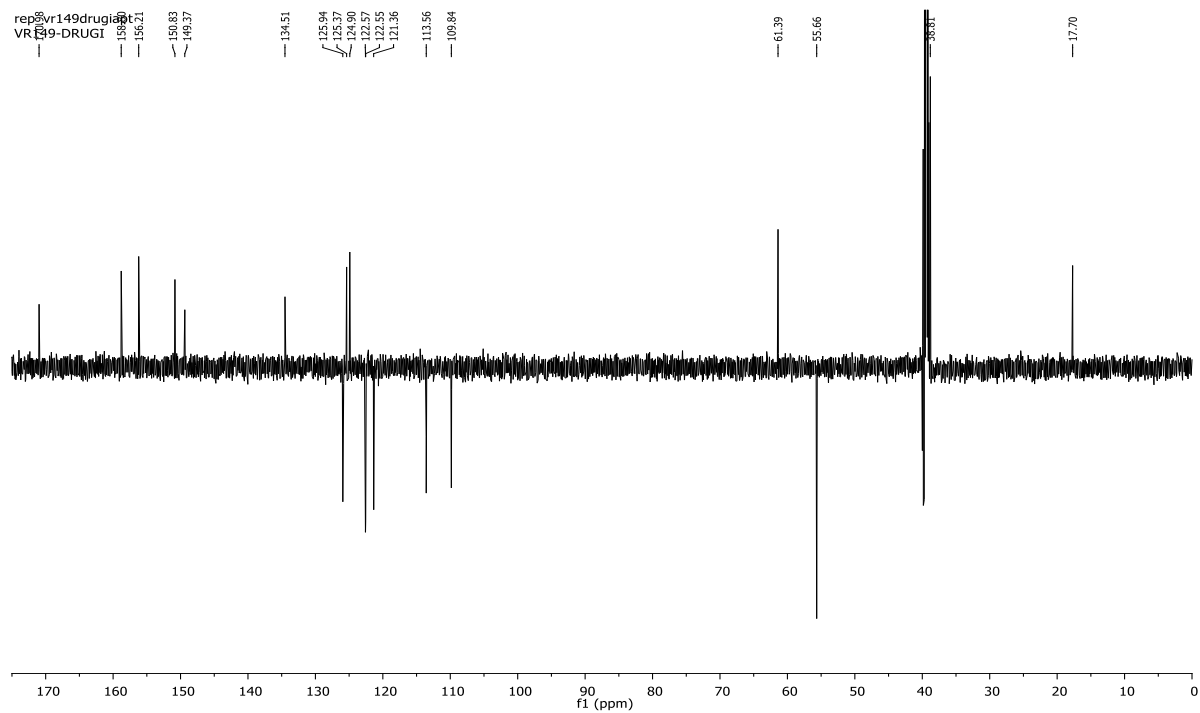
$^1\text{H}$  NMR (300 MHz, DMSO)  $\delta$  spectrum of 2-(3-Fluoro-4-((1H-1,2,3-triazol-4-yl)methoxy)phenyl)-6-(1,4,5,6-tetrahydropyrimidin-2-yl)benzothiazole hydrochloride (**23b**)



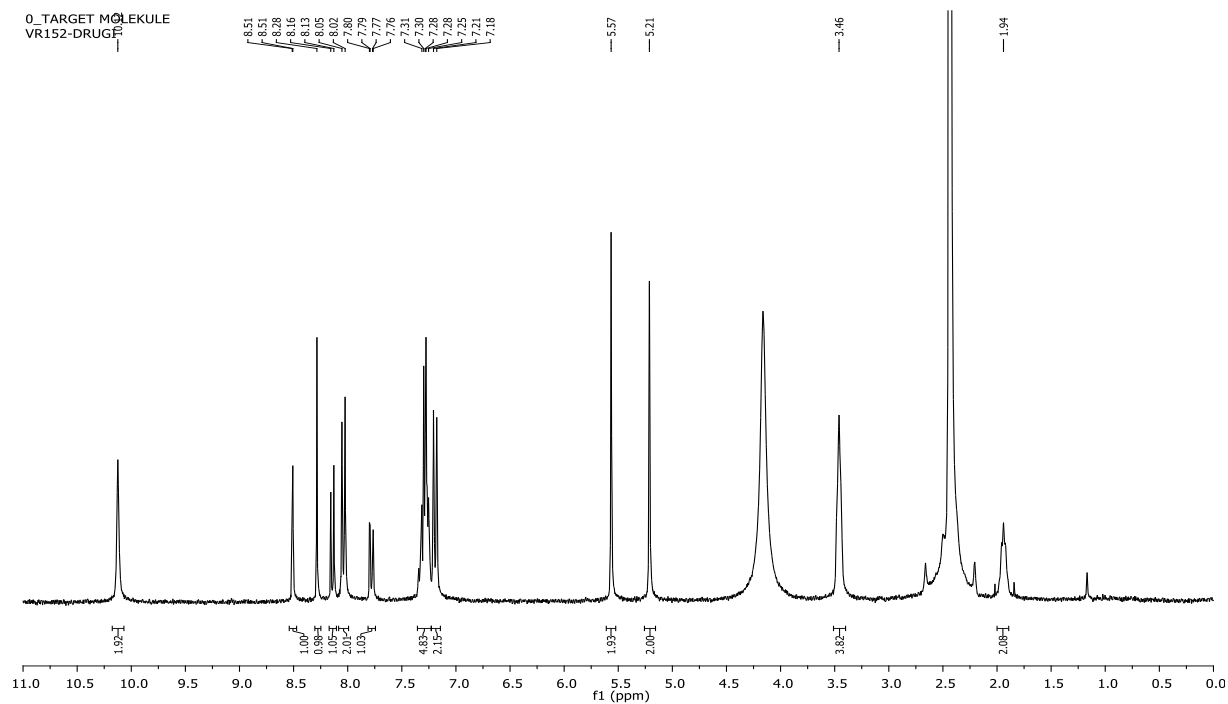
$^{13}\text{C}$  NMR (75 MHz, DMSO)  $\delta$  spectrum of 2-(3-Fluoro-4-((1H-1,2,3-triazol-4-yl)methoxy)phenyl)-6-(1,4,5,6-tetrahydropyrimidin-2-yl)benzothiazole hydrochloride (**23b**)



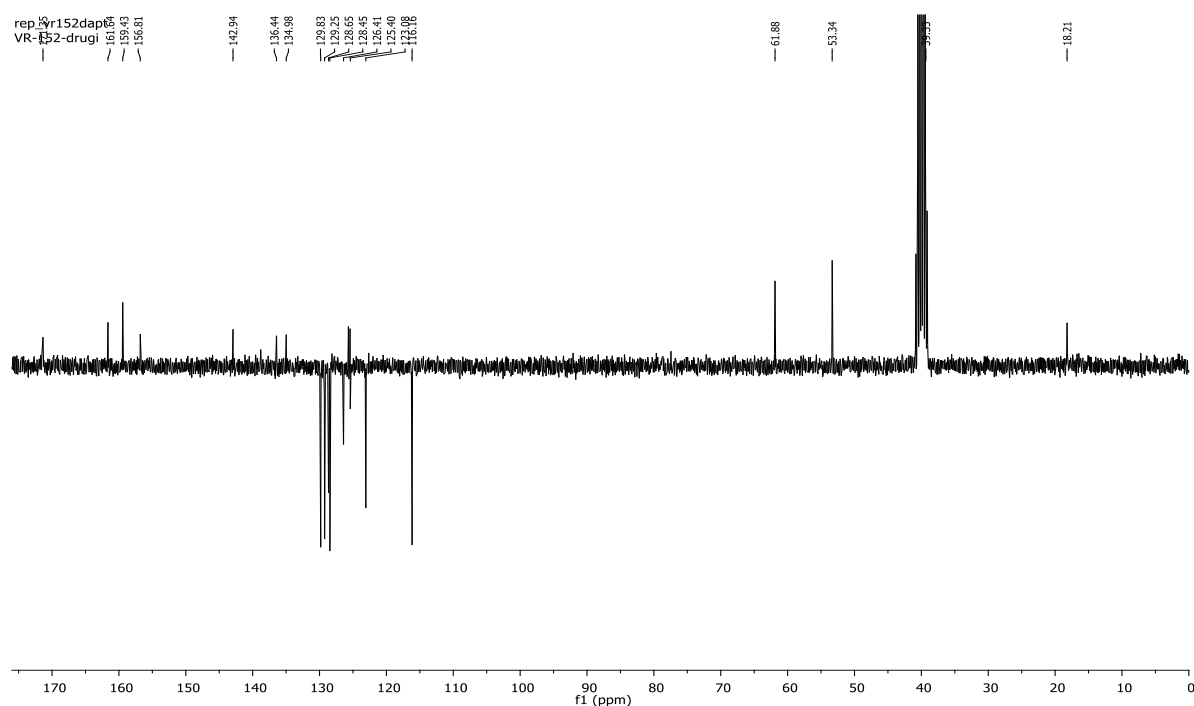
$^1\text{H}$  NMR (300 MHz, DMSO)  $\delta$  spectrum of 2-(3-Methoxy-4-((1H-1,2,3-triazol-4-yl)methoxy)phenyl)-6-(1,4,5,6-tetrahydropyrimidin-2-yl)benzothiazole hydrochloride (**23c**)



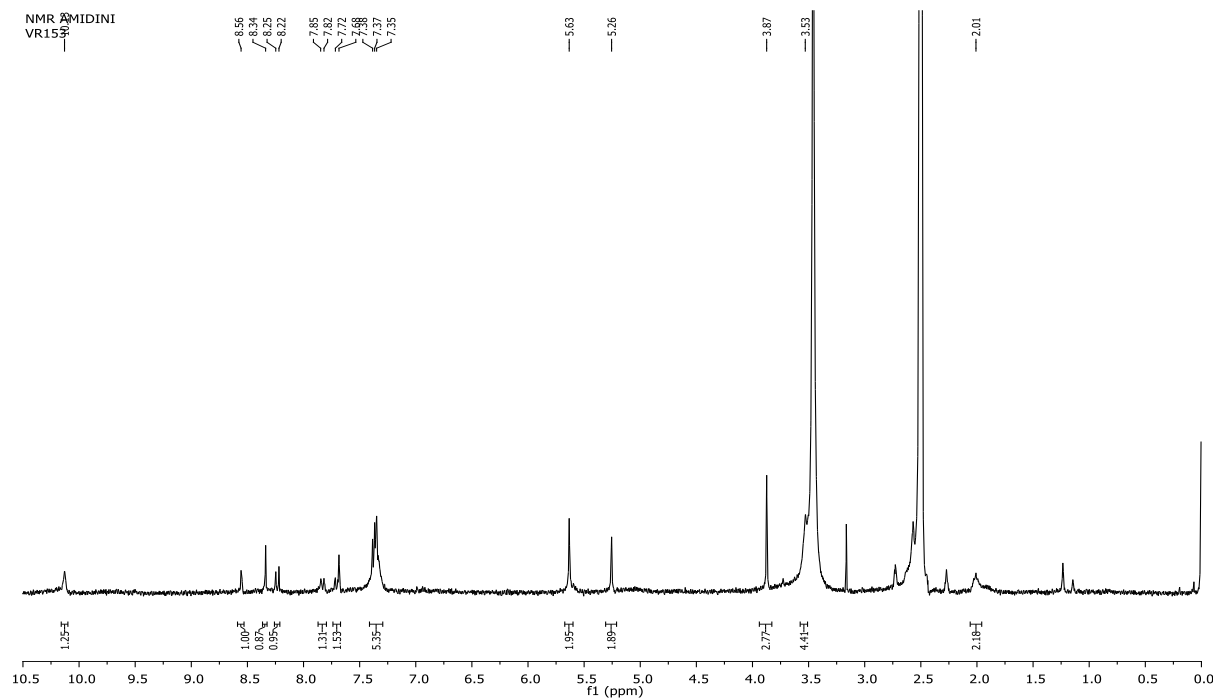
$^{13}\text{C}$  NMR (151 MHz, DMSO)  $\delta$  spectrum of 2-(3-Methoxy-4-((1H-1,2,3-triazol-4-yl)methoxy)phenyl)-6-(1,4,5,6-tetrahydropyrimidin-2-yl)benzothiazole hydrochloride (**23c**)



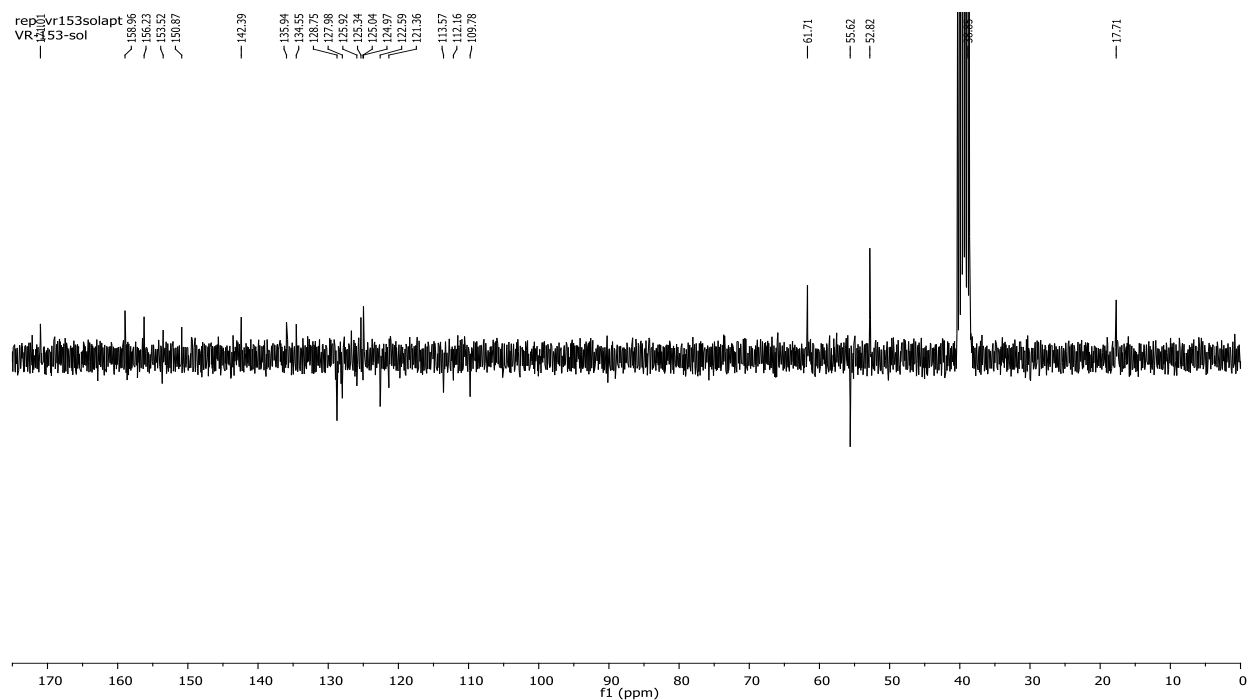
$^1\text{H}$  NMR (300 MHz, DMSO)  $\delta$  spectrum of 2-(4-((1-Benzyl-1H-1,2,3-triazol-4-yl)methoxy)phenyl)-6-(1,4,5,6-tetrahydropyrimidin-2-yl)benzothiazole hydrochloride (**24a**)



$^{13}\text{C}$  NMR (75 MHz, DMSO)  $\delta$  spectrum of 2-(4-((1-Benzyl-1H-1,2,3-triazol-4-yl)methoxy)phenyl)-6-(1,4,5,6-tetrahydropyrimidin-2-yl)benzothiazole hydrochloride (**24a**)



$^1\text{H}$  NMR (300 MHz, DMSO)  $\delta$  spectrum of 2-(3-methoxy-4-((1-benzyl-1H-1,2,3-triazol-4-yl)methoxy)phenyl)-6-(1,4,5,6-tetrahydropyrimidin-2-yl)benzothiazole hydrochloride (**24c**)



$^{13}\text{C}$  NMR (75 MHz, DMSO)  $\delta$  spectrum of 2-(3-methoxy-4-((1-benzyl-1H-1,2,3-triazol-4-yl)methoxy)phenyl)-6-(1,4,5,6-tetrahydropyrimidin-2-yl)benzothiazole hydrochloride (**24c**)